Chemical Technology Division

Chemical Technology Division
Chemical Technology Division
Chemical Technology Division
Chemical Technology Division
Chemical Technology Division
Chemical Technology Division
Chemical Technology Division
Chemical Technology Division
Chemical Technology Division
Chemical Technology Division
Chemical Technology Division
Chemical Technology Division
Chemical Technology Division
Chemical Technology Division
Chemical Technology Division
Chemical Technology Division

ANL-97/21

Separation Science and Technology Semiannual Progress Report

October 1993 - March 1994

by G. F. Vandegrift, S. B. Aase, B. Buchholz, D. B. Chamberlain, C. Conner, J. M. Copple, K. Foltz,* B. Gebby,† J. C. Hutter, R. A. Leonard, L. Nuñez, A. Philippides, M. C. Regalbuto, A. E. V. Rozeveld, J. Sedlet, S. A. Slater, B. Srinivasan, D. Strellis,* and D. G. Wygmans

*University of Illinois, Champaign-Urbana, IL
†Ohio State University, Columbus, OH

Argonne National Laboratory, Argonne, Illinois 60439
operated by The University of Chicago
for the United States Department of Energy under Contract W-31-109-Eng-38

Chemical Technology Division
Chemical Technology Division
Chemical Technology Division
Chemical Technology Division

Reproduced from the best available copy.

Available to DOE and DOE contractors from the
Office of Scientific and Technical Information
P.O. Box 62
Oak Ridge, TN 37831
Prices available from (423) 576-8401

Available to the public from the
National Technical Information Service
U.S. Department of Commerce
5285 Port Royal Road
Springfield, VA 22161

Distribution Category:
General, Miscellaneous, and Progress
Reports (Nuclear) (UC-500)

ANL-97/21

ARGONNE NATIONAL LABORATORY
9700 South Cass Avenue
Argonne, IL 60439

SEPARATION SCIENCE AND TECHNOLOGY SEMIANNUAL PROGRESS REPORT

October 1993–March 1994

by

G. F. Vandegrift, S. B. Aase, B. Buchholz, D. B. Chamberlain, C. Conner, J. M. Copple, K. Foltz,* B. Gebby,† J. C. Hutter, R. A. Leonard, L. Nuñez, A. Philippides, M. C. Regalbuto, A. E. V. Rozeveld, J. Sedlet, S. A. Slater, B. Srinivasan, D. Strellis,* and D. G. Wygmans

Chemical Technology Division

December 1997

Previous Reports in this Series

April 1993–September 1993	ANL-95/43
October 1992–March 1993	ANL-95/4
April 1992–September 1992	ANL-94/29
October 1991–March 1992	ANL-93/38

* University of Illinois, Champaign-Urbana, IL.
† Ohio State University, Columbus, OH.

TABLE OF CONTENTS

TABLE OF CONTENTS (contd)

LIST OF FIGURES

LIST OF FIGURES (contd)

LIST OF FIGURES (contd)

LIST OF TABLES

LIST OF TABLES (contd)

LIST OF TABLES (contd)

SEPARATION SCIENCE AND TECHNOLOGY
SEMIANNUAL PROGRESS REPORT
October 1993–March 1994

ABSTRACT

This document reports on the work done by the Separations Science and Technology Programs of the Chemical Technology Division, Argonne National Laboratory (ANL), in the period October 1993–March 1994. This effort is mainly concerned with developing the TRUEX process for removing and concentrating actinides from acidic waste streams contaminated with transuranic (TRU) elements. The objectives of TRUEX processing are to recover valuable TRU elements and to lower disposal costs for the nonTRU waste product of the process. Other projects are underway with the objective of developing (1) evaporation technology for concentrating radioactive waste and product streams such as those generated by the TRUEX process, (2) treatment schemes for liquid wastes stored or being generated at ANL, (3) a process based on sorbing modified TRUEX solvent on magnetic beads to be used for separation of contaminants from radioactive and hazardous waste streams, and (4) a process that uses low-enriched uranium targets for production of ^{99}Mo for nuclear medicine uses.

SUMMARY

TRUEX Technology Development

The Division's work in separation science and technology is mainly concerned with developing a technology base for the TRUEX (TRansUranic EXtraction) solvent extraction process. The TRUEX process extracts, separates, and recovers TRU elements from solutions containing a wide range of nitric acid and nitrate salt concentrations. The extractant found most satisfactory for the TRUEX process is octyl(phenyl)-N,N-diisobutylcarbamoylmethylphosphine oxide, which is abbreviated CMPO. This extractant is combined with tributyl phosphate and a diluent to formulate the TRUEX process solvent. The diluent is typically a normal paraffinic hydrocarbon or a nonflammable chlorocarbon such as carbon tetrachloride or tetrachloroethylene. The TRUEX flowsheet includes a multistage extraction/scrub section that recovers and purifies the TRU elements from the waste stream and multistage strip sections that separate TRU elements from each other and the solvent.

The objectives of TRUEX processing are to recover valuable TRU elements and to lower disposal costs for the nonTRU waste product of the process. A major thrust of the development efforts has been the Generic TRUEX Model (GTM), which is used with Macintosh or IBM-compatible personal computers for designing TRUEX flowsheets in Microsoft Excel and estimating cost and space requirements for installing TRUEX processes for treating specific waste streams.

During this report period, many improvements were made to the user interface of the GTM. These improvements included changes to user input cards to incorporate features that were not previously available from the front end but could be accessed by knowledgeable Microsoft Excel users, enhanced data reports for many options of the GTM, and removal of some input limitations.

The heart of the GTM is the Spreadsheet Algorithm for Stagewise Solvent Extraction (SASSE), which calculates multistaged, countercurrent flowsheets based on species distribution ratios calculated in the Spreadsheet Algorithm for Speciation and Partitioning Equilibria (SASPE). During this reporting period, we continued our efforts in the modeling of the extraction behavior of Zr/F by the TRUEX solvent, to be used in SASPE calculations. Results of our modeling efforts using different equations to calculate the distribution ratio for zirconium are discussed. Our zirconium modeling efforts were focused on (1) the GTM equation used to calculate the zirconium distribution ratio, (2) the values for the constants used to fit experimental data obtained with tracer zirconium in nitric acid, and (3) the values of the formation constants used to calculate the concentration of ZrF_2. Plans for further improvement to the zirconium extraction model are also addressed.

In a related effort, we have revised the macro that controls the calculation of the SASSE worksheet when extraction efficiency is less than 100% so that it can determine the proper number of iterations for each calculation. With this revision, the macro now avoids potential calculational errors and appears to be fully implemented. One can now use any value for extraction efficiency and expect well-behaved convergence of the SASSE worksheet.

The extraction behavior of bismuth in the TRUEX process is important in treating the nuclear waste at the Hanford site, since large quantities are present. The distribution of bismuth between nitric acid and TRUEX solvent was thus measured as a function of nitric acid concentration and bismuth concentration. Bismuth concentrations were measured by a calorimetric method. The initial bismuth concentration in the aqueous phase ranged from about 0.25 mM to 16 mM (0.500 mg/L to 3.3 g/L). Distribution ratios increased from about 3.5 at 0.05 M HNO_3 to a maximum of about 90 at 0.8M HNO_3 for bismuth concentrations at 0.25 mM and 2-3 mM. At a bismuth concentration of 16 mM, the ratios were about 15% higher.

Centrifugal Contactor Development

Multistage 2-cm centrifugal contactors ("minicontactors") are being used to carry out cold (nonradioactive) and hot (radioactive) tests of the combined TRUEX-SREX flowsheet, a new solvent extraction process developed to selectively extract and partition U, Am, Pu, Sr, and Tc from dissolved sludge wastes at the DOE Hanford site. The first cold tests were done to evaluate the hydraulic performance of the PS 12 solvent and to compare the experimentally observed behavior of nitric acid with that predicted by the GTM. Because the hydraulic performance of the PS 12 solvent degraded with time and with use during the cold tests, we switched to a new solvent, the PS 15 solvent, for all of the other tests.

When the HNO_3 concentration at several stages of two cold tests was compared with GTM calculations, the results indicated that minicontactor stage efficiency ranges between 80 and 100%, with most results closer to 100%. Thus, both the minicontactor and the GTM seem to be working well. Because of the erratic nature of some low flows in the interstage lines, it had been expected that the stage efficiency of the 2-cm contactor would be lowered significantly. However, based on these results, that does not appear to be the case.

Two uranium tests of the combined TRUEX-SREX process were done to evaluate the use of NaOH with THFTCA (tetrahydrofuran-2,3,4,5-tetracarboxylic acid) as the stripping agent. The results are very promising. With some NaOH present, Am, Pu, Sr, and the lanthanides can be removed in the strip section while U remains in the solvent so that it exits in the carbonate wash.

Based on the cold tests and the uranium tests, a TRUEX-SREX process flowsheet is being developed for an appropriate hot test in a 24-stage minicontactor. Flowsheet changes were made so that (1) the strontium decontamination factor will be as high as that desired for plant operation with the dissolved sludge wastes and (2) the stripping agent will be 0.3M THFTCA with 0.4M NaOH.

Another solvent extraction process, called SREX-NEPEX, separates Sr, Np, and Pu from the lanthanides, Am, and Ba. From an analysis of this process, a flowsheet to be tested was developed. We are now planning to test this flowsheet using a 20-stage minicontactor. In this test, the aqueous feed will contain small amounts of depleted U and ^{239}Np.

Pacific Northwest Laboratory is installing a pilot-scale centrifugal contactor system for the study of solvent extraction flowsheets, especially the TRUEX process, to clean up tank wastes. In support of this work, we built a multistage minicontactor system especially modified to meet their needs and have started hydraulic testing on the system.

We are supporting the Radiochemical Engineering Development Center (REDC) of Oak Ridge National Laboratory (ORNL) in the TRUEX processing of Mark 42 targets (aluminum-clad PuO_2) and in evaluation of the results using the GTM. We have also identified some areas of the GTM that need more work. Overall, we are very pleased with the results. A TRUEX flowsheet generated by the GTM was able to meet process goals the first time it was tested. We have asked ORNL to rerun the GTM using an extraction efficiency of 84%, which should yield the best comparison of the GTM calculations with the experimental data.

Advanced Evaporator Technology

Hanford is considering the use of a Compact Processing Unit (CPU) for treating their underground storage tank waste. The CPU concept is briefly described, along with the application of the concept to an evaporator/concentrator CPU. Hanford's current plans for a processing scheme called Case BETA are summarized in the Case BETA flowsheet so as to focus on the use of the evaporators.

The concentrator to be included in the evaporator/concentrator CPU will be based on an Artisan Rototherm. An overview of the Rototherm is given. A preliminary test plan has been prepared for the evaporator/concentrator CPU. During the first year, the CPU will be employed to concentrate a low-level waste stream from which the cesium has been removed. The evaporator/concentrator system will be designed such that maintenance-free operation is possible. Next, the system will be prepared for processing high-level waste. During the second year, the CPU will be used to process either a simulated or real acidic eluant.

A LICON model C-3 evaporator is being used for laboratory-scale evaluations of the evaporator/concentrator CPU. Work within the reporting period included hardware installation and software design for the data acquisition system being added to the laboratory-scale evaporator. A test plan was generated to guide the laboratory-scale tests, and the first in the series of tests was begun. Approximately 45 L of feed was evaporated down to 11 L of concentrate over 8.5 hours of operation. No major operational difficulties were encountered.

Technical Support for ANL Waste Management

We are cooperating with ANL Waste Management to develop treatment processes for all liquid wastes stored or being generated at ANL. Early work was directed toward the treatment of

mixed waste slurries; a hydroxide/sulfide precipitation process followed by filtration was developed for this waste. This process was tested using (1) a waste simulant containing 2M HNO_3 and 25 g/L of copper nitrate and (2) actual mixed waste containing Se, As, Pb, Cd, Ag, Cr, Ba, U, Mo, and Fe. The process was successfully demonstrated with both types of waste.

Another project is underway to treat aqueous TRU wastes in temporary storage at ANL. After volume reduction, these wastes would be shipped to the Waste Isolation Pilot Plant in Carlsbad, New Mexico, for permanent storage. A literature review of potential methods for waste solidification was completed. Magnetite carrier precipitation was chosen for processing the liquid TRU waste. Tests have been started to evaluate this process.

We are also participating in the installation, testing, and startup of new evaporators and concentrators for low-level wastes and the development of a process to treat liquid scintillation cocktail waste.

Magnetically Assisted Chemical Separation

Magnetically assisted chemical separation (MACS) processes are being developed for removing contaminants (^{137}Cs, ^{90}Sr, transuranics) from waste solutions. The MACS process combines the selective and efficient separation afforded by chemical sorption with the high physical separation afforded by magnetic recovery of ferromagnetic beads. Studies during this reporting period involved evaluating polymeric coatings for magnetic particles and measuring the hydrolytic and radiolytic damage to coated particles during processing.

Processing of ^{99}Mo Target

Efforts have been renewed to determine the feasibility of substituting low-enriched uranium (LEU) for the high-enriched uranium used in the production of ^{99}Mo for medical applications. As a part of this program, we are studying two LEU target designs. The LEU targets will contain either uranium-metal foil or uranium silicide (U_3Si_2). Either UO_2 or various UAl_x alloys are used in current high-enriched uranium (HEU) targets. The silicide fuel is being developed as a LEU substitute for UAl_x alloys, and the uranium metal foils are being developed as LEU substitute for UO_2.

The autodestruction rate of hydrogen peroxide in sodium hydroxide solutions at 70-100°C was measured. These data will be used to optimize the silicide dissolution process. The results of experimental work on the dissolution of depleted uranium metal foil in mixtures of nitric acid and sulfuric acid are also reported. These data show that several combinations of nitric and sulfuric acid mixtures and temperatures will yield the desired dissolution rate. The work will be continued in order to design a satisfactory ^{99}Mo recovery scheme from irradiated LEU-metal foil target; the scheme will resemble the Cintichem process, which was developed for HEU-UO_2 targets and was used for the commercial production of ^{99}Mo until February 1990.

I. INTRODUCTION
(G. F. Vandegrift)

A high-priority need exists to develop processes that can be applied to restore DOE sites to conditions that meet state and federal environmental regulations. The Division's work in separation science and technology is concerned with developing such processes for radioactive, mixed, and hazardous wastes. The TRUEX (TRansUranic EXtraction) solvent extraction process continues to be developed and demonstrated for recovering TRU elements from solutions containing a wide range of nitric acid and nitrate salt concentrations. An important part of this effort is developing and validating the Generic TRUEX Model (GTM). The GTM allows users to design flowsheets for specific waste streams and estimate the cost and space requirements for implementing a site- and feed-specific TRUEX process. The GTM is also a useful tool for plant operators to vary, monitor, and control the process once it is in place. Flowsheets for other solvent extraction processes are also being designed and tested.

Our other work in separation science and technology includes the development of (1) a process based on sorbing modified TRUEX solvent on magnetic beads to be used for separation of contaminants from radioactive and hazardous waste streams, (2) evaporation/concentration technology for processing supernatant solution removed from underground storage tanks, and (3) a process that uses low-enriched uranium targets in place of high-enriched uranium for production of ^{99}Mo for nuclear medicine uses. Several other projects are also underway to develop advanced processes for treating radioactive, mixed, and hazardous wastes.

II. TRUEX TECHNOLOGY DEVELOPMENT

The major effort in TRUEX technology-base development involves developing a generic data base and modeling capability for the TRUEX process, referred to as the Generic TRUEX Model (GTM). The GTM will be directly useful for site-specific flowsheet development directed to (1) establishing a TRUEX process for specific waste streams, (2) assessing the economic and facility requirements for installing the process, and (3) improving, monitoring, and controlling on-line TRUEX processes. The GTM is composed of three sections. The heart of the model is the SASSE (Spreadsheet Algorithm for Stagewise Solvent Extraction) code, which calculates multistaged, countercurrent flowsheets based on distribution ratios calculated in the SASPE (Spreadsheet Algorithm for Speciation and Partitioning Equilibria) section. The third section of the GTM, SPACE (Size of Plant and Cost Estimation), estimates the space and cost requirements for installing a specific TRUEX process in a glovebox, shielded-cell, or canyon facility. The development of centrifugal contactors for feed- and site-specific applications is also an important part of the effort.

A. General Improvements to Generic TRUEX Model

(J. M. Copple)

Although the Generic TRUEX Model (GTM) is a user friendly program, some features in GTM version 2.7, distributed in September 1993, were not accessible from the front end. The user was instructed on how to change or add information in the export file (the file generated based on the user input to the front end) to use these features. Changes have since been made to the front end: Version 3.0 of the GTM incorporates these features, which include accepting multiple organic feeds and allowing the reroute of aqueous and organic effluent streams to other sections.

Another improvement made to the GTM involves the reporting of results. In prior versions, the card display size was static and was small enough to fit on the standard (9-in.) display screen that came with the Macintosh Plus and SE; so for many options, reports were displayed on numerous output cards and could only be viewed one at a time and printed together. Multiple-report cards have been combined into a single screen display, and if the card is larger than the screen, scroll bars are displayed. Since the size of the report can vary, the report cards were modified to contain input and output values that give a complete accounting of the run on one display. A "Save to File" button has been added on all the result cards. When this button is clicked, the card results are saved to a file in the same layout as shown on the screen. This feature gives the user a computer-readable form of the results. In GTM 2.7 some reports were saved to file, but others could only be printed.

In GTM 2.7, there were constraints on the number of feeds that could be used in a flowsheet calculation from the front end. Only one extraction, three scrubs, four strips, a component wash, a carbonate wash, an acid rinse, and one organic feed could be entered. The front end could only accept this number of feeds because a section feed card existed for each section. Now there are only three feed cards, one extraction type, one scrub/strip type, and one organic type. For each section, a card is displayed and the user enters the feed. The feed is then stored in another location, so the feed card can be reused if needed. When running Options 1 and 8 of the GTM,[1] the constraints remain because of limitations in the SPACE section.

Some changes were made to the calculation section of the GTM. If the user specifies a stage efficiency of less than 0.85, a routine called the "Ea_macro" is automatically called to correctly set up the calculations. In GTM 2.7, the user only received a message stating that because of convergence problems, the stage efficiency (E_a) should not be set too low and recommends that a value >0.85 be used. In GTM 2.7, the user could manually call the Ea_macro to handle a smaller stage efficiency. This message is

no longer displayed and values <0.85 are now handled automatically. The equations for calculating distribution ratios and constants for ZrO and F were also improved.

Other changes to the front end include the following. The ability to enter initial concentrations for CMPO and TBP was added to Option 7. On the input card, the user may specify values for CMPO and TBP or leave them blank. If they are left blank, the initial values are based on the diluent specified in this card. Also the organic-phase concentrations of HNO_3, $CMPO_{free}$, and TBP_{free} equilibrated with the user-specified aqueous phase are displayed on the Option 2 results card.

B. Development of Spreadsheet Algorithm for Speciation and Partitioning Equilibria
(M. C. Regalbuto and G. F. Vandegrift)

We continue our efforts in the modeling of the extraction behavior of Zr/F by the TRUEX solvent for use in SASPE. In previous report periods, we attempted to correlate the experimental distribution ratio (D value) measured at different Zr/F ratios (0 to 6) and different HNO_3 concentrations (0.16-5.02M). Different forms of the equation used to calculate the distribution ratio for zirconium were tested. We will discuss the results of our modeling efforts using the different equations, as well as plans for further improvements to the model for zirconium behavior. Our previous assumption, that only ZrF_2 extracts and that the distribution ratio for zirconium could be modeled as a function of the concentration of ZrF_2 and total Zr, did not account for the nitrate activity dependence. Nitrate activity becomes important at lower F/Zr ratios when the amount of free zirconium in the aqueous phase is large.

To improve our predictions at low F/Zr ratios, we added a term to our equation that calculates the distribution ratio for zirconium. This equation will account for the nitrate activity dependence at large zirconium-free concentrations, i.e., low F/Zr ratios.

Our efforts were then focused on (1) the form of the equation used to calculate D_{ZrO}, (2) the values for the constants used to fit the nitrate-alone data, and (3) the values of the formation constants used to calculate the concentration of ZrF_2 and its partitioning into the TRUEX solvent. The following equation was the best form to fit data with and without fluoride present:

$$D_{ZrO} = \frac{[K_0 + K_1 \{NO_3\}]\,[Zr\_free] + K_3\,[ZrF_2]}{[Zr\_total] + K_2\{NO_3\}\,[Zr\_free]} \qquad (1)$$

where brackets indicate concentration; braces indicate activity; K_i's are equilibrium constants; and Zr_free and Zr_total indicate the free and total zirconium, respectively. During this reporting period, we decided to revise the values for K_0, K_1, and K_2, employing zirconium-tracer experimental data originally used in the GTM (tracer zirconium, fluoride absent). Equation 1 reduces nitrate-only data to the following:

$$D_{ZrO} = \frac{K_0 + K_1\{NO_3\}}{1 + K_2\,\{NO_3\}} \qquad (2)$$

Figure 1 shows a plot of the experimental distribution ratios measured for the zirconium tracer data versus nitrate activity. We also show the values calculated for D_{ZrO} for the given nitrate activities using Eq. 2. The values of K_0, K_1, and K_2 were determined in such a way that the errors between the calculated and the measured values are minimized. These values for the constants satisfy this condition: $K_0 = 4.04$, $K_1 = 44.9$, and $K_2 = 0.19$. Unfortunately, the value of K_2 that satisfies the experimental tracer data is too

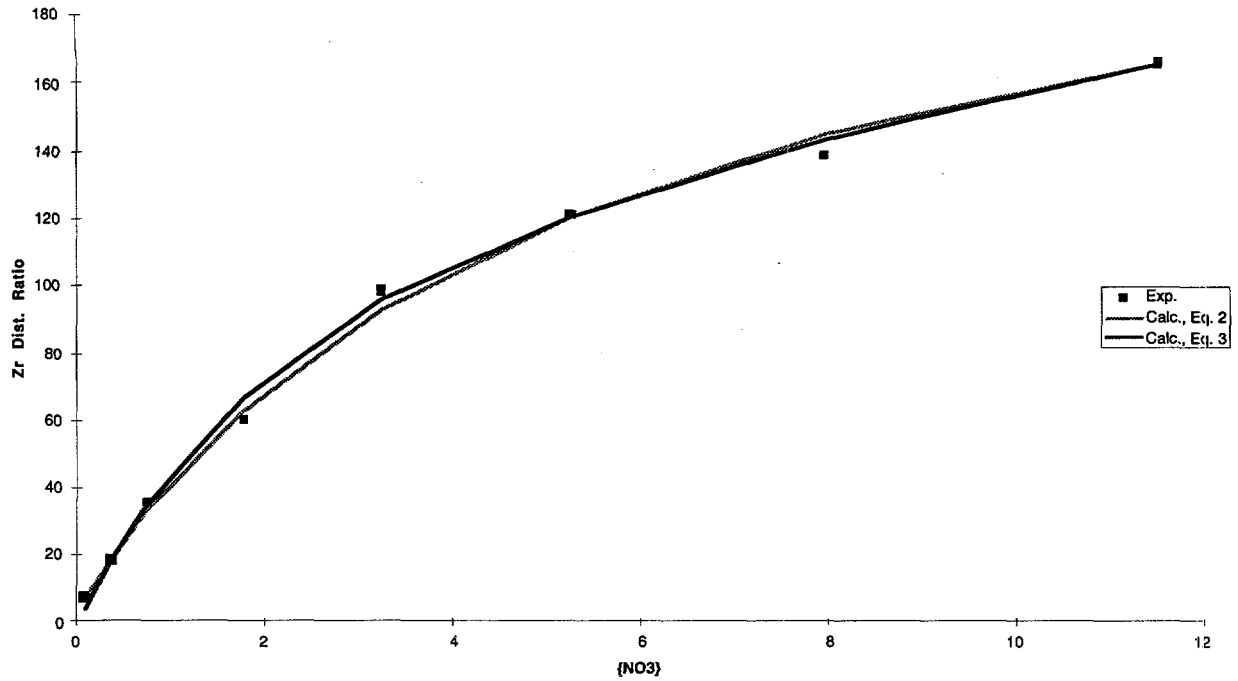

Fig. 1. Experimental and Calculated Distribution Ratios for Zirconium Extraction at Various Nitrate Activities

low to predict the nitric acid dependence that was experimentally determined for the data with fluoride present.

To be able to determine the nitrate dependence in the distribution ratio for zirconium in the presence of fluoride, we changed Eq. 2 such that, when the nitric acid concentration increases, the distribution ratio for zirconium increases at the proper rate. We can write D_{ZrO} as follows:

$$D_{ZrO} = \frac{[K_0\{NO_3\} + K_1\{NO_3\}^2]\,[Zr\_free] + K_3[ZrF_2]}{[Zr\_total] + K_2\{NO_3\}\,[Zr\_free]} \quad (3)$$

where K_0, K_1, and K_2 are equilibrium constants that were fit using experimental data; $\{NO_3\}$ is the activity of nitrate; Zr_free is the amount of zirconium in the aqueous phase that is not associated with fluoride or any other component; Zr_total is the total zirconium in the aqueous phase; $[ZrF_2]$ is the concentration of ZrF_2 in the aqueous phase; and K_3 is the equilibrium constant between the organic and aqueous phase for ZrF_2. The values of K_0, K_1, K_2, and K_3 that best fit the experimental data for F/Zr ratios of 1-6 are given in Table 1. Table 2 has the values of the formation constants for the different zirconium fluoride species that best fit the experimental values. Comparisons of the estimated distribution ratios and the experimental values obtained for different F/Zr ratios as a function of $\{NO_3\}$ are given in Figs. 2 through 5.

Note that the values of the constants K_0, K_1, and K_2 used in Eq. 3 were fit using the experimental data for the distribution ratio for zirconium in the presence of fluoride. If K_0, K_1, and K_2 are fit with the tracer data originally used by the GTM, their values will be 58.2, 0.97, and 0.33, respectively, and will not fit the fluoride data. In Fig. 1, we show the values for D_{ZrO} calculated using Eq. 3 and the values for K_0, K_1, and K_2 obtained from fitting the tracer data.

Table 1. Values for the Constants Used to Calculate the Distribution Ratio for Zirconium in GTM 3.0

Equil. Constant	Equation 2 Using Tracer Data	Equation 3 Using Tracer Data	Equation 3 Using F/Zr Data
K_0	4.04	58.2	1.3
K_1	44.9	0.97	17
K_2	0.19	0.33	0
K_3	---	---	1.5

Table 2. Formation Constants for ZrF Species

Species	Values from GTM 2.7	Values from GTM 3.0
ZrF	6.5E+8	6.5E+8
ZrF_2	2.15E+16	4.02E+16
ZrF_3	2.37E+22	2.96E+20
ZrF_4	5.84E+27	2.98E+27
ZrF_5	1.9E+32	4.96E+31
ZrF_6	2.32E+36	6.73E+35

Figures 2 and 3 indicate reasonably good agreement between the calculated (Eq. 3) and experimental distribution ratios at F/Zr ratios of 2, 3, and 4. For the F/Zr ratio of 5, the calculated value is much higher (Fig. 4), indicating that our value for the formation constant for ZrF_5 is too low. For the F/Zr ratios between 5 and 6, the calculated value is much lower (Fig. 5), indicating that our value for the formation constant for ZrF_6 is set too high. We are working on ways to improve our zirconium extraction model so that we can fit both tracer and fluoride data. We will also include new data collected at F/Zr ratios of zero and one.

C. Development of Spreadsheet Algorithm for Stagewise Solvent Extraction
(R. A. Leonard, J. M. Copple, M. C. Regalbuto, and G. F. Vandegrift)

The SASSE (Spreadsheet Algorithm for Stagewise Solvent Extraction) worksheet was developed for detailed evaluation of proposed TRUEX flowsheets in conjunction with distribution ratios calculated by the SASPE worksheet. It works for any amount of other-phase carryover and gives the steady-state concentration profile for each feed component without requiring any iterations. When SASSE is used independently, the appropriate distribution-ratio values or equations must be supplied by the user. When it is used within the Generic TRUEX Model, these ratios are calculated by SASPE. All worksheets and macros are based on Microsoft Excel.

The macro called SASSE_Generator generates the SASSE worksheets whether it is used independently or as a part of the GTM. In the previous report period, the SASSE worksheet had been upgraded to include stage efficiency. To implement this upgrade, a macro called Ea_Macro was developed for controlling the calculation of the SASSE worksheet when the extraction efficiency (E_a) is less than 1.0 (100%). An improvement to the Ea_Macro is reported here.

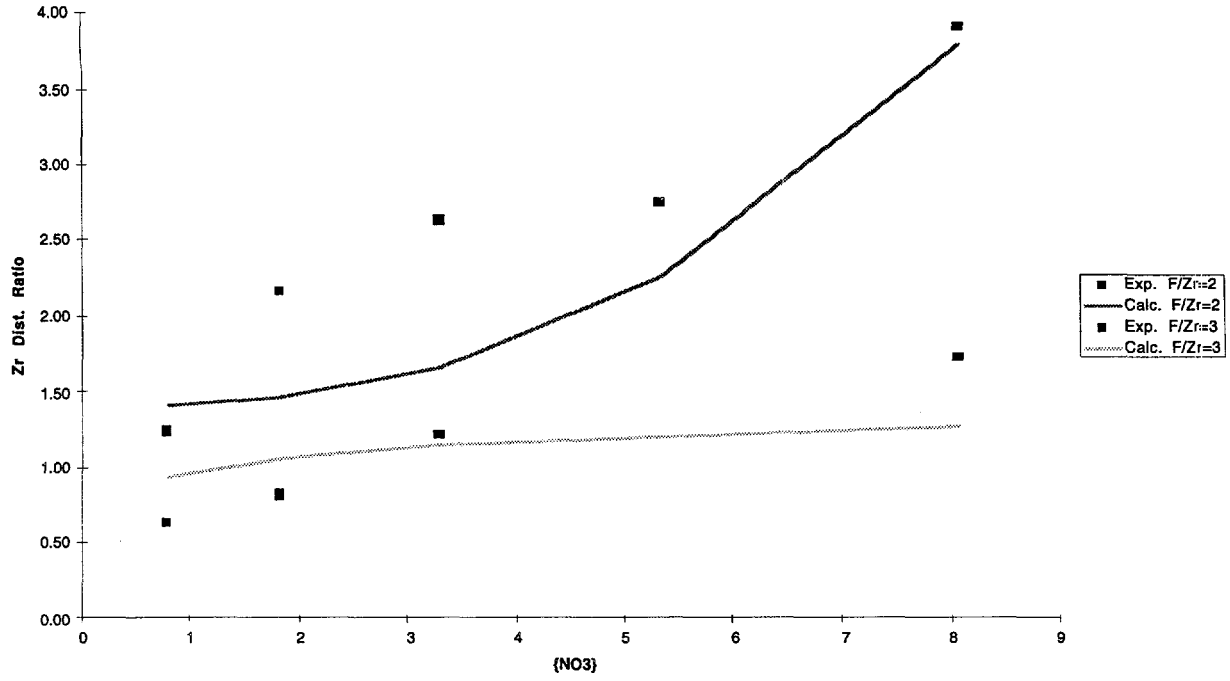

Fig. 2. Distribution Ratio for Zirconium as a Function of Nitrate Activity for F/Zr Ratios of 2 and 3

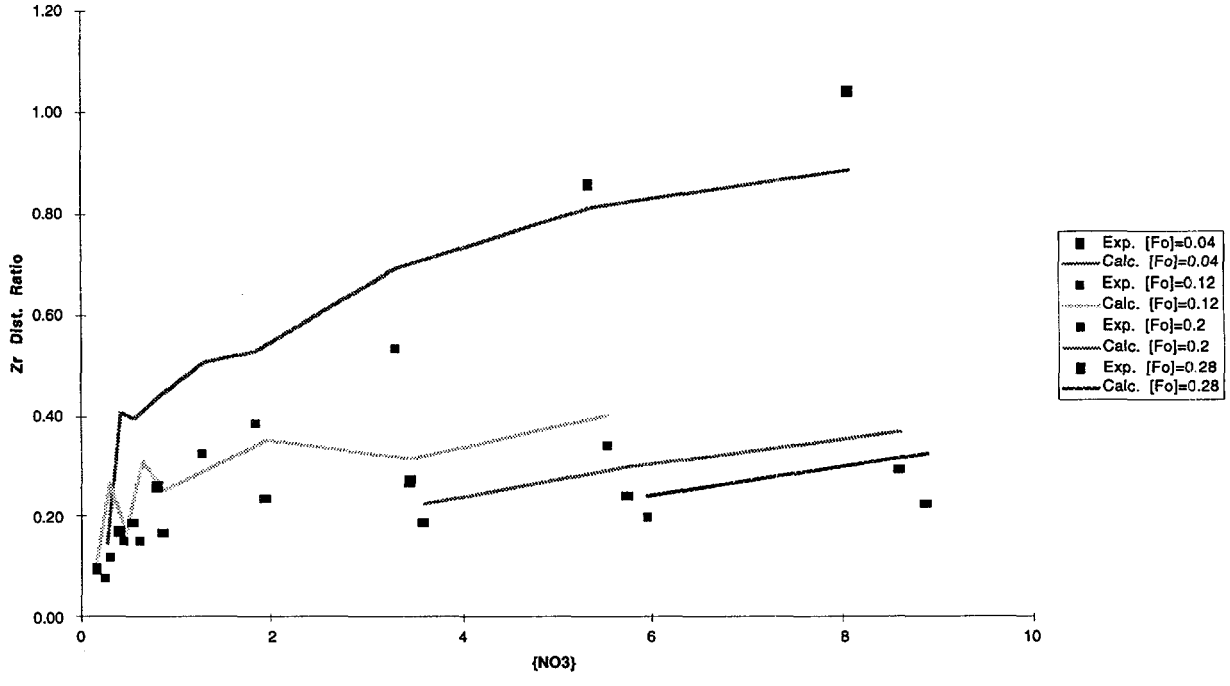

Fig. 3. Distribution Ratio for Zirconium as a Function of Nitrate Activity for F/Zr Ratio of 4 and Various Initial Fluoride Concentrations

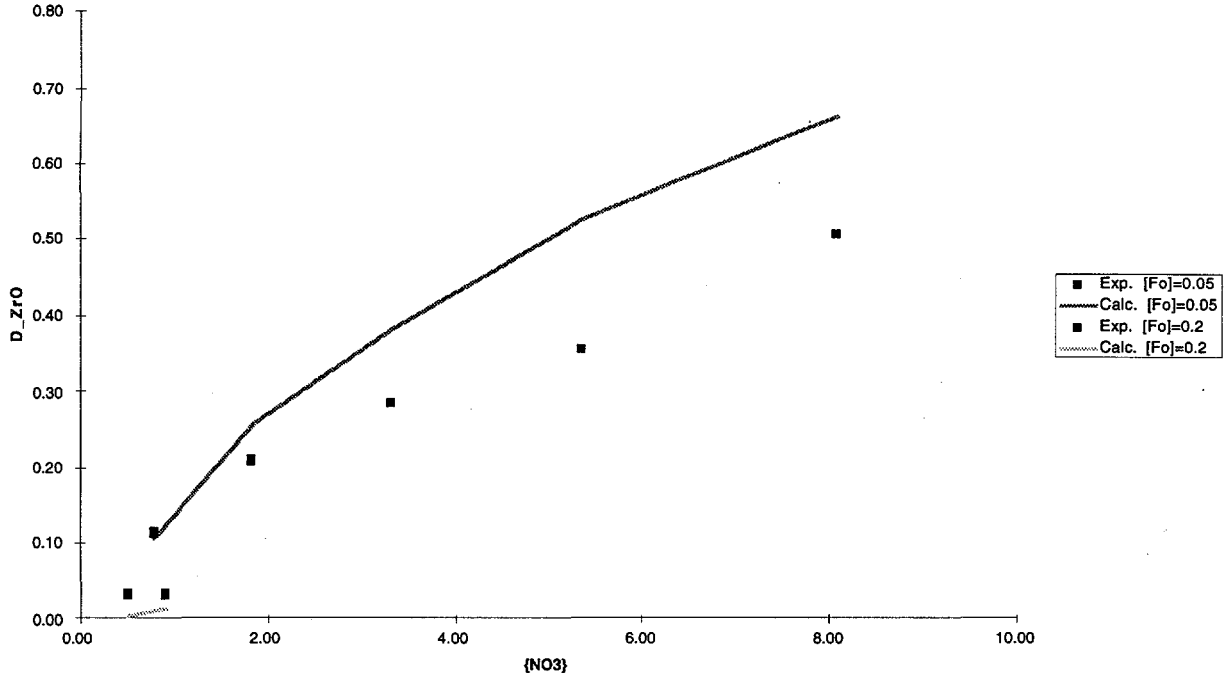

Fig. 4. Distribution Ratio for Zirconium as a Function of Nitrate Activity for F/Zr Ratio of 5 and Various Initial Fluoride Concentrations

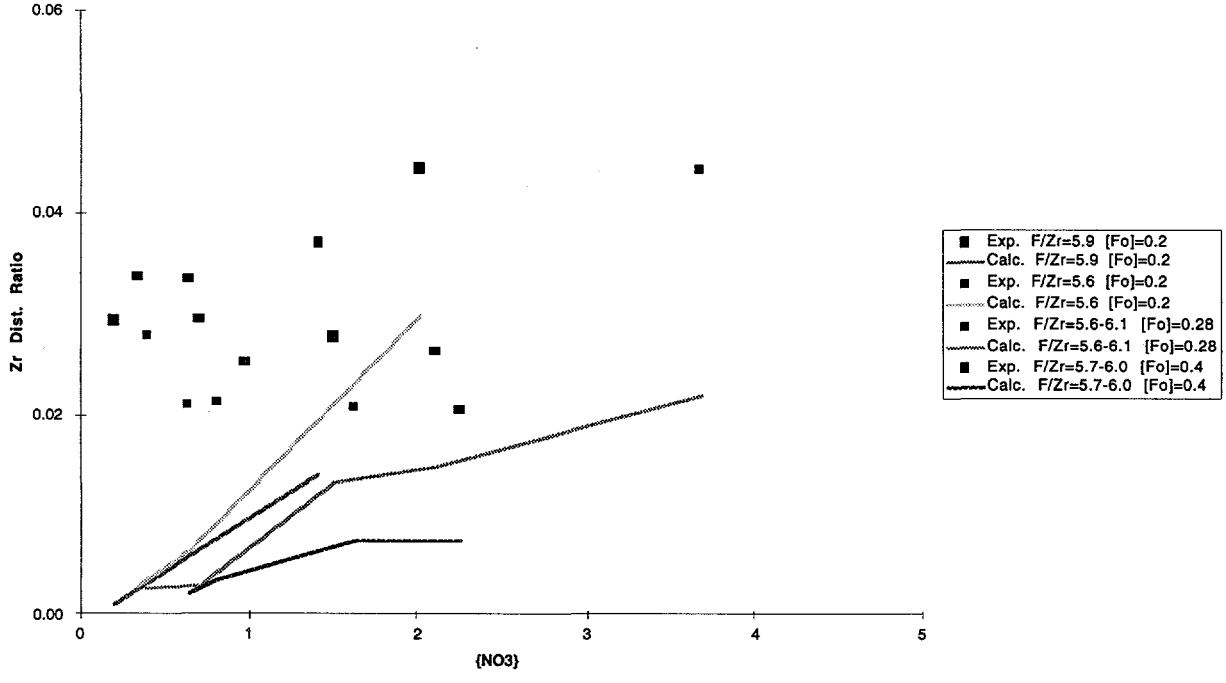

Fig. 5. Distribution Ratio for Zirconium as a Function of Nitrate Activity for F/Zr Ratio of 5-6 and Various Initial Fluoride Concentrations

The Ea_Macro, which controls the calculation of the SASSE worksheet when the extraction efficiency (E_a) is less than 1.0 (100%), works as follows. It controls the value of S_i used in the SASSE worksheet, where S_i is the ratio of two concentrations of component i. The S_i ratio is the concentration of component i in the organic phase going from stage j - 1 to stage j divided by its concentration in the aqueous phase going from stage j to stage j - 1. The macro calculates the SASSE worksheet while holding the S_i values constant. Then, it updates all the S_i values (S_i) with the new values (S_i_new) and recalculates the worksheet. Up to now, the Ea_Macro had performed this iteration a fixed number of times, namely five.

In evaluating the Mark 42 flowsheet tests at Oak Ridge National Laboratory by using the GTM, we encountered some cases where more than five iterations of the Ea_Macro were needed. If there were not a sufficient number of iterations, some D values would be very much larger than their final values. For some components, the D values were so large that impossibly large concentrations were calculated. When such concentrations were passed to SASPE, it was not able to calculate a new set of D values.

We have improved the Ea_Macro and corrected this problem as follows. After each iteration of the Ea_Macro, the ratio of S_i/S_i_new for each component is reviewed for all process stages. If any ratio differs from 1.0 by more than 1%, the Ea_Macro goes through another iteration; otherwise, it stops. If 100 iterations are required, the macro also stops and gives the user an error message. In practice, no more than 10 iterations have been required. The number of Ea_Macro iterations changes with each iteration between SASSE and SASPE. As the SASSE-SASPE iteration converges, the number of Ea_Macro iterations becomes small, with only one or two being required.

With the current SASSE worksheet and the new Ea_Macro, the calculation of E_a is now so stable that it can be used within the GTM after each SASSE-SASPE iteration. In the past, when the iterative solution for E_a <1.0 was less stable, E_a was kept at 1.0 until a solution was obtained, then the actual E_a value was introduced. Now this is not necessary. Using the new E_a procedure in the GTM, we observed that for one flowsheet an E_a of 0.85 required fewer SASSE-SASPE iterations than when E_a was 1.0. Thus, the Ea_Macro now appears to be fully implemented and allows the use of various values for extraction efficiency with well-behaved SASSE convergence in each case.

D. Data Base Enhancement
(D. Strellis)

The behavior of bismuth in the TRUEX process is important in treating the nuclear waste stored at the Hanford site, since large quantities (grams per liter) are present. The bismuth comes from the bismuth phosphate that was used as a carrier and the sodium bismuthate that was used as an oxidizing agent in the initial process for separating plutonium from neutron-irradiated uranium. Distribution ratio measurements are being made for Bi(III). A spectrophotometric method is being used to measure the absorbance of the iodobismuthate complex in both the aqueous and organic phases. This complex forms when potassium iodide is added to a solution containing bismuth. Distribution ratios, thus far, have ranged from 3 to 120, depending on the HNO_3 concentration in the aqueous phase.

During this reporting period, the distribution of Bi(III) in the TRUEX process was studied by contacting the TRUEX-NPH solvent with aqueous solutions containing various bismuth and nitric acid concentrations. In some experiments, the initial HNO_3 concentration was varied throughout the set. In others, the initial bismuth concentration was varied.

In Exp. 4, both forward and reverse extractions were done using nine initial concentrations of HNO_3. A 5.01 mM bismuth stock solution was prepared by dissolving bismuth nitrate pentahydrate

crystals in 0.1M HNO_3. This stock solution was used to spike the initial aqueous phase. It was also used in preparing the spectrophotometric standards for the analysis. An Excel spreadsheet was compiled to calculate the initial bismuth and HNO_3 concentrations for the aqueous phase after adding all the constituents.

The calibration curve in Fig. 6 shows the aqueous-phase data for forward extraction with the standards shown in Table 3. The best-fit line to these data has a slope of 289.49 M^{-1} and a correlation coefficient of 99.90%.

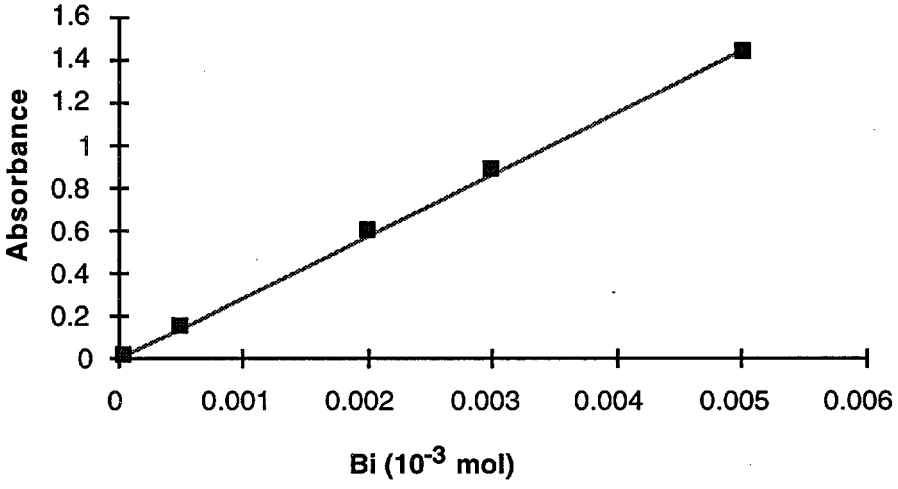

Fig. 6. Spectrophotometer Calibration Curve for Forward Extraction with Aqueous Phase

Table 3. Absorbance of Photometric Standards Used for Forward Extraction with Aqueous Phase

Sample Name	Bi, 10^{-3} mol	Absorbance
1S	0.0000501	0.021
2S	0.000501	0.158
3S	0.002004	0.598
4S	0.003006	0.89
5S	0.00501	1.43

For the forward extraction with organic samples, five standards were measured to create a calibration curve (Table 4 and Fig. 7). The organic photometric standards for this experiment included 1 mL of unequilibrated TRUEX solvent. The same calibration curve was used in quantifying the bismuth concentration for the reverse extraction with organic samples. This increased the absorbance of the solution around 450 nm, thus giving an inaccurate calibration curve. From the results of these standards, the best-fit line in Fig. 7 through the data has a slope of 272.37 M^{-1} and a correlation coefficient of 99.50%.

A new set of photometric standards was prepared for the reverse extraction with the aqueous phase. Table 5 shows the data for the reverse extraction with aqueous standards, while Fig. 8 shows the calibration curve. The best-fit line has a slope of 215.84 M^{-1} and a correlation coefficient of 100.00%.

Table 4. Absorbance of Photometric Standards Used for Forward and Reverse Extraction with Organic Phase

Sample Name	Bi, 10^{-3} mol	Absorbance
1S	0.0000501	0.024
2S	0.000501	0.145
3S	0.001503	0.368
4S	0.00501	1.521
5S	0.01002	2.71

Table 5. Absorbance of Photometric Standards Used for Reverse Extraction with Aqueous Phase

Sample Name	Bi, 10^{-3} mol	Absorbance
1S	0.0000501	0.009
2S	0.0003507	0.073
3S	0.001002	0.219
4S	0.003507	0.757
5S	0.00501	1.081

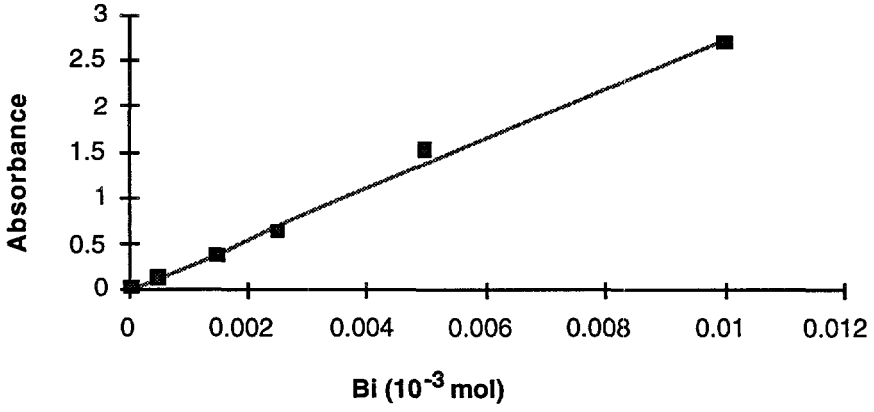

Fig. 7. Spectrophotometer Calibration Curve for Forward and Reverse Extraction with Organic Phase

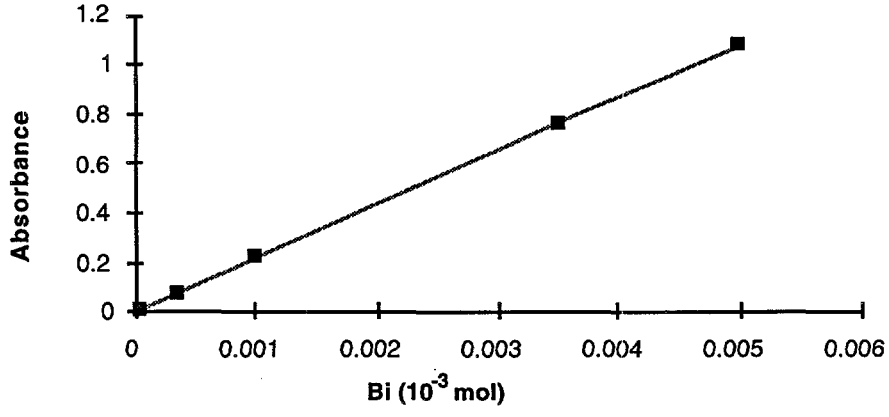

Fig. 8. Spectrophotometer Calibration Curve for Reverse Extraction with Aqueous Phase

Over the course of these experiments, the bismuth concentration of the feed solution was varied. It is important to know how this concentration affects the distribution ratio. Following the procedures for TRUEX pre-equilibration and forward extraction, aqueous samples were prepared by the potassium iodide (KI) photometric method. Two 1-mL samples of each separated phase were run through the KI method. The forward-extraction organic phases were analyzed in a similar manner, except that the isopropyl alcohol-potassium iodide (IA-KI) method was used. To analyze the organic phase, a 1-mL sample of each separated phase was run through the IA-KI method.

The D values of a given element were then calculated by dividing its concentration in the organic phase by that in the aqueous phase. Since the aqueous analysis was run in duplicate, an average of the two measurements of bismuth concentration was taken to arrive at the concentration in the aqueous phase. To check the accuracy of these data, a mass balance was done for the experiment. To obtain the mass of bismuth for either the aqueous or the organic phase, the volume of the phase used in the experiment is multiplied by the bismuth concentration of the phase.

After the forward-extraction experiment, a set of reverse extractions was performed. This was done by contacting the separated organic phases from the forward extractions with fresh aqueous solutions. As in the forward-extraction procedure, two 1-mL samples of each separated aqueous phase were run through the KI method.

The bismuth distribution ratios for the forward and reverse extractions (Exp. 4) are shown in Tables 6 and 7. Included in this table are the nitric acid concentrations and bismuth concentrations in the initial aqueous phases.

Table 6. Bismuth Distribution Ratios for Forward Extraction in Exp. 4

$[HNO_3]$, M	Initial Aq. [Bi], mM	Dist. Ratio	Mat. Bal., %
0.05	2.23	3.47	103
0.10	1.56	14.2	97.7
0.30	1.80	59.2	93.8
0.48	1.68	76.0	91.9
1.98	1.18	56.3	97.0
5.05	0.48	11.0	99.5
8.01	2.23	3.40	98.2
10.2	2.67	3.27	92.9

Table 7. Bismuth Distribution Ratios for Reverse Extraction in Exp. 4

$[HNO_3]$, M	Initial Org. [Bi], mM	Dist. Ratio	Mat. Bal., %
0.05	3.70	4.46	116
0.10	5.93	14.4	120
0.30	8.59	68.3	109
0.48	9.84	88.5	112
0.91	8.77	73.2	110
1.98	7.20	46.0	112
5.04	3.73	8.98	131
8.01	3.48	3.30	129
10.2	3.52	2.45	132

Experiment 5 was performed with exactly the same procedures that were used for Exp. 4; therefore, a complete description of the experiment is not included here. These contacts were done with aqueous phases whose nitric acid concentrations varied from 0.07 to 10.3M and whose bismuth concentrations ranged from 2.06 to 6.40 mM. Only a forward extraction was performed for this experiment. The composition of each aqueous phase is shown with its distribution ratio in Table 8.

Table 8. Bismuth Distribution Ratios for Exp. 5

$[HNO_3]$, M	Initial Aq. [Bi], mM	Dist. Ratio	Mat. Bal., %
0.07	3.56	4.91	107
0.16	2.99	28.0	103
0.30	2.88	64.9	102
0.47	2.30	89.1	101
0.91	2.06	96.7	102
1.98	2.27	53.9	101
5.05	2.67	9.98	106
8.07	5.33	3.39	107
10.3	6.40	4.40	146

Experiment 6 contacts were done with aqueous phases whose nitric acid concentrations varied from 0.05 to 9.52M and whose bismuth concentrations ranged from 0.21 to 0.29 mM. Only a forward extraction was performed for this experiment. Duplicate extractions were performed at each nitric acid concentration. The composition of each aqueous phase is shown with its distribution ratio in Table 9.

Table 9. Bismuth Distribution Ratios for Exp. 6

$[HNO_3]$, M	Initial Aq. [Bi], mM	Dist. Ratio	Mat. Bal., %
0.05	0.250	4.60	100
0.19	0.254	41.9	102
0.30	0.246	63.9	102
0.48	0.254	87.7	99.3
0.90	0.290	76.0	104
1.98	0.240	57.4	102
4.92	0.277	11.3	98.2
7.96	0.214	3.94	107
9.52	0.214	3.11	110

Experiment 7 contacts were done with aqueous phases whose nitric acid concentrations varied from 0.27 to 8.0M but whose bismuth concentration was a constant 16 mM. One forward and two reverse extractions were performed for this experiment. Duplicate extractions were performed for each nitric acid concentration. The composition of each aqueous phase is shown with its distribution ratio in Tables 10 through 12.

Experiment 8 was identical to Exp. 7 except that the aqueous phases were allowed to sit for 20 days before being contacted with the pre-equilibrated TRUEX-NPH, which also sat for 20 days. The composition of each aqueous phase is shown with its distribution ratio in Tables 13 through 15.

Table 10. Bismuth Distribution Ratios for Forward Extraction in Exp. 7

$[HNO_3]$, M	Initial Aq. [Bi], mM	Dist. Ratio	Mat. Bal., %
0.27	16.0	56.1	102
0.50	16.0	96.9	109
1.00	16.0	83.2	85.2
2.01	16.0	64.7	147
5.00	16.0	14.7	142
8.00	16.0	4.28	119

Table 11. Bismuth Distribution Ratios for First Reverse Extraction in Exp. 7

$[HNO_3]$, M	Initial Org. [Bi], mM	Dist. Ratio	Mat. Bal., %
0.30	23.8	63.3	96.7
0.48	25.8	92.1	88.8
0.91	20.0	89.8	110
1.98	34.4	76.3	98.5
5.04	30.8	11.4	76.0
8.00	21.1	3.62	80.6

Table 12. Bismuth Distribution Ratios for Second Reverse Extraction in Exp. 7

$[HNO_3]$, M	Initial Org. [Bi], mM	Dist. Ratio	Mat. Bal., %
0.30	22.3	84.6	102
0.48	22.5	103	95.6
0.91	22.6	90.5	99.4
1.98	32.8	36.7	81.7
5.04	20.7	8.14	92.2
8.00	12.0	4.20	71.3

Table 13. Bismuth Distribution Ratios for Forward Extraction in Exp. 8

$[HNO_3]$, M	Initial Aq. [Bi], mM	Dist. Ratio	Mat. Bal., %
0.27	16.0	47.4	98.7
0.50	16.0	83.4	101
1.00	16.0	76.7	94.3
2.01	16.0	37.3	96.5
8.00	16.0	2.41	94.8

Table 14. Bismuth Distribution Ratios for First Reverse Extraction in Exp. 8

$[HNO_3]$, M	Initial Org. [Bi], mM	Dist. Ratio	Mat. Bal., %
0.30	22.9	63.0	100
0.48	23.9	91.6	101
0.91	22.2	85.1	103
1.98	22.2	50.3	105
5.04	na[a]	9.93	na[a]
8.00	14.0	3.41	105

[a]A forward extraction organic sample was not analyzed at this nitric acid concentration; thus a feed concentration for bismuth and a material balance could not be calculated.

Table 15. Bismuth Distribution Ratios for Second Reverse Extraction in Exp. 8

$[HNO_3]$, M	Initial Org. [Bi], mM	Dist. Ratio	Mat. Bal., %
0.30	22.4	84.6	102
0.48	23.6	103	95.6
0.91	22.3	90.5	99.4
1.98	22.6	36.7	81.7
5.04	17.4	8.14	92.2
8.00	9.87	4.20	71.3

Figure 9 shows the D values reported in Tables 6 and 8-15. This graph shows a distinct inverted parabolic trend. The peak extraction point occurs at around 0.8M nitric acid. As the nitric acid concentration is increased from this point, we see a drop in the bismuth D value. This trend probably arises from the competition between nitric acid and bismuth for the CMPO bonding sites. At 0.05M nitric acid, the D value is about 3; as nitric acid is increased to 0.8M, the bismuth extraction efficiency increases. However, beyond the peak, an increasing nitric acid concentration causes nitric acid to extract more efficiently than bismuth; thus, the bismuth D values decrease steadily. These data will be incorporated into the GTM.

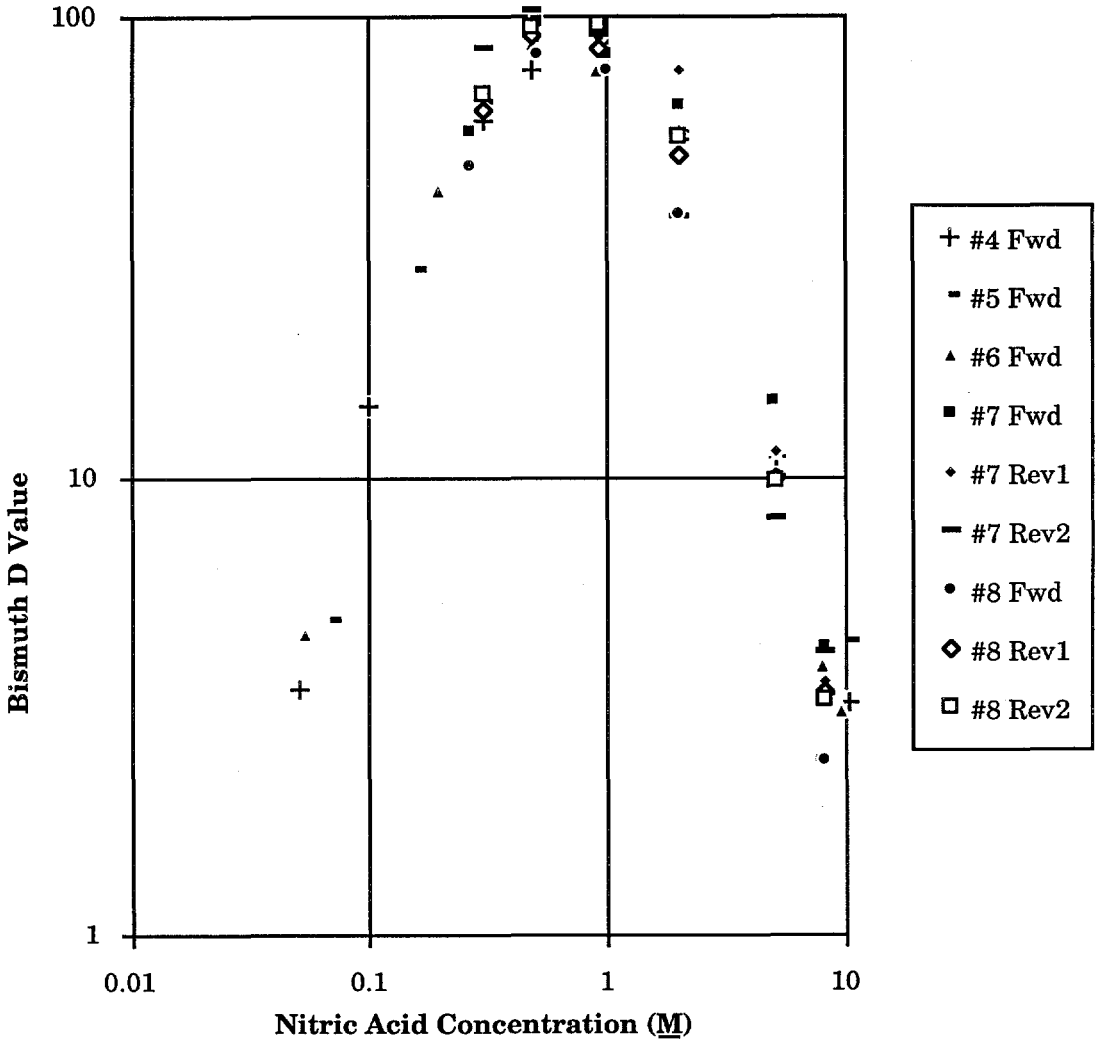

Fig. 9. Bismuth Distribution Ratios Measured with Macroscopic Bismuth Quantities Present in the Aqueous Phase

III. CENTRIFUGAL CONTACTOR DEVELOPMENT

(R. A. Leonard, D. B. Chamberlain, C. Conner, A. Philippides,
S. A. Slater, D. G. Wygmans, and G. F. Vandegrift)

The ANL centrifugal contactor is modified as necessary to work with specific solvent extraction processes. For each new process, solution densities and organic-to-aqueous (O/A) flow ratios are reviewed, and if necessary, the rotor weirs are modified. In support of our contactor development efforts, we have the capability of making vibrational measurements by using proximity probes and real-time analyzers. We can relate the results to the rotor design by using a vibrational model for rotating systems.

In our current efforts, we are using the centrifugal contactors to carry out cold and hot tests of the flowsheets developed for TRUEX-SREX and the SREX-NEPEX processes. In addition, we are analyzing data from the TRUEX processing of Mark 42 targets at Oak Ridge National Laboratory (ORNL) and building a 28-stage minicontactor for Pacific Northwest Laboratory (PNL).

A. Combined TRUEX-SREX Processing

A new solvent extraction process has been developed at Argonne that will selectively extract and partition U, Am, Pu, Sr, and Tc from Hanford dissolved sludge wastes (DSW). This process is a combination of the TRUEX process and the recently developed SREX (strontium extraction) process. In this program, we are undertaking cold and hot tests of the TRUEX-SREX flowsheet in our 2-cm multistage contactor. This work is being done in cooperation with E. P. Horwitz, M. Deitz, R. Chiarizia, and H. Diamond of the Chemistry Division (CHM) at Argonne.

The combined TRUEX-SREX solvent for this work (referred to as PS 12) consists of 0.2M CMPO, 0.2M crown ether [the specific crown ether is 4,4'(5')-di-t-butylcyclohexano-18-crown-6, referred to here as CE] and 1.2M diamyl amylphosphonate (DAAP) in Isopar L. However, as discussed below, the PS 12 solvent has proved to be less than satisfactory when used in centrifugal contactors. As a result, a new solvent, PS 15, has been developed. It consists of 0.15M CMPO, 0.15M CE, and 1.2M TBP in Isopar L. Tetrahydrofuran-2,3,4,5-tetracarboxylic acid (THFTCA) dissolved in water was being used as the stripping agent. However, we have now found that THFTCA works better when NaOH is added to form the mono sodium salt of THFTCA (called mono-sodium THFTCA or MST) and some of the di-sodium salt of THFTCA (called di-sodium THFTCA or DST). In particular, we are using 0.3M THFTCA with 0.4M NaOH, yielding 0.2M MST and 0.1M DST.

In this work, we first performed cold tests of the TRUEX-SREX process and compared the experimentally observed behavior of nitric acid with that predicted by the GTM. Based on these tests, we decided to switch from solvent PS 12 to PS 15. We then completed two tests of the TRUEX-SREX process with uranium to evaluate the use of NaOH with THFTCA as the stripping agent. We are now preparing for a hot (radioactive) test of the process flowsheet.

1. Cold Tests

The cold tests of the TRUEX-SREX process were done with a 20-stage 2-cm centrifugal contactor (minicontactor) that was set up in a vac-frame hood. These tests allowed us to check nitric acid extraction experimentally and compare it with that predicted by the GTM. As a part of the cold tests, aqueous samples were taken from the bottom of selected minicontactor stages when THFTCA was used as the stripping agent. After the cold tests, we addressed the problem of the poor

performance of the PS 12 solvent. As a result, a new solvent, PS 15, was developed and is being used for all subsequent tests of the combined TRUEX-SREX flowsheet.

a. Preparation

In preparation for the first TRUEX-SREX cold test (C1), FMI pumps (Fluid Metering, Inc., Oyster Bay, NY) were installed and calibrated for each feed stream. These low-flow positive-displacement pumps are self-priming and have generally worked well for us. They can be calibrated so that they deviate from the desired flow rate by 5% or less (1% or less of the maximum flow rate for the pump).

We had a problem with one pump, a FMI QC-20 pump drive (20 rpm) with a 3.2-mm (1/8-in.) diameter piston. This pump was started dry and was pulling water up a feed tank. When the water was only 10 cm above its level in the tank, the piston, which had been noisy, froze up and pulled out of the ball-bearing socket connecting the piston to the pump drive motor, becoming bent into an unusable shape. Possible factors contributing to the bending of the piston were (1) the small diameter of the piston, (2) the lack of liquid in the piston, (3) a long period of not using the piston, (4) the operation of the piston near its maximum stroke length, and (5) the possible presence of 2.0M $Al(NO_3)_3$, which may not have been flushed out after previous use. In a review of this problem, it was found that only the smallest FMI pistons, that is, those with 3.2-mm (1/8-in.) diameters, have bent before. Thus, we plan to use larger pistons in the future. In addition, we will clean out pumps after use, try to keep them wet between uses, and operate at 50% or less of the maximum piston stroke if the pump is dry and has not been used for a long time.

To evaluate the movement of THFTCA in the strip section of the TRUEX-SREX flowsheet for the PS 12 solvent, the distribution ratio for THFTCA (D_{THFTCA}) was correlated as a function of the molar concentration of THFTCA, [THFTCA]. Using unpublished data (M. D. Mendoza and K. L. Nash, CHM Division) as well as the results of test C3 below, the data were fit by

$$D_{THFTCA} = \frac{8}{1 + 40\,[THFTCA]} \qquad (4)$$

where a least-squares technique was used to determine the values for the two constants. The results, given in Fig. 10, show that the effect of nitric acid concentration is small.

With the model for D_{THFTCA} and the TRUEX-SREX flowsheet for test C1 (see Fig. 11), an additional strip feed containing 1.0M THFTCA was added at stage 14. The concentration profile for THFTCA in the strip section (stages 12 through 19) was then calculated by using a SASSE worksheet from the GTM (Option 6--Using SASSE Independently). For these calculations, the organic (PS 12) flow rate was 12 mL/min to stage 12. The aqueous (strip scrub) feed of 0.01M HNO_3 was 9 mL/min to stage 19. There was aqueous feed to stage 14, but none to stage 12. If the aqueous (strip) feed of 1.0M THFTCA is 3 mL/min to stage 14, most of the THFTCA will exit with the organic solvent from stage 19 as shown in Fig. 12. Thus, the carbonate wash may not be able to neutralize the THFTCA. In addition, the concentration of THFTCA in stage 12 (the first strip stage) is too low (less than 0.2M THFTCA) to be effective.

To increase the THFTCA in stage 12, the 1.0M THFTCA feed was moved from stage 14 to stage 12, and its flow rate was increased from 3 to 7 mL/min. With these changes, we

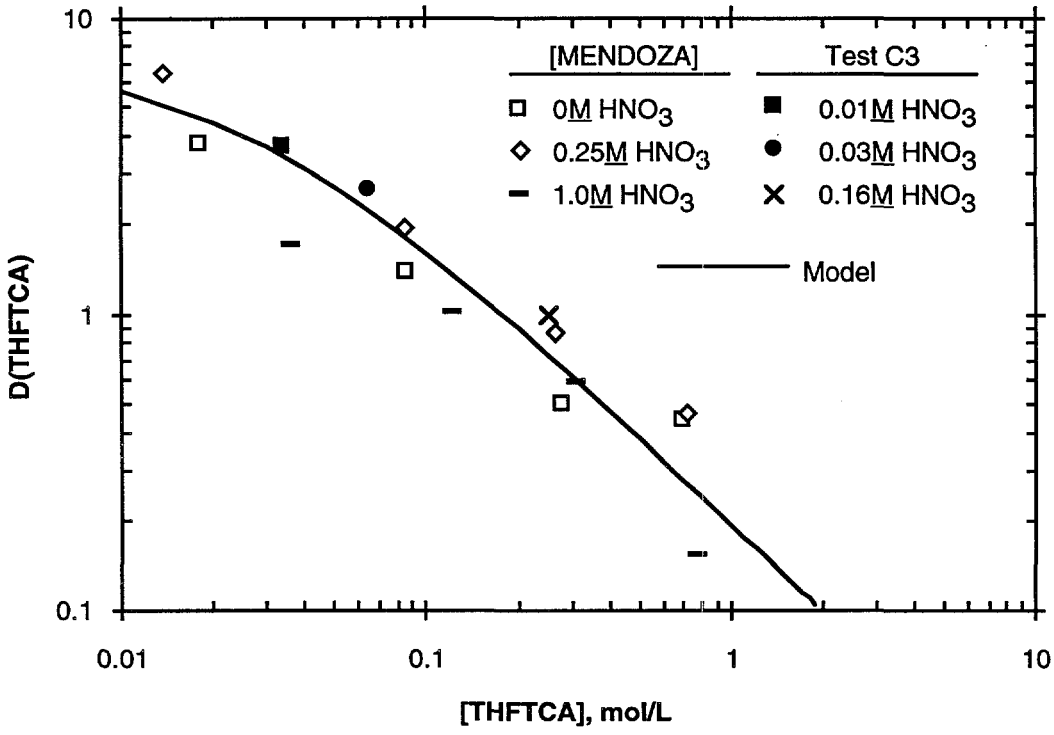

Fig. 10. Effect of the Concentration of THFTCA and Nitric Acid on the Distribution Ratio for THFTCA with Solvent PS 12. The data labeled [MENDOZA] is from Mendoza and Nash, CHM Division.

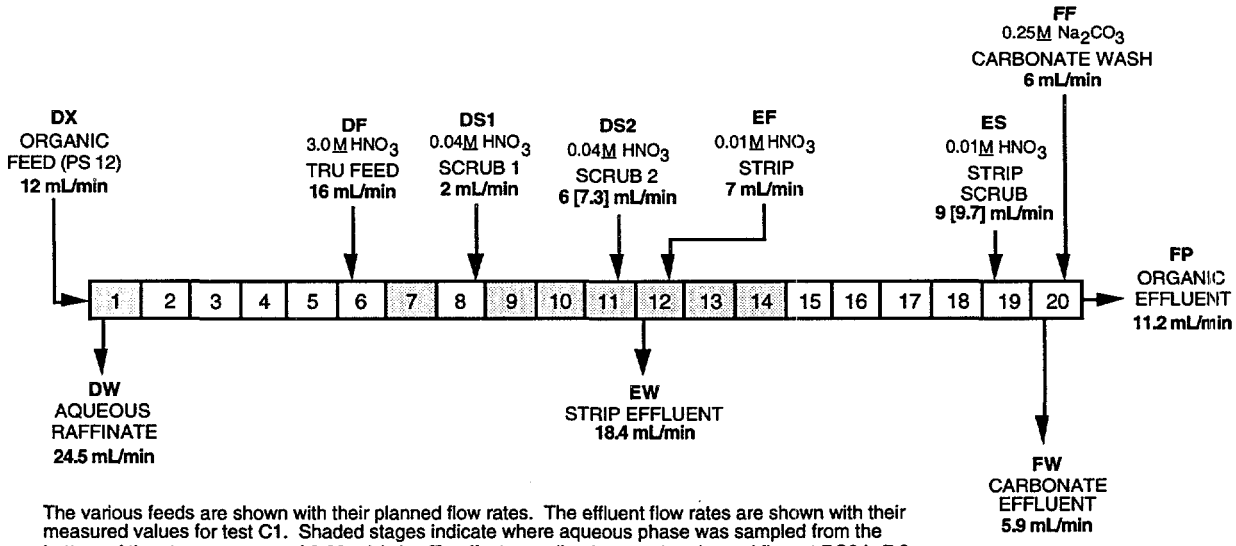

The various feeds are shown with their planned flow rates. The effluent flow rates are shown with their measured values for test C1. Shaded stages indicate where aqueous phase was sampled from the bottom of the stage at a rate of 0.33 mL/min. To offset sampling losses, the planned flow at DS2 is 7.3 rather than 6.0 mL/min; at EF, 4.0 rather than 3.0 mL/min. Numbers in [ ] show planned flow in mL/min to accommodate stage sampling.

Fig. 11. Schematic for Test C1 of the TRUEX-SREX Flowsheet with Nitric Acid and Sodium Carbonate

obtained the required aqueous phase concentration, 0.2M THFTCA, in stage 12 as shown in Fig. 13. However, the concentration of THFTCA being carried by the solvent from stage 19 into the carbonate wash section (stage 20) is slightly higher than before.

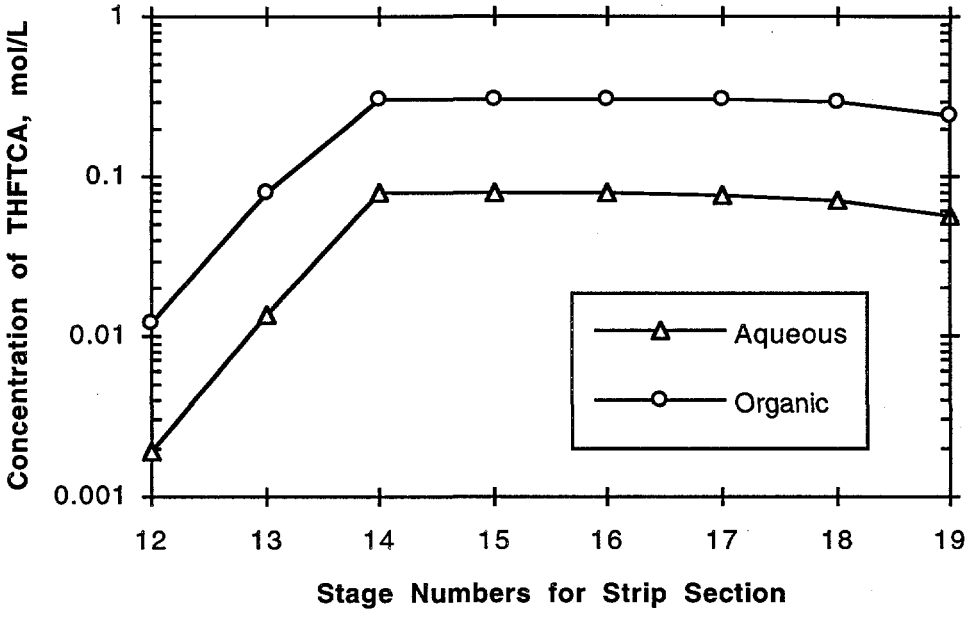

Fig. 12. Concentration Profile of THFTCA in the Strip Section with 1.0M THFTCA Feed to Stage 14 at 3 mL/min

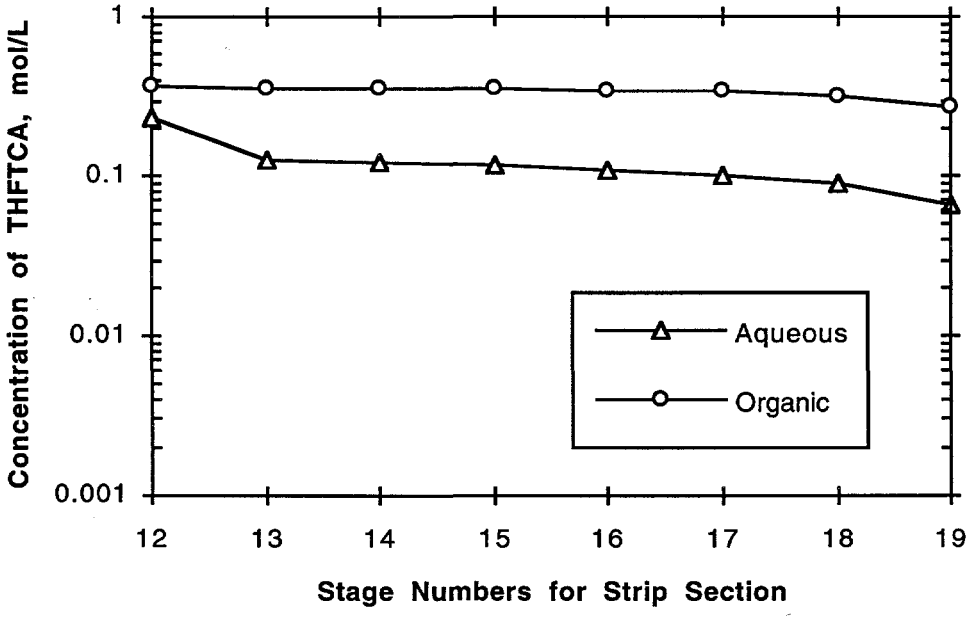

Fig. 13. Concentration Profile of THFTCA in the Strip Section with 1.0M THFTCA Feed to Stage 12 at 7 mL/min

As a result of this analysis of the THFTCA profile, the THFTCA feed (EF in Fig. 11) was moved from stage 14 to stage 12, and its flow was increased to 7 mL/min. This is the basis for the flowsheet shown in Fig. 11. Note that, for test C1, the EF feed contains only 0.01M HNO_3. Thus, the HNO_3 concentration in the strip (EW) effluent could be measured easily.

A question raised by this analysis is whether or not too much THFTCA is going to the carbonate wash section. Will the 0.25M Na_2CO_3 feed at 6 mL/min be able to strip the THFTCA from the PS 12 solvent with a feed rate of 12 mL/min? The results, given below for test C3, suggest that the Na_2CO_3 flow rate may need to be doubled.

In tests C1 and C2, aqueous phase was sampled from the bottom of eight stages at the rate of 0.33 mL/min. The stages sampled are the shaded stages in Fig. 11. To offset these sampling losses, the various feed flow rates were increased as appropriate.

b. Test C1

The first cold test, C1, was run on the morning of November 17, 1993, following the flowsheet shown in Fig. 11. This test used only nitric acid in the various aqueous feeds for the first 19 stages so that we could generate a good concentration profile for nitric acid. These values were then compared with calculated values from the GTM. This work checks the ability of the GTM to calculate the acid profile accurately. The ability of the GTM to do this is very important because distribution ratios for most of the other components strongly depend on the nitric acid concentration. This check was also important because it was the first test of the GTM with the crown ether as one of the extractants in the solvent.

Sodium carbonate was used in the aqueous feed to stage 20, the carbonate wash section. The PS 12 solvent, which was a light yellow color in the feed tank, was observed to turn orange in the sodium carbonate wash stage. After the test, when the solvent was subjected to an acid rinse with 0.1M HNO_3 in a separatory funnel, the solvent turned a dirty green. This solvent was used as the organic (DX) feed for test C2. The planned feed flow rates are shown in Fig. 11 along with the measured effluent flow rates. The hydraulic performance of the contactor during test C1 was good, with no significant other-phase carryover in any effluent.

The bottom sampling system proved to be of limited value because, for some stages, organic phase was drawn into the Viton tubing that made up the sampling lines. When this happened, the tubing, which had an inside diameter of only 0.8 mm so that sampling system volume was minimized, became sticky and swelled. Eventually, it closed up so that no more sample could be drawn through. In addition, our experience with setting up the tubing in the Masterflex three-roller cartridge pump head (Cole-Parmer Instrument Co., Niles, IL) shows that it would be difficult to use in a glovebox and almost impossible to use in a shielded cell facility. In spite of these problems, at the end of the run we were still observing aqueous liquid from each stage sampled except for stages 13 and 14.

(1) Titration Results for Nitric Acid Concentration

The aqueous effluents and stage samples from test C1 were titrated using a Metrohm 670 Titroprocessor. Sodium hydroxide (0.0983M) was the base used as the titrant. Titration volumes of the samples were chosen such that 20 to 80% of the 10-mL burette volume was used during the titration. The results, given in Table 16, are identified by stage number, sampling location (sample taken from effluent port or from the bottom of the stage at 0.33 mL/min), the time

into the test when sampling started (time zero was when the organic flow was started after all aqueous flows were established), and the time interval over which the sample was collected. Note that the HNO_3 concentration in the DW effluent (stage 1) increased with time at first. After 30 min into the run, the HNO_3 concentration in this effluent had reached an average value of 1.92M and slowly fluctuated between 1.87 and 1.95M. The HNO_3 concentration in the EW effluent (stage 12) also increased with time at first. After 30 min into the run, the HNO_3 concentration in this effluent had reached an average value of 0.050M and slowly fluctuated between 0.047 and 0.053M. The bottom samples from stage 1 initially follow the same pattern as the effluent samples. However, the high concentration of HNO_3 in the last bottom sample is much higher than we expected from the other results. The bottom samples from stage 12 follow the same pattern as the EW effluent samples, although the last three samples are higher in acid concentration than we expected from the corresponding EW effluent results. (Note that, for the bottom samples, there is a 3-min residence time in the sampling line.)

Table 16. Titration Results from TRUEX-SREX Cold Test C1

Stage Number	Sampling Location	Time into Test When Start Sampling, min	Time over Which Sample Collected, min	Avg. HNO_3 Conc., M
1	Bottom	10	10	1.324
		20	10	1.783
		30	10	1.987
		40	10	2.082
		50	10	2.184
		60	10	2.795
	Effluent (DW)	12	0.2	1.362
		17	0.2	1.704
		22	0.2	1.817
		27	0.2	1.869
		32	0.2	1.916
		37	0.2	1.951
		42	0.2	1.935
		47	0.2	1.926
		52	0.2	1.900
		54	2.0	1.874
		57	0.2	1.895
		62	0.2	1.929
		67	0.2	1.904
7	Bottom	10	10	0.561
		20	10	1.153
		30	10	1.287
		40	10	1.306
		50	10	1.322
		60	10	1.313
9	Bottom	10	10	0.107
		20	10	0.390
		30	10	0.500
		40	10	0.550
		50	10	0.568
		60	10	0.566
10	Bottom	10	10	0.055
		20	10	0.215
		30	10	0.267
		40	10	0.307
		50	10	0.314
		60	10	0.310

(contd)

Table 16. (contd)

Stage Number	Sampling Location	Time into Test When Start Sampling, min	Time over Which Sample Collected, min	Avg. HNO_3 Conc., M
11	Bottom	10	10	0.047
		20	10	0.151
		30	10	0.200
		40	10	0.258
		50	10	0.241
		60	10	0.244
12	Bottom	10	10	0.010
		20	10	0.028
		30	10	0.046
		40	10	0.055
		50	10	0.069
		60	10	0.055
	Effluent (EW)	13	0.3	0.012
		18	0.3	0.020
		23	0.3	0.034
		28	0.3	0.042
		33	0.3	0.048
		38	0.3	0.050
		43	0.3	0.047
		48	0.3	0.052
		53	0.3	0.054
		58	0.3	0.053
		63	0.3	0.049
		64	2.0	0.051
		68	0.3	0.050

The variations in the HNO_3 concentration coming from the DW and EW effluents may be the result of the erratic flow (cyclic intermittent slugs of liquid) observed in some aqueous-phase interstage lines. This behavior may also cause some degradation in the stage efficiency of the 2-cm contactor. Such a loss in stage efficiency would disappear in larger contactors, that is, 4-cm and larger, where interstage flow is continuous.

(2) Modeling of Nitric Acid Concentration

In Fig. 14 the titration results given in Table 16 are compared with GTM model calculations for extraction efficiencies (E_a) of 0.8, 0.9, and 1.0 (80, 90, and 100%). The GTM model used the "DAAP" option and followed the TRUEX-SREX flowsheet shown in Fig. 11. This comparison indicates that the extraction efficiency in the minicontactors is high, close to 100%.

As noted above, we had expected that the erratic flow observed in the aqueous-phase interstage lines would cause some degradation in E_a for the minicontactor (2-cm contactor). However, the results in Fig. 14 indicate that stage efficiency was essentially 100%.

c. Test C2

The second cold test, C2, was run on the afternoon of November 17, 1993, following the TRUEX-SREX flowsheet shown in Fig. 15, with some metals and oxalic acid. As noted above, the organic (DX) feed was the organic effluent from test C1 that had been rinsed with 0.1M nitric acid. The liquids in the stages had not been drained; instead, they were kept in place so

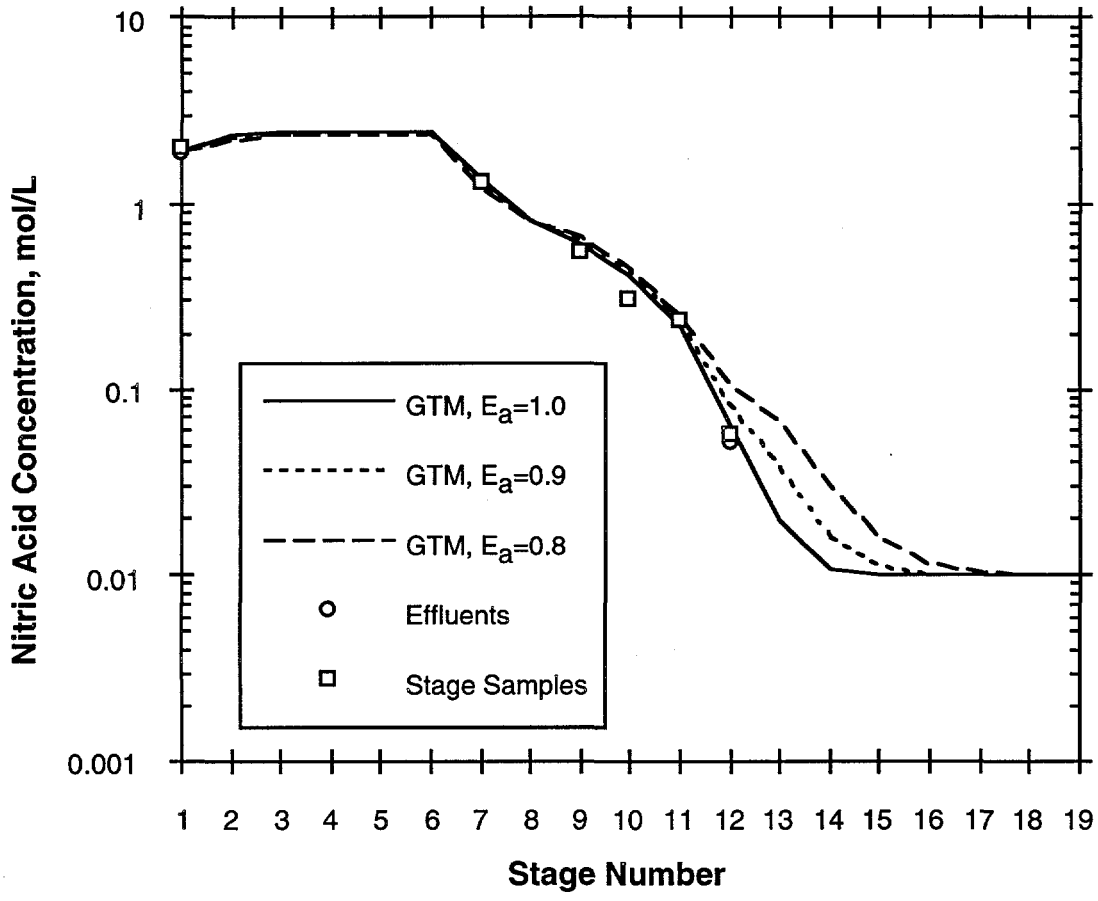

Fig. 14. Measured and Calculated Concentration Profile of HNO_3 for Test C1

that test C2 could be started up quickly. For this test, iron, samarium, and oxalic acid were added to the nitric acid in the DF feed. To keep the oxalate ion out of the strip, 2.0M aluminum nitrate was used as the DS1 feed. Later in the run we had planned to switch the EF feed to 1.0M THFTCA. However, because of poor hydraulic performance (0 to 6% O in A phase for the DW effluent and 13 to 18% O in A phase for the EW effluent), we never switched the EF feed from 0.01M HNO_3 to 1.0M THFTCA. Instead, we cut off the DX flow for 10 min, from 23 to 33 min into the test, trying to establish good (aqueous continuous) conditions. Then, the test was continued for another 37 min until the DX feed was processed. During this time, we continued to find significant other-phase carryover in two of the four effluents.

As before, 0.25M sodium carbonate was used as the aqueous feed to stage 20, the carbonate wash section. The PS 12 solvent, which was now a dark green in the feed tank, was again observed to turn orange in the sodium carbonate wash stage. After the test, when the solvent was subjected to an acid rinse with 0.1M HNO_3 in a separatory funnel, the solvent again turned a dirty green. This rinsed solvent was used as the organic (DX) feed for test C3.

The planned feed flow rates are shown in Fig. 15 along with the effluent flow rates measured during the last 15 min of the test. The other-phase carryover for the DW effluent was initially zero. It gradually built up over the course of the test to the 6% value deductible from Fig. 15. The other-phase carryover for the EW effluent fluctuated between 13 and 18% throughout the test, including the final 14% value deductible from Fig. 15. The aqueous FW effluent had no other-phase

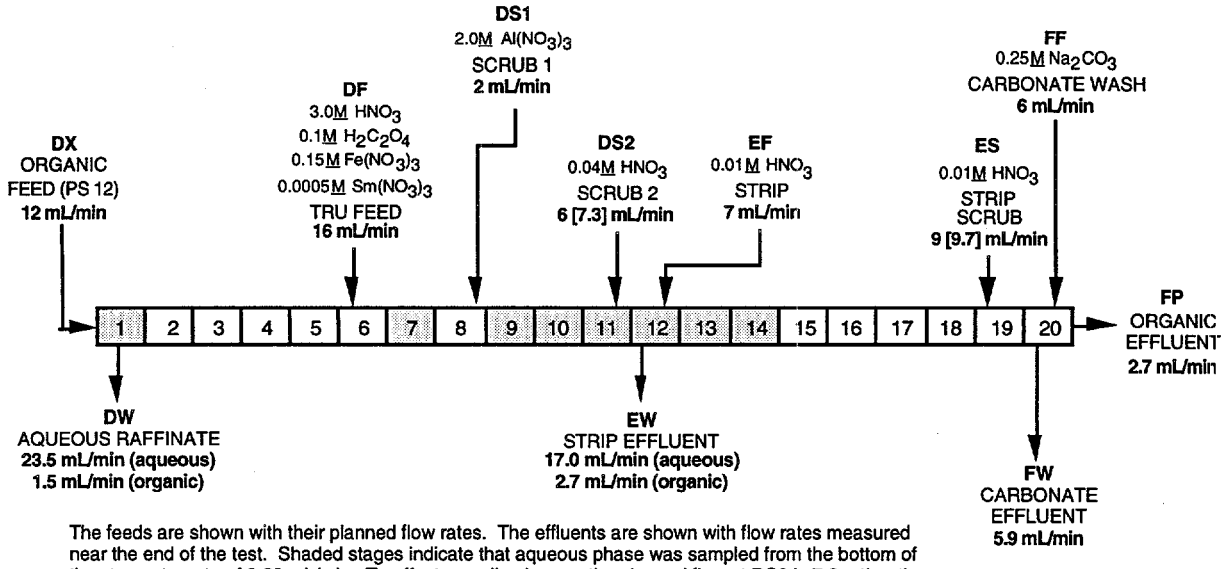

The feeds are shown with their planned flow rates. The effluents are shown with flow rates measured near the end of the test. Shaded stages indicate that aqueous phase was sampled from the bottom of the stage at a rate of 0.33 mL/min. To offset sampling losses, the planned flow at DS2 is 7.3 rather than 6.0 mL/min; at EF, 4.0 rather than 3.0 mL/min. Numbers in [ ] show the planned total flow in mL/min to accommodate stage sampling.

Fig. 15. Schematic for Test C2 of the TRUEX-SREX Flowsheet with Some Metals and Oxalic Acid

carryover and kept a fairly constant flow rate, 5.7 ± 0.2 mL/min. While the organic FP effluent had no other-phase carryover, it never reached its expected value of 12 mL/min. At 20 min into the test, just before the DX flow was turned off, the flow rate of FP effluent was 5.5 mL/min; at 40 min, just after the DX flow was restarted, its flow rate was 3.7 mL/min; and at 60 min, its flow rate was only 2.7 mL/min. Thus, at the end of the test, the organic flow was not at steady state: 12 mL/min of feed was entering while, as can be deduced from Fig. 12, only 6.9 mL/min (all organic effluents) was exiting. The bottom sampling system continued to deteriorate during this test. By the end of test C2, aqueous samples were emerging only from the bottom of stages 1, 7, and 12.

(1) Titration Results for Nitric Acid Concentration

The aqueous effluent and stage samples from test C2 were titrated for nitric acid, just like the test C1 samples. The results, given in Table 17, are identified by stage number, sampling location (sample taken from effluent port or from the bottom of the stage at 0.33 mL/min), the time into the test when sampling started (time zero was when the organic flow was started after all aqueous flows were established), and the time interval over which the sample was collected. Note that the nitric acid concentration for the effluent samples is somewhat higher than that of the bottom samples in both stage 1 and stage 12, the opposite of the results for test C1.

(2) GTM Modeling of Nitric Acid and Metal Concentrations

Assuming that the contactor was fairly close to steady-state operation in the last 10 to 20 min of the test, the nitric acid data were compared with the concentration profile for HNO_3 at extraction efficiencies of 0.8, 0.9, and 1.0 (80, 90, and 100%). The results of this comparison, shown in Fig. 16, again indicate that the extraction efficiency in the minicontactors is high, 80 to 100%. The GTM model used the "DAAP" option and followed the TRUEX-SREX flowsheet for the C2 test (Fig. 15). The model included the 0.3-mL/min sampling flow rates at the bottom of eight stages (1, 7, and 9-14) as well as 15% O in A phase throughout the strip section,

Table 17. Titration Results for TRUEX-SREX Cold Test C2

Stage Number	Sampling Location	Time into Test When Start Sampling, min	Time over Which Sample Collected, min	Avg. HNO_3 Conc., M
1	Bottom	50	10	2.484
		60	10	2.534
	Effluent (DW)	52	0.2	2.630
		54	2.0	2.568
		57	0.2	2.640
		62	0.2	2.621
		67	0.2	2.794
7	Bottom	50	10	1.128
		60	10	1.313
12	Bottom	50	10	0.101
		60	10	0.110
	Effluent (EW)	53	0.3	0.125
		58	0.3	0.144
		63	0.3	0.136
		64	2.0	0.160
		68	0.3	0.176

stages 12-19. The apparent high nitric acid concentration at stage 1 was expected; it was caused by the metal ions in the DW effluent, which interfere in the titration. Based on our measurements of nitric acid in the DF feed, which also contained the metal ions, we had expected the measured nitric acid concentration to be about 0.5 to 0.7M higher than was actually present.

At the end of test C2, the measured concentrations of Fe, Al, and Sm in the aqueous (EW) effluent from the strip section were as shown in Table 18 (see the results in the "ICP" column). Essentially all of the samarium is extracted in the EW effluent. Thus, the extraction efficiency in the minicontactors was adjusted in the GTM until its value agreed with the measured (ICP) value. The calculated results summarized in Table 18 show that the best estimate for extraction (stage) efficiency is 90%. However, since the stated error for the ICP values is ±10%, the extraction efficiency could be anywhere between 80 and 100%.

Essentially all of the aluminum appears in the aqueous (DW) effluent from the extraction section. Thus, higher-than-expected concentrations in EW can be attributed to other-phase carryover in the scrub section. As shown in Table 18, the GTM calculations indicate that an average other-phase carryover of 3.8% in the scrub section, including the DF feed stage (stages 6 through 11), would yield the observed EW value for aluminum with 90% extraction efficiency in all contactor stages. Based on the observed values for other-phase carryover in the DW and EW effluents, other-phase carryover of 3.8% seems very reasonable.

Analyzing the iron concentration in the EW effluent in a similar fashion, one would predict 24.6% other-phase carryover in the scrub section, including the DF feed stage. This value for other-phase carryover appears to be too high. Instead, the differences between the measured and calculated values for the iron concentration in EW effluent are thought to reflect the difficulty in modeling iron extraction. This difficulty arises because the distribution ratio for iron is time dependent.

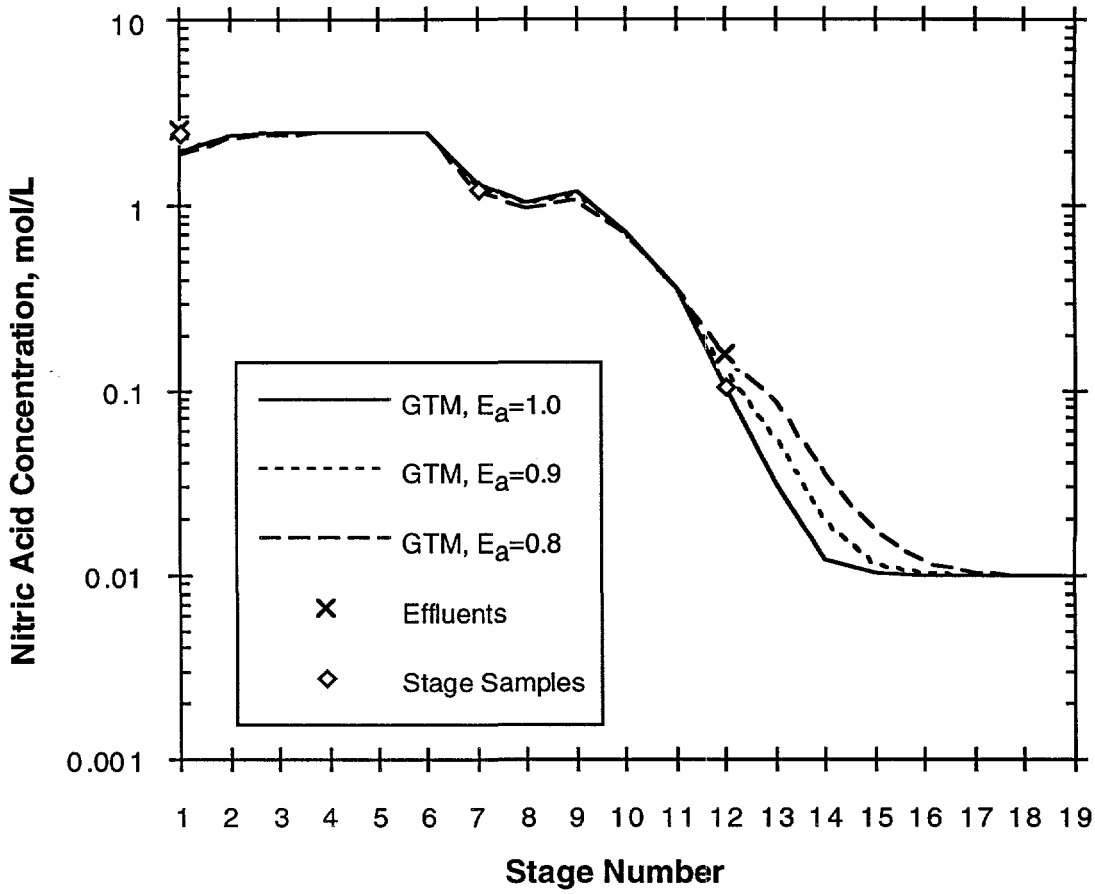

Fig. 16. Calculated and Measured Concentration Profile of HNO_3 for Test C2

Table 18. Measured and Calculated Metal Ion Concentrations in the Aqueous (EW) Effluent from Strip Section

	Metal Ion	Component Conc., M					
Source		ICP[a]	GTM	GTM	GTM	GTM	GTM
Extraction Efficiency, %		Actual	100	90	80	90	90
Other-Phase Carryover, %		Actual	0.5	0.5	0.5	3.8[b]	24.6[b]
	Fe	3.1E-03	1.6E-07	7.9E-05	1.3E-04	1.8E-04	3.1E-03
	Al	4.2E-05	5.4E-09	3.1E-06	2.1E-05	4.2E-05	1.3E-02
	Sm	3.6E-04	3.9E-04	3.6E-04	3.4E-04	3.6E-04	3.1E-04

[a]Analysis by inductively coupled plasma-atomic emission spectrometry.
[b]This increased value for other-phase carryover was used in stages 6 through 11.

Further tests (Sec. III.A.1.e and f) were made to determine the reason for the poor hydraulic performance observed during test C2 and to determine whether the PS 12 solvent is a viable process solvent. Before this was done, a batch test of the strip and carbonate wash sections (test C3) was carried out so that the extraction and stripping behavior of THFTCA in those two sections could be determined.

d. Test C3

The third cold test, C3, was done so that we could estimate how much THFTCA will appear in the carbonate wash and how well the carbonate wash will be able to scrub it out. This test consisted of seven batch contacts carried out in a 1-L separatory funnel, using 200 mL of the PS 12 solvent. The solvent, which had been used for tests C1 and C2, was pre-equilibrated for test C3 by contacting with 3M HNO_3 and then with 0.5M HNO_3. Aqueous feed concentrations and volumes, shown in Fig. 17, were chosen to give the approximate concentrations in the strip and carbonate wash sections for the flowsheet shown in Fig. 15. These are the two sections where THFTCA will be present.

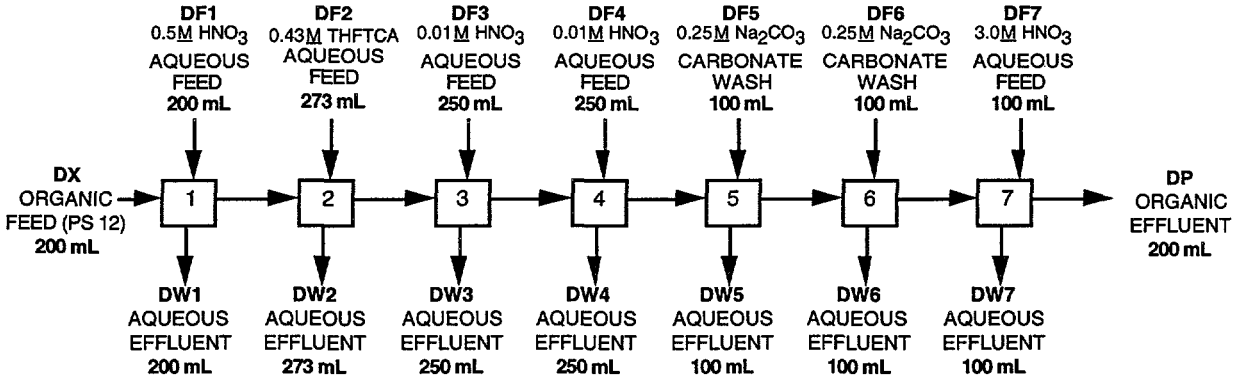

Fig. 17. Schematic for Test C3 of THFTCA Strip for TRUEX-SREX Flowsheet by Seven Batch Contacts of PS 12 Solvent

The results for test C3 are listed in Table 19. They include aqueous concentration of HNO_3 and THFTCA after each contact measured by titration, the O/A volume ratio, and the solvent color. This table also includes the THFTCA concentration in the organic phase calculated by material balance and the D_{THFTCA} values obtained from these THFTCA concentrations. The D_{THFTCA} results are plotted in Fig. 10 along with earlier results from Mendoza and Nash (CHM Division). The two sets of results agree fairly well.

The ability of Na_2CO_3 to neutralize or at least strip out the THFTCA that is carried into the carbonate wash section is indicated indirectly by the color of the solvent: Its turning orange suggests that it has been neutralized by the Na_2CO_3, and that consequently, the THFTCA has been removed. On this basis, it appears that the solvent was stripped of THFTCA after two contacts at an O/A volume ratio of 2.0. For a centrifugal contactor, two carbonate wash stages with an O/A flow ratio of 1.0 will be even more effective than the two-contact batch strip of test C3, because of the additional benefit from countercurrent operation.

In actual practice, enough Na_2CO_3 must remain after THFTCA neutralization to strip out those other components (e.g., U and Pu) that the Na_2CO_3 is supposed to remove. No work has been done to define how much Na_2CO_3 has to be available. However, from the amount of THFTCA found in the carbonate wash with the solvent, it appears that only one of the four acid groups in the THFTCA has to be neutralized by the Na_2CO_3 for the THFTCA to be stripped out of the solvent.

Table 19. Summary of Test C3

Contact Number	O/A Volume Ratio	Measured Aq. HNO_3 Conc. after Equil., M	Measured Aq. THFTCA Conc. after Equil., M	Calc. Org. THFTCA Conc. after Equil.,[a] M	D_{THFTCA}	Solvent Color	Notes
1	1.00	0.527	—	—	—	Green	
2	0.73	0.161	0.251	0.248	0.99	Green	
3	0.81	0.030	0.640	0.169	2.64	Green	
4	0.80	NM[b]	0.345	0.126	3.64	Green	
5	1.96	NM[b]	NM[b]	—	—	Yel. green	Carbonate Wash
6	2.00	0.011	NM[b]	—	—	Orange	Carbonate Wash
7	1.96	1.390	NM[b]	—	—	Dark green	

[a]Based on material balance for the THFTCA.
[b]Not measurable.

e. Test C4

The fourth cold test, C4, was run to explore the hydraulic performance of the PS 12 solvent with the full cold test, including use of THFTCA, oxalic acid, $Al(NO_3)_3$, and, at 31 min into the test, the metal ions in the DW feed. The flowsheet used for this test is shown in Fig. 18. The test was started with the introduction of the aqueous phases. Solvent flow was not introduced until the aqueous flow was fully established in all stages. The timing for the test was set to zero when the solvent flow was started. Eighteen minutes later, the solvent started exiting from stage 20.

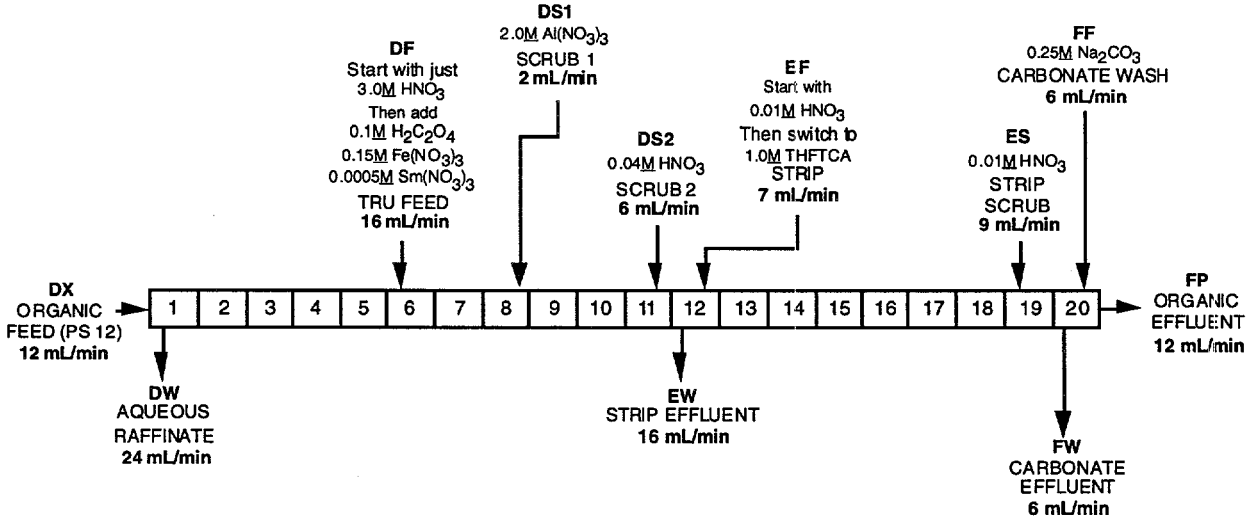

Fig. 18. Schematic of Test C4 of the TRUEX-SREX Flowsheet

A problem developed during test C4 that caused us to terminate it early. At 50 min into the test, we discovered that the rotors in stages 1 through 8 were not turning because the motor for stage 2 had tripped the ground fault circuit interrupter (GFCI), cutting the power to the first eight stages. The stage 2 motor was then given its own electrical outlet, but it continued to trip the GFCI. Because this motor could not be made to work, the test was terminated 54 min after it started.

After the test, the stages were drained. Then, the stage 2 motor was checked again and found to be functioning properly. In the future, the need for GFCI devices in the electrical lines supplying the contactor motors and pumps will be given a critical review. In addition, a running light will be put on the motor junction box of each new contactor stage that is built. Because the minicontactor motors are so quiet, we cannot always hear if one or more shut down. However, we will be able to see if a motor's running lights are off and so be immediately apprised of a problem.

Notes made during the test indicate that the GFCI was tripped at 23 min into the test, shutting down the first eight contactor stages. Thus, observations made before this time can be used to evaluate the hydraulic performance of the PS 12 solvent. At 15 min into the test, no organics were in the aqueous DW effluent. At 20 min into the test, 8% organics were in the aqueous EW effluent. Thus, before the first eight stages shut down, the hydraulic performance for test C4 was much like that for test C2. Consequently, the poor hydraulic performance of the PS 12 solvent in test C2 was not simply the result of having both phases in each stage at startup.

f. Test C5

The fifth cold test, C5, was run to evaluate further the GFCI problem, as well as the hydraulic performance of the PS 12 solvent. The flowsheet used for this test, shown in Fig. 19, consisted of the six stages of the extraction section for the cold TRUEX-SREX flowsheet. The aqueous DF feed was the DW raffinate from test C1. The organic DX feed was the PS 12 solvent used in tests C1 through C4. This solvent was a very dark green.

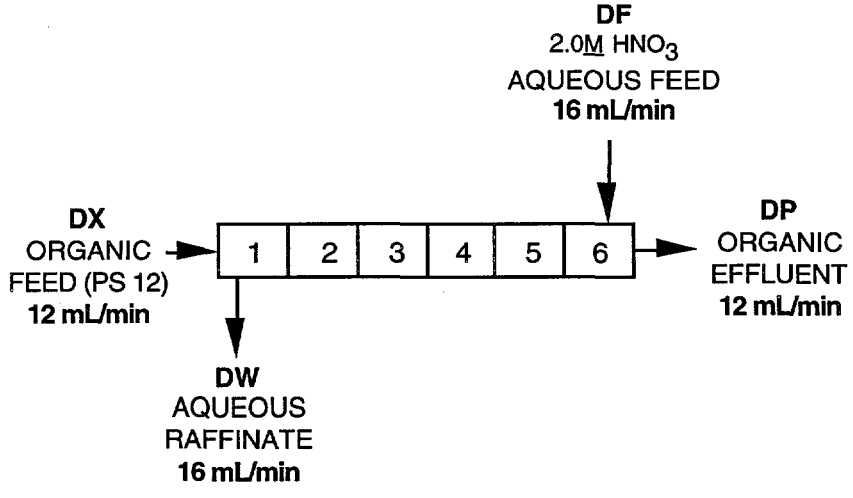

Fig. 19. Schematic for Test C5 of Extraction Section of TRUEX-SREX Flowsheet

The GFCI problem did not reappear during this test. Initially, the liquid level in the interstage lines was erratic, and significant other-phase carryover was noted in both effluents. However, by 16 min into the test, no aqueous phase was found in the organic DP effluent. At 29 min into the test, 11% organic phase was still in the aqueous DW raffinate; at 49 min, this amount had dropped to 6%. At 50 min into the test, the erratic levels in the interstage lines had more or less disappeared. Thus, the poor hydraulic performance for the PS 12 solvent that was seen earlier for tests C2 and C4 was seen again in test C5.

g. Summary of Cold Test Results

The results for the hydraulic performance of the minicontactor during tests C1 through C5 are summarized in Table 20. The hydraulic performance, which was good for the C1 test, was not satisfactory for subsequent tests. For the C1 test, the PS 12 solvent was light yellow. For the subsequent tests, its color was dark green in contact with acid solutions and orange in contact with basic solutions (0.25M Na_2CO_3). The FW and FP effluents always had less than 1% other-phase carryover, and thus, are not shown in Table 20. Based on these tests, the PS 12 solvent has been rejected as unsatisfactory because of the deterioration of its hydraulic performance with use.

Table 20. Summary of Hydraulic Performance for Cold Tests

	Organics in Aqueous,[a] %		
Test	DW	EW	Notes
C1	<1	<1	
C2	0	18	
	0.6	13	
	2.5	15	
	6	14	
C3	N/A	N/A	b
C4	0	8	c
C5	11	N/A	d
	6	—	

[a]Less than 1% other-phase carryover is considered satisfactory hydraulic performance.
[b]Not applicable (N/A) as minicontactor was not used.
[c]Results shown were obtained before problems developed, that is, during the first 23 min of the test.
[d]No EW effluent, as only the six-stage extraction section was tested.

Based on test C4, we decided to put a running light on the junction box for each motor of each new contactor stage to make it easy to assess whether or not each motor has power. It will not, of course, indicate whether the contactor rotor is actually turning. If the rotor is turning and the hydraulic performance is good, the liquid level in the mixing zone of the stage will be low.

2. Solvent Evaluation

a. Dispersion Number Tests

Based on cold tests C1 through C5, it appeared that significant deterioration had occurred in the hydraulic performance of the PS 12 with time and use. To confirm this, the density, viscosity, and dispersion number (N_{Di}) were measured again for the PS 12 solvent. (The procedure used to measure N_{Di} is described elsewhere.[2]) These results, summarized in Table 21, show that the density was about the same, the viscosity was increased by 14%, the dispersion number for 0.1M HNO_3 was significantly less (about three times lower while the A in O phase increased), and the dispersion number for 0.25M Na_2CO_3 was essentially unchanged. Thus, the dispersion number for 0.1M HNO_3 appears to give the best indication of solvent deterioration.

Table 21. Solvent Properties[a]

	PS 12				PS 15
Date	10/92	6/93	8/93	12/93-1/94	12/93-1/94
Condition	new	new	new	used	new
Density, g/L	865	866	866	867	859
Viscosity, mPa•s	5.4	5.2	5.3	6.0	3.3
0.1M HNO_3:					
$N_{Di}x10^4$	4.5	2.9	—	1.38	6.0
Max A in O, %	1.0	1.6	—	3.6	1.4
Avg. A in O, %	0.9	1.0	—	3.6	1.4
0.25M Na_2CO_3:					
$N_{Di}x10^4$	8.3	2.6	—	4.8	11.4
Max A in O, %	6	2	—	1.4	1.6
Avg. A in O, %	6	2	—	1.4	1.6
3.0M HNO_3:					
$N_{Di}x10^4$	—	—	—	4.7	6.7
Max A in O, %	—	—	—	4.0	2.2
Avg. A in O, %	—	—	—	2.7	2.0
3.0M HNO_3:[b]					
$N_{Di}x10^4$	—	—	—	15	17
Max A in O, %	—	—	—	2.1	0.8
Avg. A in O, %	—	—	—	1.5	0.8

[a]Conditions: O/A=1.0; aqueous phase is dispersed phase except as noted; room temperature (24 ± 2°C).
[b]Organic phase is dispersed.

A new solvent, PS 15, was developed by E. P. Horwitz et al. (ANL Chemistry Division) to give better hydraulic performance while keeping the important extraction properties of the solvent. This solvent, which uses 25% less of both extractants and replaces DAAP with TBP, consists of 0.15M CE, 0.15M CMPO, 1.2M TBP, and the rest Isopar L. The properties of this solvent, which are included on Table 21, show that it is better than fresh PS 12 solvent. In addition, if the replacement of DAAP by TBP solves the problem of degradation with time and use, then the long-term characteristics for PS 15 should be better as well.

The desired solvent characteristic, the one used in the design of the centrifugal contactor, is that the solvent have an N_{Di} of 8×10^{-4} or greater with less than 1% other-phase carryover. None of the solvents in Table 21 meets these criteria. However, the PS 15 solvent is closer to the desired solvent characteristic than the PS 12 solvent. The viscosity for PS 15 is only 60% that of PS 12. This may be a major reason why the hydraulic performance of PS 15 is better than that for PS 12.

Information on N_{Di} for 3M HNO_3 was obtained for the used PS 12 solvent as well as the fresh PS 15 solvent. These data, which are included in Table 21, show that the used PS 12 solvent works significantly better at higher acid concentrations. This may be why we had higher other-phase carryover for the EW effluent relative to the DW effluent. When the viscous organic phase is the dispersed phase, both solvents give better (higher) N_{Di} values. However, based on past experience with 30% TBP in normal dodecane, we expect the centrifugal contactor to operate with the aqueous phase as the dispersed phase, except at low O/A flow ratios.

b. Hydraulic Performance Tests

To determine hydraulic performance, the maximum throughput (both phases) was measured for both PS 12 and PS 15 in a one-stage minicontactor test. The tests were done at an O/A flow ratio of 1.0 using 0.1M HNO_3 for the aqueous phase. The results, given in Table 22, show that PS 12 performance is very dependent on which phase is the initial continuous phase, while PS 15 performance is not. In addition, the maximum throughput for initial-organic-continuous operation is 25% lower for PS 12 after the five cold tests. The maximum throughput for initial-organic-continuous operation for PS 15 is 50% higher than that for PS 12, even when the PS 12 was fresh. Thus, this hydraulic performance test also confirms that the PS 15 solvent is better than the PS 12 solvent.

Table 22. Maximum Throughput for Two Solvents in a Minicontactor with 0.1M HNO_3 at an O/A Flow Ratio of 1.0

Solvent	Date	Initial Cont. Phase	Max. Throughput (both phases), mL/min	Mode of Failure
PS 12	9/93 (Before cold tests)	A	86 ± 5	>1% A in O
		O	41 ± 5	>1% both phases
	2/94 (After cold tests)	A	104 ± 4	>1% A in O
		O	32 ± 2	>1% A in O
PS 15	2/94	A	61 ± 5	>1% A in O
		O	63 ± 5	>1% both phases

3. Uranium Tests

Because it is difficult to keep the THFTCA from being extracted in the strip section and carried by the solvent into the carbonate wash, a new strip feed consisting of mono-sodium THFTCA (MST) and di-sodium THFTCA (DST) was developed and tested at the CHM Division. Some of their results, summarized in Table 23, show that the distribution ratio of THFTCA at 0.25M THFTCA is 0.18 with 0.25M NaOH. With HNO_3 (no NaOH), this concentration of THFTCA gives a THFTCA distribution ratio of 0.7 (see Fig. 10). Thus, the use of NaOH at this concentration reduces the THFTCA distribution ratio by a factor of four. This makes it easy to keep the THFTCA in the aqueous phase and, at the same time, reduce the aqueous feed rate to the strip section. In addition, if there is not too much NaOH, that is, if the amount of DST is low, the distribution ratio for uranium remains high so that most of the uranium will end up in the carbonate wash. Based on these results, the composition chosen for the strip feed was 0.2M MST and 0.1M DST, which can also be written as 0.3M THFTCA with 0.4M NaOH.

Table 23. Effect of Various THFTCA and NaOH Concentrations on Distribution Ratios of U and THFTCA

PS 15 Pre-equilibrated with HNO_3,[a] M	THFTCA Conc., M	NaOH Conc., M	Distribution Ratio for U	Distribution Ratio for THFTCA
0.04	0.25	0.25	11.0 ± 0.4	0.18
	0.25	0.50	0.7 ± 0.1	NM[b]
0.4	0.40	0.50	5.3 ± 0.6	NM[b]

[a] After being pre-equilibrated with HNO_3 using the HNO_3 concentration shown below in the aqueous phase, the PS 15 was loaded with the uranium.

[b] Not measured.

a. Methods

In the uranium tests (U1 and U2), we evaluated the ability of the strip section to keep the uranium in the organic phase and the THFTCA in the aqueous phase. These tests were done using flowsheets with 7 or 8 contactor stages. The single-stage extraction section has a special extraction (DF) feed that includes Al, HNO_3, Sm, Sr, and U. The high concentration of aluminum causes the PS 15 solvent to load with HNO_3, Sm, Sr, and U. In the four-stage strip section, the flow rate for the strip (EF) feed, 0.3M THFTCA with 0.4M NaOH, was varied from 4 to 15 mL/min. In the one- or two-stage carbonate wash section, 0.25M Na_2CO_3 was used to wash the PS 15. In the single-stage acid rinse section, 0.1M HNO_3 was used to rinse the PS 15.

(1) Test U1

Test U1 was carried out as shown in Fig. 20. Two strip feed (EF) flow rates were used, 15 mL/min (Test U1.1) and 8 mL/min (Test U1.2). The hydraulic performance of the minicontactor was excellent for both U1 tests. The interstage lines all remained open throughout the test, and no significant other-phase carryover was seen in any effluent. In addition, most of the yellow color, indicating uranium, was observed to end up in the FW effluent.

(2) Test U2

Test U2 carried out as shown in Fig. 21. The strip feed (EF) flow rate of only 4 mL/min allowed us to evaluate the effect of even less NaOH present to neutralize the nitric acid being carried into stage 2 by the PS 15 solvent (and so, to determine the low end of the strip feed rate). The hydraulic performance of the minicontactor was good in that the interstage lines remained open, and no significant other-phase carryover was seen in any effluent. As before, most of the uranium (indicated by yellow color) was observed to exit in the carbonate wash (FW) effluent, as desired.

However, at 18 min into the test, that is, 18 min after the organic flow was started, we observed the partial backup of organic (60 to 80%) and aqueous (25 to 30%) interstage liquids flowing into stage 6. At 23 min into the run, the partial backup of organic (60 to 80%) interstage liquid flowing into stage 5 occurred as well. At 31 and 35 min, we observed the partial backup of organic (80%) and aqueous (60%) interstage liquids flowing into stage 4, while at the same time, the backup into stage 6 dropped down to the 15 to 25% range. At 38 min, the test was completed.

b. Results

The results for the three tests, the two U1 tests (U1.1 and U1.2) and the U2 test, are summarized in Table 24 along with a material balance for each component. The concentration of THFTCA was measured by J. V. Muntean (CHM Division), using a one-pulse proton nuclear magnetic resonance following 1:1 dilution of the sample with deuterated water. With this equipment, THFTCA can be analyzed at concentrations as low as 0.003M. The various metal ions were measured by E. A. Huff (ANL Analytical Chemistry Laboratory) using ICP-spectrochemical analyses, which are accurate to within ±10%. The composition of the various feeds, which were the same for all three tests, are shown in Figs. 20 and 21, along with the measured flow rates for the effluent streams.

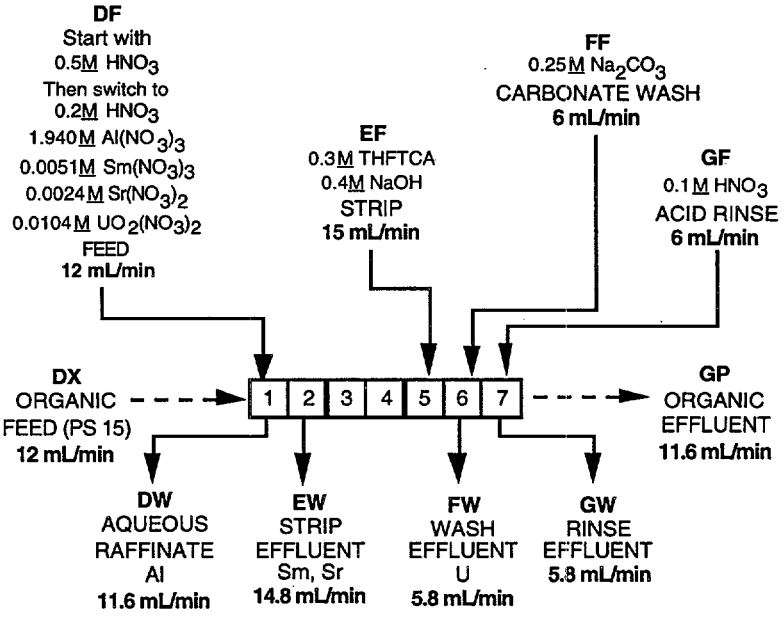

Feed flows shown were the planned flows, the effluent flows shown were the measured flows. After 30 min into 60-minute test, when the EF flow was lowered from 15 (as shown above) to 8 mL/min, it was observed that EW dropped from 14.8 (as shown above) to 7.9 mL/min.

Fig. 20. TRUEX-SREX Flowsheet for First Strip-Section Test with Uranium (U1)

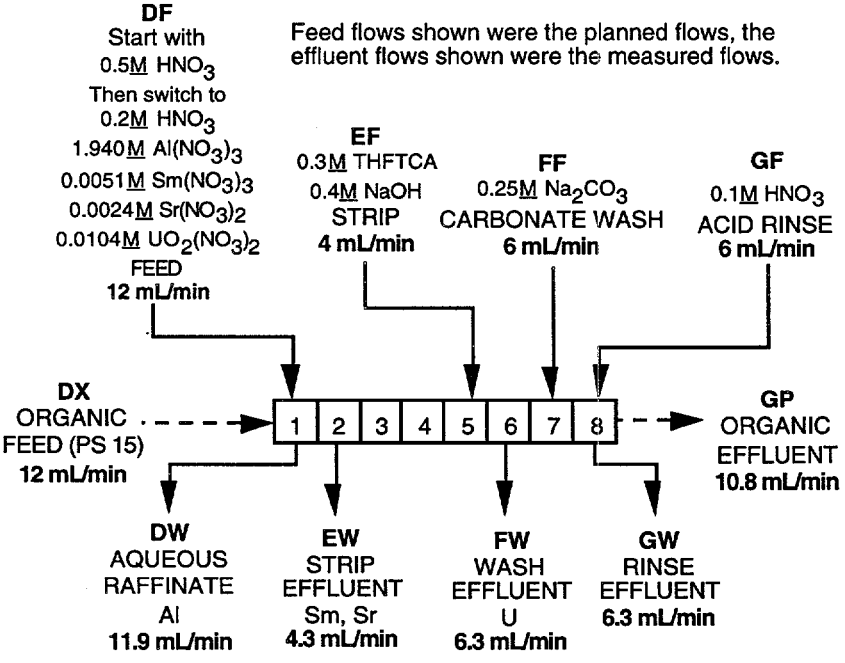

Fig. 21. TRUEX-SREX Flowsheet for Second Strip-Section Test with Uranium (U2)

Table 24. Component Concentrations in Various Effluents for Uranium Tests[a]

Test	Component	Component Concentration, M					Amount of Component Recovered, %
		DW	EW	FW	GW	GP	
U1.1	THFTCA	<3E-04	0.231	0.084	NM	NM	88
	Al	TH	0.039	<0.0007	NM	NM	–
	Sr	3.06E-05	2.07E-03	<2E-06	NM	NM	107
	Sm	<2E-06	4.00E-03	<7E-05	NM	NM	103
	U	<2E-05	9.70E-04	0.0166	NM	NM	95
U1.2	THFTCA	<3E-04	0.197	0.055	NM	NM	79
	Al	TH	0.071	<0.0007	NM	NM	–
	Sr	3.29E-05	3.86E-03	<2E-06	NM	NM	106
	Sm	<2E-06	7.12E-03	<7E-05	NM	NM	97
	U	<2E-05	2.66E-04	0.0193	NM	NM	98
U.2	THFTCA	<5E-04	0.0445	0.092	ND	ND	61
	Al	TH	0.152	<0.0007	NM	NM	–
	Sr	2.68E-05	3.12E-03	1.31E-04	<2E-06	<2E-06	49
	Sm	<2E-06	7.20E-03	8E-05	<3E-06	<3E-06	53
	U	<2E-05	<4E-05	0.01655	<4E-05	<4E-05	88

[a]ND: not detected.
NM: not measured; concentration thought too small to detect.
TH: concentration too high to be measured without dilution.

The only difference in the three tests (U1.1, U1.2, and U2) was that the strip (EF) feed rate was decreased from 15 to 8 to 4 mL/min. As the EF feed rate decreased, the concentration of aluminum in the EW effluent increased. Analysis of these concentrations shows that 2.4 to 2.7% of the aluminum was carried out of the extraction stage (stage 1) by the organic effluent. Since the distribution ratio for aluminum in the first stage was low (that is, 0.001 or less), these results indicate that the aqueous-phase carryover in the organic phase from stage 1 was close to 2.3%. This amount of other-phase carryover is higher than the 1% or less that is desired in contactor operation. However, this level of other-phase carryover can be tolerated for most centrifugal contactor operations, and it can be modeled by the GTM since other-phase carryover is included in the SASSE worksheet calculations.

The strip section takes out the strontium, lanthanides, and transuranic elements in the EW effluent but leaves most of the uranium in the organic phase so that it comes out in the carbonate wash section in the FW effluent. As the EF feed rate decreased, the concentration of uranium in the EW effluent also decreased. This result, which can be seen in Table 24, is summarized in Table 25. Note that, even in the worst case, test U1.1, only 13% of the uranium was found in the EW effluent.

In tests U1 and U2, the addition of NaOH to the THFTCA in the strip (EF) feed was done to keep the THFTCA in the strip section so that it can be effective in removing the lanthanides and transuranic elements. A review of Table 24 shows that THFTCA was best kept in the aqueous phase, that is, in strip (EW) effluent for test U1.1. This test had the highest EF flow rate, and so, the highest concentration of NaOH entering the strip section. As the EF flow rate decreased, the amount of THFTCA in the strip (EW) effluent also decreased relative to that in the carbonate wash (FW) effluent. In addition, as the EF flow decreased, the amount of THFTCA recovered decreased from 88% down to 61%. This suggests that the THFTCA is being pinched in the strip section. At the

Table 25. Distribution of Uranium between the Various Effluents

Test	EF Feed Rate, mL/min	Amount of U in Various Effluents, %				
		DW	EW	FW	GW	GP
U1.1	15	0	13	87	0	0
U1.2	8	0	2	98	0	0
U.2	4	0	0	99	0	0

right end of the strip section, the THFTCA entering with the NaOH keeps the THFTCA in the aqueous phase; at the left end, the HNO_3 entering with the organic phase from the extraction section (stage 1) neutralizes much of the NaOH. As NaOH is lost, the THFTCA is extracted into the organic phase.

The amount of HNO_3 that would end up in the EW effluent if there were no NaOH in the EF feed has been calculated for a nitric acid distribution ratio of 10 in the extraction section and 0.2 in the strip section. The results are summarized in Table 26. Since there was 0.4M NaOH in the EF feed, the HNO_3 concentrations in Table 26 must be subtracted from 0.4 to determine how much NaOH is left with the THFTCA in the EW effluent. In the worst case, test U.2, all the NaOH was neutralized, and the EW effluent would have had about 0.1M HNO_3. This test is the one where only 61% of the THFTCA was recovered, the one with most of the THFTCA exiting in the FW effluent.

Table 26. Concentration of Nitric Acid in Strip Effluent without Sodium Hydroxide

Test	HNO_3 Conc.,[a] M
U1.1	0.14
U1.2	0.27
U.2	0.48

[a]Calculated for EW effluent based on HNO_3 carried in by the PS 15 solvent from the extraction section.

As planned, most of the Sr and Sm came out in the strip (EW) effluent (see Table 24). However, for the U.2 test, we were detecting Sr and Sm in the carbonate wash (FW) effluent. In addition, only 49 and 53% of these two components, respectively, were recovered. This suggests that they were also pinched in the strip section. In future tests, we will take stage samples at the end of the test. Analysis of these stage liquids can provide some estimate of how much material is being pinched in a stage or section.

Based on these tests, we now have a reasonable basis for designing the strip section of the TRUEX-SREX flowsheet. In particular, the scrub section must be designed so that the HNO_3 in the organic phase entering the strip section does not neutralize all the NaOH entering with the THFTCA. At the same time, the HNO_3 concentration in the scrub section must be kept high enough to prevent the strontium from being pinched there. In addition, based on these uranium tests, one should set the strip (EF) feed rate so that the NaOH concentration in the strip (EW) effluent will be between 0.1 and 0.2M.

4. Hot Test

Based on the results of cold tests and the uranium tests, we are preparing for a hot test (H1) of the TRUEX-SREX flowsheet. The preparation of the glovebox and the development of the flowsheet are summarized here.

a. Preparation

An empty glovebox in CMT was decontaminated in preparation for the hot test of the TRUEX-SREX flowsheet in a 24-stage 2-cm contactor (minicontactor). A glovebox window was removed so that the glovebox could be cleaned out and painted. While the window was still off, various items (including a contactor table, a contactor tray, and the 24-stage contactor system) were put into place. The contactor table was a new structure designed so that all the pumps, feed tanks, and effluent tanks can be placed under the contactor, where they are easily accessible. The contactor system is now being prepared for the TRUEX-SREX hot test. The interstage lines on the organic side of the contactor have already been installed; the aqueous interstage lines will be installed as soon as the flowsheet design is finalized.

b. Flowsheet Development

Based on the cold tests reported above, a combined TRUEX-SREX flowsheet was developed for the hot test (H1), as shown in Fig. 22. To obtain a decontamination factor of 10^5 for strontium in the extraction section, eight extraction stages are used along with a DF feed flow rate of 8 mL/min and a HNO_3 concentration in the DF feed of 4.5M. The strip section has been designed so that THFTCA can be used alone, and the amount of THFTCA that does pass through to the carbonate wash section can be handled by the 0.25M Na_2CO_3 feed.

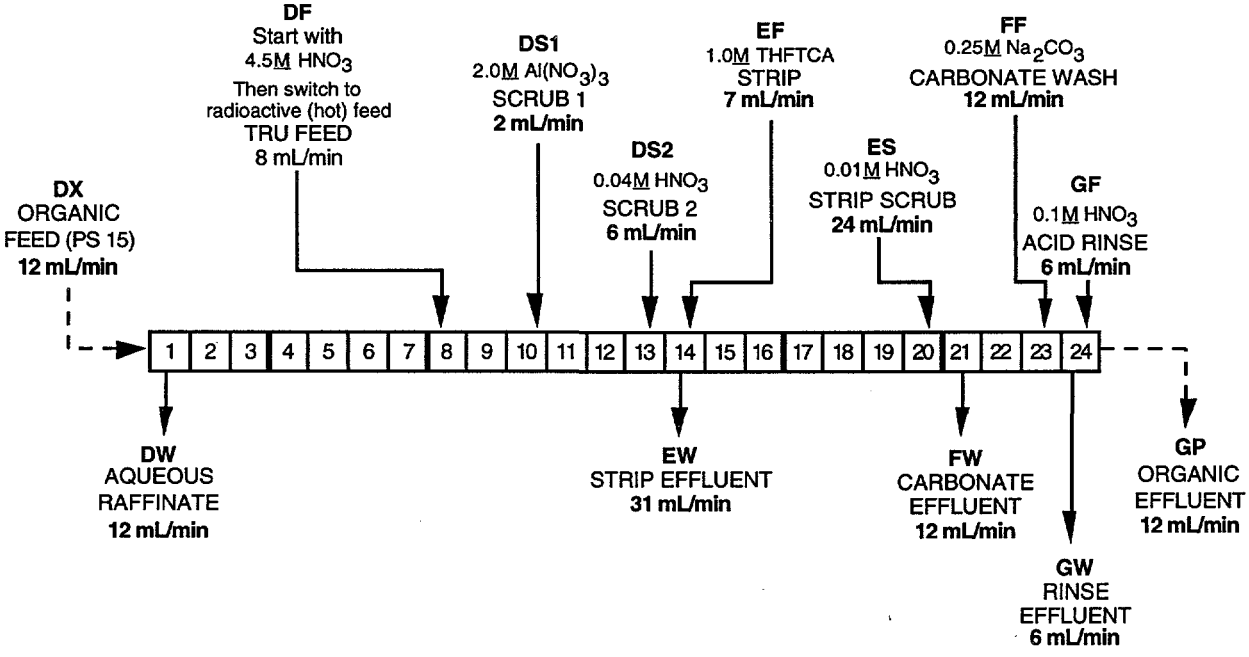

Fig. 22. TRUEX-SREX Flowsheet for the First Hot Test (H1)

The strip and carbonate wash sections of the TRUEX-SREX flowsheet shown in Fig. 22 follow closely the design verified by cold test C3. As such, the flowsheet should be able to handle the THFTCA. However, based on the successful uranium tests, we are planning to revise the H1 flowsheet to incorporate a strip feed of 0.3M THFTCA with 0.4M NaOH.

5. SREX-NEPEX Processing

A second solvent extraction process is being developed in the ANL Chemistry Division to process the strip effluent from the TRUEX-SREX process. This new process, called SREX-NEPEX (where NEPEX stands for neptunium-plutonium extraction), will separate Sr, Np, and Pu from the lanthanides, Am and Ba. The solvent for this process, PS 16, consists of 0.15M CE and 1.2M TBP in Isopar L. We have designed a SREX-NEPEX flowsheet and are preparing to test it in a 20-stage 2-cm contactor.

B. Minicontactors for Pacific Northwest Laboratory

Pacific Northwest Laboratory (PNL) is setting up a pilot-scale centrifugal-contactor system at the Hanford site in Richland, Washington. This system will be used to evaluate solvent extraction flowsheets, especially the TRUEX process, for processing of dissolved sludge from Hanford waste tanks. Up until October 1993, we had been planning to build 68 minicontactor stages for PNL. Because of funding reductions, however, only 28 contactor stages were actually built along with three spare motor/rotor assemblies. In addition, four stages were built for ANL use. In one-phase tests, we will measure the no-flow volumes for each mixing zone and rotor. We will also measure the zero-point flow rate, that is, the flow rate at which one-phase flow starts to come out the less-dense-phase exit. Then, based on these tests, three stages will be chosen for two-phase testing at three O/A flow ratios (0.33, 1.0, and 3.)

As contactor fabrication progressed, we made four changes to the minicontactor design. These changes reflect our past experiences in testing the TRUEX-SREX flowsheet with a 20-stage minicontactor. The first change was to add a purge-air manifold to the contactor housing. The manifold design was required to be convenient to use but out of the way for contactor testing. It also had to be easy to remove if a different contactor design is required at a later date, e.g., upon installation of the contactor system in a shielded-cell facility. The design chosen has a removable bracket that fits under one of the clamping nuts at the top of selected contactor stages.

The second change was made to ensure that any given motor/rotor assembly could be inserted in any stage. To do this, each contactor housing cavity was measured to determine the distance between the top surface to the lip of the upper collector ring and the top of the vanes in the bottom of the mixing zone. In addition, the length of each rotor was measured from the bottom of the slinger ring to the bottom of the rotor. Both sets of measurements were found to be uniform from contactor to contactor. Using these dimensions, we were able to attach to the rotor to the motor in such a way that the rotor would touch neither the lip of the upper collector ring nor the bottom vanes. A gauge is now being designed so that the motor/rotor can be assembled in a glovebox or shielded-cell facility, if necessary.

The third change allows workers to determine whether power is on at each motor. To accomplish this, a red neon power light was added to the junction box at the top of each motor. When this light goes out, the motor has no power. This feature was added because we were having problems with the ground fault circuit interrupter. Note that this running light indicates that the motor has

power, it does not guarantee that the rotor is turning, or that operation is normal. This can be determined by an appropriate liquid-level probe in the liquid-level detector port, which is available at each stage. If the interstage lines are transparent or translucent—if, for example, the lines are made of Teflon FEP (fluorinated ethylene polypropylene) or Teflon PFA (perfluoroalkoxyl) tubing—one can see if the liquid level in the mixing zone is high by observing its level in these lines.

The need for a fourth change, a better motor/rotor connection, has been identified, but the appropriate change has not yet been fully implemented. The existing connector has worked quite well for several years. However, we recently experienced two cases where the rotor had slipped down the motor shaft, so that the slinger ring of the rotor rested on the lip of the upper collector ring and stopped the rotor from rotating. In one of the cases, the problem was observed during hydraulic testing of the newly fabricated PNL contactor. Currently, each minicontactor rotor is held onto the motor shaft by a small set screw, 6-32 UNC x 0.187-in. long. The screw is turned using a 1/16-in. allen wrench. There are two parts to this problem. First, because of the small size of the set screw and the allen wrench, the screw cannot be turned very tightly. Second, if the screw does not hit the flat of the motor shaft straight on, the shaft may turn relative to the contactor rotor and leave the set screw not touching the motor shaft. When this happens, the rotor is free to slip down the motor shaft.

A special review of the problem with the motor/rotor connection indicated that the best way to improve the design is to use a bigger set screw. With a 10-32 UNC x 0.125-in. long set screw, which uses a 3/32-in. allen wrench, one should be able to set the screw much tighter. In addition, the motor/rotor assembly procedure will be changed so that the set screw hits the flat of the motor shaft close to perpendicular. To do this, the distance that the set screw extends into the hollow center region of the rotor shaft will be preset with a gauge. The distance will be such that the rotor can be connected to the motor shaft only if the set screw is directly over the flat on the motor shaft.

C. TRUEX Processing of Mark 42 Targets

We have supported the ORNL Radiochemical Engineering Development Center (REDC), formerly the Solvent Extraction Test Facility (SETF), in the TRUEX processing of Mark 42 targets (aluminum-clad PuO_2). As a part of this work, we designed a TRUEX flowsheet so that Pu, Am, and Cm could be recovered using the three existing banks of 16-stage mini-mixer-settlers in a hot cell at REDC (see previous report). We are now helping L. K. Felker and D. E. Benker of ORNL analyze the test data. The preliminary results look good. However, we have recommended that ORNL rerun the GTM using an extraction efficiency of 84%, which should yield the best comparison of the GTM calculations with experimental data. To run the GTM at this extraction efficiency, it was necessary to modify the SASSE procedure so that E_a can be less than 1.0. Details of this modification are discussed in Sec. II.C. Summarized here are the accomplishments from our involvement with ORNL in the TRUEX processing of Mark 42 targets and the problem areas identified.

1. Accomplishments

The GTM was successfully used to develop a TRUEX flowsheet for processing Mark 42 targets. In the flowsheet, Pu, Am, Cm, and the rare earth elements are recovered from the dissolved targets. Then, the Pu is separated from the Am, Cm, and the rare earths. This flowsheet has been tested at REDC and found to work well. By using the GTM, we were able to design a very complex TRUEX flowsheet so that the very first experimental flowsheet to be tested performed as expected. We were also able to identify and resolve key design problems and make appropriate flowsheet changes before the first experimental test.

With the aid of the GTM, we were able to design a flowsheet in which the plutonium is separated from the Am, Cm, and the rare earths with ≤ 0.1% cross-contamination. This result was demonstrated in an experiment with the full concentration of all feed components. A key feature of this design was a complex scrub section that removed essentially all the oxalate ion ($\leq 10^{-7}$M) from the solvent, and that carefully controlled the nitric acid concentration in the organic phase transported from the last scrub section to the strip section.

Using literature data along with the improved SASPE portion of the GTM, we were able to determine solubility products for oxalate with Pu and with Am, Cm, and the rare earth elements. This capability allowed us to design a flowsheet with high oxalate concentrations but without significant oxalate precipitation. The ability to observe the settling zones of the mini-mixer settlers allowed us to verify this flowsheet.

From the data obtained using the Mark 42 TRUEX flowsheet tests, we determined the extraction efficiency to be 84% for the mini-mixer settlers used in the tests. Using this extraction efficiency (rather than the default of 100%) will result in better agreement between the GTM and the experimental tests and allow other problems to be more clearly identified.

With the improvement in extraction efficiency for the GTM (see Sec. II.C), we were able to model mini-mixer settler operation closely, even in regions where Cm and Pu stage-to-stage concentrations were changing rapidly. With the improved capabilities of the GTM to handle solvent loading, we were able to analyze the high loadings required by the Mark 42 TRUEX flowsheet. In addition, data obtained from the experimental tests will allow us to improve further the ability of the GTM to model high solvent loadings.

Finally, the tests of the flowsheet demonstrated the ability to cleanup and reuse the TRUEX solvent, and to use the TRUEX solvent with very high levels of radiation (10^9 dpm/mL of alpha) and with very high residence times in the process equipment (2 to 3 min/stage with a total of 48 stages).

2. Problem Areas

One of the problems encountered was that there were not enough stages in the existing extraction/scrub section to make the TRUEX process as robust as desired. If we had not been constrained to design the process for the existing ORNL mini-mixer settlers, however, this would not have been a problem.

For good operation of the mini-mixer settler, the O/A flow ratio should be between 1 and 10. We were able to meet this design criterion for most of the flowsheet; however, for the organic scrub section of the first strip, we needed an O/A flow ratio of 0.5. In spite of this, the section worked well for the first two tests. On the third test, the mixer-settler acted up by allowing other-phase carryover to occur at some stages and the aqueous flow had to be decreased until the O/A flow ratio was very close to 1.0. With other solvent extraction equipment, this low O/A flow ratio would not have been a problem.

The flowsheet performance deteriorated when the component concentrations in the feed was lowered to 4% of their design values. This poorer operation was probably due to excess oxalate concentration in the scrub section. Without metal ions such as zirconium to tie up the oxalate, more oxalate is extracted into the solvent and appears in the strip section. There it keeps the

plutonium from being extracted into the solvent so that much of the plutonium appears in the effluent containing the Am, Cm, and rare earths.

While we accomplished the desired separation of Pu from Am, Cm, and the rare earths, this separation was not easy. In particular, it required the addition of an organic scrub section for the first strip. For the Hanford tank wastes, separation of Pu from Am will not be required. This will greatly simplify the Hanford process and make it easier to operate.

IV. ADVANCED EVAPORATOR TECHNOLOGY

(D. B. Chamberlain, C. Conner, B. Gebby, A. E. V. Rozeveld, D. G. Wygmans, and G. F. Vandegrift)

A program was funded this year by the Underground Storage Tank Integrated Demonstration (UST-ID) to determine whether an evaporator Compact Processing Unit (CPU) was feasible. This CPU evaporator would be used to remove the significant amount of water that will likely be added to underground storage tanks during retrieval operations at the DOE Hanford site. Early estimates indicate that the volume of waste will increase by at least a factor of three through water addition. Further, approximately 30 wt% of the current waste inventory at Hanford is water. To minimize the volume of waste requiring treatment and disposal, removal of this water is important. In fact, removal of the water before processing in the low-level vitrification facility at Hanford is needed to improve operation of the melters and reduce the size of the off-gas system. Decontaminated water recovered from the evaporators could be recycled to support further retrieval operations and/or discharged to the site effluent treatment plant.

The initial focus for DOE's compact processing units was to process waste from Hanford's underground storage tanks. The evaporator CPU was one of several CPUs being developed by the UST-ID; these included units for waste retrieval, filtration, cesium removal, evaporation, and organic destruction. Tank 241-AW-101 was chosen to be the first tank to be processed[3]; therefore, we initially focused on the composition of this tank for our evaporator system.

In addition to processing cesium-free salt solutions, the evaporator/concentrator system will be designed to test the feasibility of processing nitric acid regeneration solutions from the cesium removal process. In the cesium removal CPU, nitric acid is used to regenerate the ion exchange resin. The regeneration operation will produce a nitric acid waste stream containing significant amounts of cesium. The recovered cesium product stream is slated for neutralization and return to the Hanford waste tanks. The objectives of this application of an evaporator CPU are twofold: (1) to reduce the volume of cesium waste that is returned to the waste tanks and (2) recover the nitric acid (the distillate) and recycle this acid to the ion exchange process. This nitric acid could then be used to remove additional cesium from the ion exchange columns. By removing and recovering nitric acid from this stream, neutralization requirements are greatly reduced. Meeting these objectives requires high decontamination factors (DFs).

As currently envisioned, the system will consist of an evaporator followed by a concentrator. The bulk of the water will be removed by the evaporator; additional concentration will be completed in a concentrator designed to handle high suspended-solids concentrations (slurries). The evaporator system will be based upon a LICON, Inc. (Pensacola, FL) design. A second company, Artisan Industries, Inc. (Waltham, MA), will be involved in the design of the concentrator; their Rototherm unit will be used as a basis for this unit.

To help in these evaluations, evaporator tests using waste simulants will be completed by LICON and Artisan. LICON will complete tests using a 3 gal/h (11 L/h) evaporator in their pilot-plant facility. The purpose of these tests is to (1) familiarize LICON with the processing of typical (simulated) waste solutions and (2) suggest equipment modifications and instrumentation required for the effective processing of these wastes. Additional objectives will be to study scaling tendencies, volume reduction, solids handling, product quality, and decontamination factors. Artisan will complete tests using a 1 ft^2 (0.9 m^2) Rototherm concentrator in their pilot-plant facility. The purpose of Artisan's tests is the same as LICON's. In addition, potential automatic process control schemes for the Rototherm unit will be investigated.

A. General Description of Compact Processing Units
(D. G. Wygmans)

Hanford is considering the use of CPU's for processing their tank waste. A CPU is a portable, self-contained chemical process module that can be located near a waste storage tank or a diversion box in the Hanford waste transfer system and used to process radioactive tank waste. The CPU can be deployed as needed and provides both scheduling and economic advantages relative to a larger, fixed facility. Currently demonstration CPUs are being pursued for a number of processing-module needs. These CPUs are not full-scale units that would fit into the final implementation of the entire processing flowsheet, but rather pilot-scale units for process demonstrations. Whether the final modules, for full-scale processing, will be CPUs or fixed units in a central facility has yet to be determined.

As envisioned, the evaporator/concentrator CPU will consist of an evaporator followed by a concentrator. The bulk of the water will be removed by the evaporator, which can attain high decontamination factors and thus produce distillate sufficiently clean for recycle or disposal. The evaporator bottoms will be fed to a concentrator, which is specially designed to handle high solids concentrations (slurries). The concentrator will further evaporate the waste, producing a thick pumpable sludge. Water recovered in the concentrator will be reprocessed in the evaporator. Thus, only one waste stream exits the evaporator/concentrator CPU: the concentrated product. In cases where a high solids concentrate is undesirable, a concentrator would not be included in the CPU.

B. Case BETA
(D. G. Wygmans)

A scheme for the processing of Hanford tank waste is being developed by Hanford personnel. In its current form, the processing scheme is called "Case BETA." A simplified Case BETA flowsheet, highlighting the four evaporators in the flowsheet, is shown in Fig. 23. As seen in Fig. 23, Case BETA calls for the vitrification of both the low-level waste (LLW) and high-level waste (HLW) fractions. Prior to vitrification of either waste fraction, the evaporation of a considerable amount of water is desirable. Concentrating the tank waste in an evaporator/concentrator system not only allows for smaller melters in the vitrification facilities, but also allows for the recycle of waste water to the waste-retrieval and sludge-washing operations. Evaporative recovery of nitric acid is also desirable. Nitric acid can be recovered from the eluant of the cesium ion-exchange (Cs IX) process and recycled for further regeneration of the ion-exchange bed.

An Aspen code is being developed in support of the flowsheet to predict stream compositions. Assumptions within the Aspen code presently include the following: the decontamination factor for all evaporators is infinite, and the solubility of dissolved solids is infinite. Thus, all solids in the feed remain in the concentrate, and all dissolved solids remain in solution. A brief overview, outlining the information contained in the Aspen code for each of the evaporators in the flowsheet, is included in Sec. IV.F.2.

C. Evaporator/Concentrator Designs
(D. B. Chamberlain)

1. Mobile Evaporator Designs of Oak Ridge National Laboratory

Martin Marietta Energy Systems at the Oak Ridge National Laboratory (ORNL) currently has two evaporator programs underway that incorporate various mobile design features.

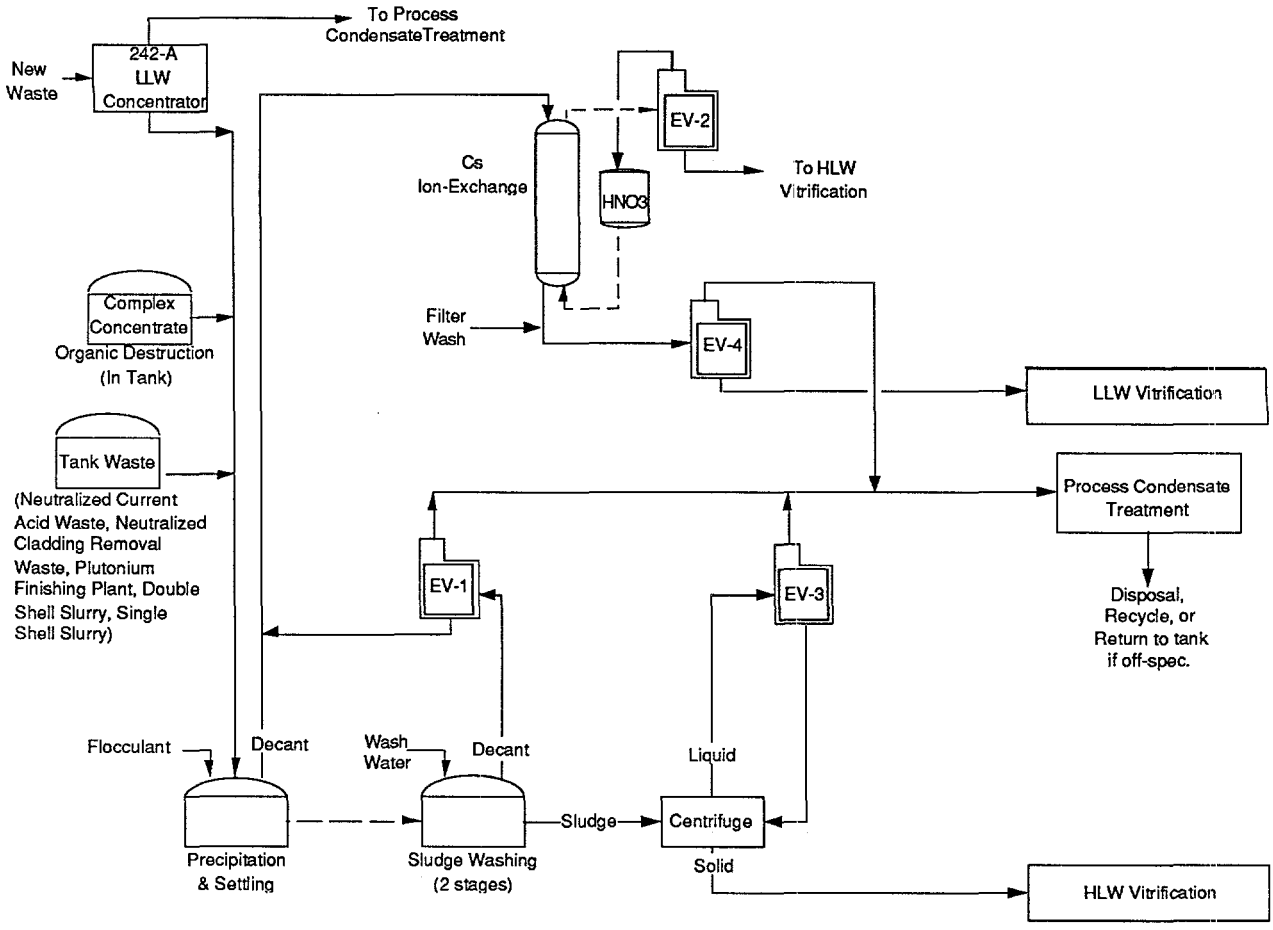

Fig. 23. Simplified Flowsheet for Case BETA

One unit (LICON VC-75 evaporator) is being designed to process water from the decontamination of contaminated surfaces. A second unit is being designed to process Melton Valley Storage Tanks (MVST C-90) waste. The designs of both these systems are described in the following two sections because they incorporate various ideas that are important in the design of a mobile evaporator system. In addition, ANL personnel have been actively involved in the design of the MVST C-90.

a. VC-75 D&D Evaporator

During the decontamination of metal and concrete surfaces, water contaminated with solids, radionuclides, hazardous materials, oil, and grease is generated. Purifying this water and recycling it to the decontamination processes significantly reduce the volume of waste generated. In this program, ORNL is designing and fabricating an evaporator system to decontaminate and purify this water (Fig. 24). The distillate from the evaporator will be suitable for recycle without further processing. The evaporator bottoms, containing the solids, hazardous materials, radionuclides, and organics is further concentrated in the pot dryer. The feed to the system is filtered to remove suspended solids before processing in the evaporator. The evaporator portion of the system is a LICON VC-75. This vapor compression unit will have a minimum processing capacity of 190 L/h (50 gal/h).

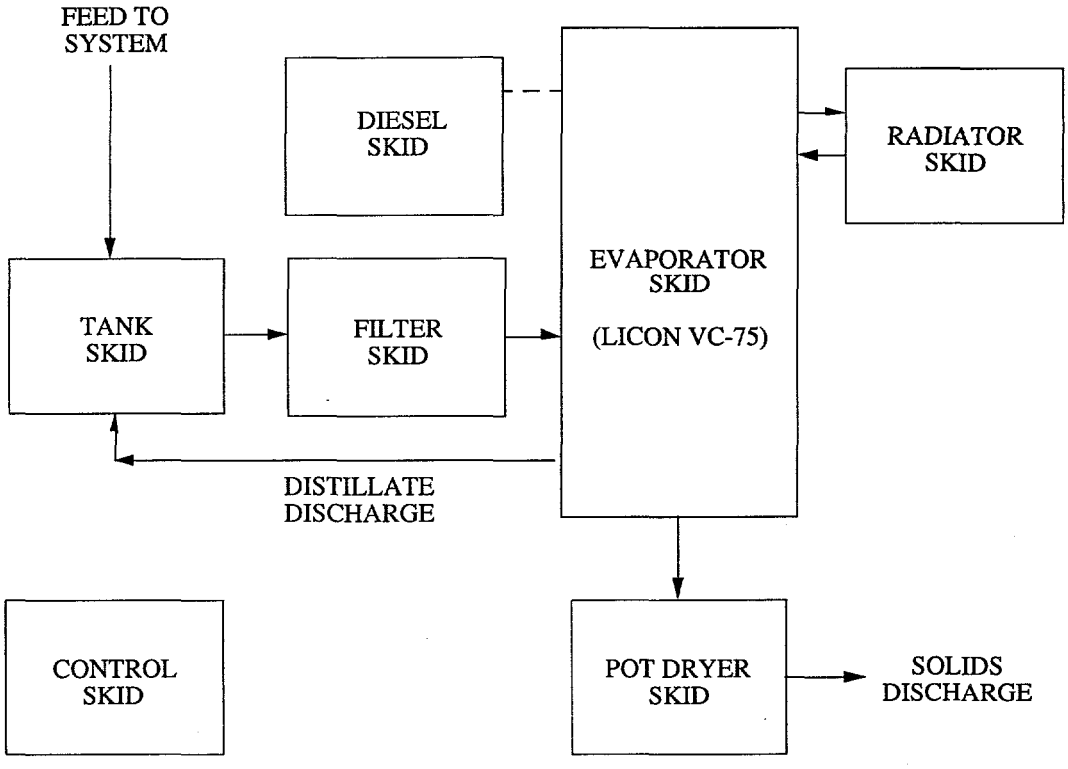

Fig. 24. Schematic of Oak Ridge D&D Mobile Evaporator

The ORNL system is designed to separate the various modules into skids. Piping and utility connections connect the various skids together. A separate skid contains the instrument displays and the computer control system. The system is self-contained: the required storage, electrical, heating, and cooling systems are included.

The equipment is separated into various skids to separate the radioactive portion of the system from the nonradioactive support systems. In addition, the highly radioactive portion of the system, the pot dryer, is separated from the other radioactive portions to reduce shielding requirements. The concentrate tank, normally included on a LICON-designed evaporator, was eliminated to reduce the volume of highly contaminated concentrate in the system. The completed system is skid mounted and will be transportable on a standard forty-foot trailer. The skids are designed to be moved separately (if necessary).

b. MVST C-90 Evaporator

The second mobile evaporator system is being purchased to process waste from the Melton Valley Storage Tanks. A schematic of the proposed system is shown in Fig. 25. This system is being sized to generate 340 L/h (90 gal/h) of distillate. Unlike Oak Ridge's D&D evaporator, this system is not self-contained. Power will be supplied to the various skids from external systems. The system is also split into various skids to separate the radioactive systems from the radioactive ones and to separate the highly radioactive systems from those requiring little shielding. However, system shielding will not be as significant as the D&D system; the system will be installed in a building with limited access, so shielding requirements are not as demanding.

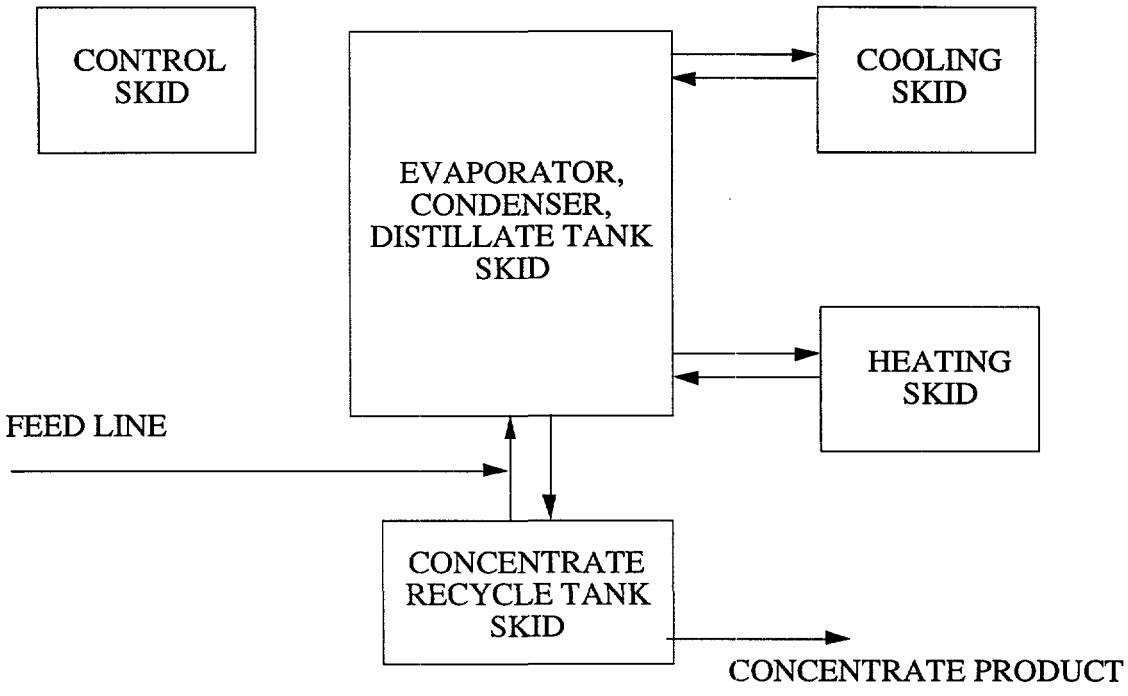

Fig. 25. Schematic of Proposed System for Oak Ridge D&D Mobile Evaporator

2. LICON System
(D. B. Chamberlain)

LICON specializes in the design and manufacture of horizontal-tube vacuum evaporators that are compact and energy efficient. Sizes range from 11 L/h (3 gal/h) to approximately 1900 L/h (500 gal/h). Many innovative features have been incorporated into their evaporators, including some that were developed in the early 1980s with support from DOE. LICON's designs incorporate horizontal heat exchangers, which require less headroom than vertical-tube heat exchangers. This design feature is important, since the evaporator must be mobile: that is, movable from site to site without dismantling process equipment.

LICON also incorporates bayonet tubes in their heat exchangers. A diagram of a single bayonet tube is shown in Fig. 26. For heating, the heating fluid flows down through the center lance and exits through the heat exchanger tube (i.e., the annular region). The outside of the tube is in contact with the boiling solution. Bayonet tubes, although more expensive to manufacture, are effective because they allow for (1) high velocities and turbulence that improve heat transfer coefficients, (2) high heat transfer area, and (3) easy venting of noncondensables from the heat exchanger. These tubes are typically manufactured from titanium.

Because LICON evaporators operate under vacuum, operating temperatures are much lower than atmospheric units. Lowering system temperatures often allows less expensive construction materials, such as fiberglass and/or CPVC/PVC (PVC = polyvinylchloride, CPVC = chlorinated polyvinylchloride) to be used. For nuclear applications, however, stainless steel and other alloys are available. Also, by lowering the boiling temperature, corrosion rates and scaling on the heat transfer surfaces are greatly reduced. Barker[4] found that the corrosion rates typically double for every 15°C rise in temperature.

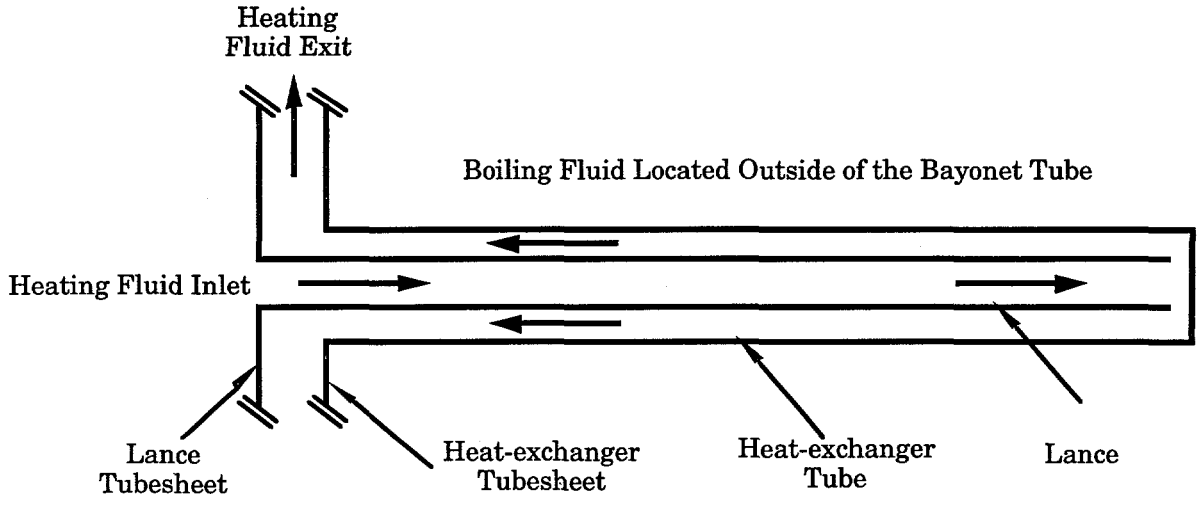

Fig. 26. Schematic of LICON Bayonet-Tube Design

System vacuum is produced by eductors, not by vacuum pumps, which increase the operating reliability of the units. LICON also relies on forced circulation of the concentrate solution through the evaporator, which aids in heat transfer, decreases scaling tendencies, and maintains solids suspended in solution. Flow rates of the concentrate are typically 10 times the rated capacity of the evaporator. Advanced microprocessor control systems to make the units fully automated are also available from LICON. This development is important since remote operation is necessary.

A flow diagram for a standard, commercially available LICON evaporator is shown in Fig. 27. A typical LICON evaporator has four distinct recirculation loops: heating, cooling, distillate, and concentrate. The feed is normally pumped into the concentrate tank. This preheats the feed by mixing with the concentrate and allows a place to vent noncondensables from the feed solution.

Recirculating hot water is used as the energy source for a LICON evaporator. Direct use of steam can be incorporated into the design, but temperatures on the heat exchange surface would be much higher (160°C vs. 88°C), which in turn increases scaling and corrosion. To generate hot water, a secondary heat exchanger is used; a pump recirculates this water through the evaporator. The hot water is located on the tube side of the exchanger. The medium being boiled is located on the shell side.

Cooling water is circulated through the condenser bayonet tubes to condense the vapor. Cooling water is also circulated through the distillate tank to cool the solution (not shown in Fig. 27) so as to improve operation of the eductor. A heat exchanger (not shown) is also located in the distillate loop so that water from the cooling loop can further lower the distillate temperature.

Distillate is circulated via a pump from the distillate tank, through the eductor, and then back to the distillate tank. The flow of solution through the eductor provides the motive force for drawing a vacuum on the system. Distillate is also discharged from the system via valves in this loop.

The concentrate is the fourth loop in a LICON evaporator. Concentrate is vacuum dragged from the concentrate tank into the evaporator shell and is withdrawn from the shell via a

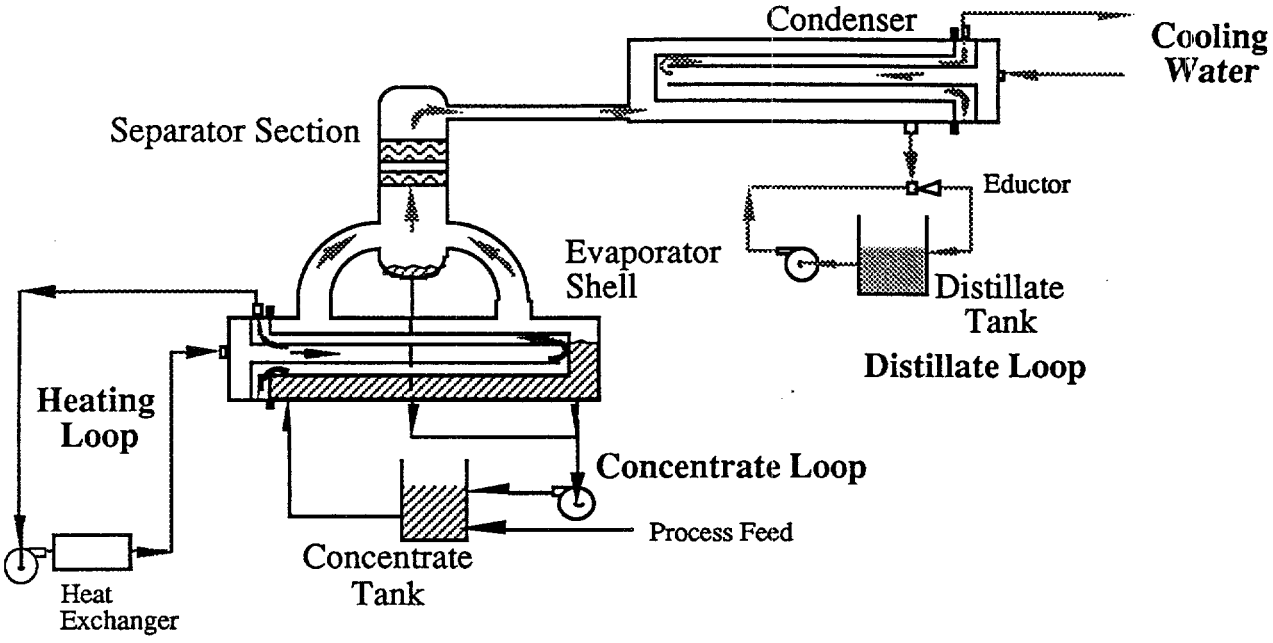

Fig. 27. Flow Schematic for LICON Evaporator

pump, where it is returned to the concentrate tank. Flow rates are about 10 times the distillate production rate to improve heat transfer in the evaporator shell and to reduce solids settling.

3. Artisan Rototherm
(D. G. Wygmans)

Artisan Industries, Inc. (Waltham, MA) has developed a concentrator called "Rototherm" that appears to be well suited to the mission of the concentrator within the CPU. The Rototherm is a horizontal, agitated-film concentrator able to handle high-solids slurries. A schematic of the Rototherm is shown in Fig. 28. The counter-current flow of vapor and feed make the unit energy efficient. The turbulent thin film created by the rotor minimizes dry spots and fouling of the heat-transfer surface, allowing the processing of highly viscous feeds and the generation of a highly concentrated product, up to granulates and powders if desired. Due to the simplicity of design and a minimal number of parts, remote operation and maintenance are facilitated. Flushing operations are also accomplished easily and with minimal volumes of flushing solution.

Transportable skid-mounted Rototherms have been fabricated by Artisan, as have fully remote-operable units. The Rototherm will be used as a basis for the Hanford waste concentrator. Artisan will be involved in the concentrator design and fabrication for the evaporator/concentrator CPU.

D. Design Criteria
(D. G. Wygmans)

Current plans are for an evaporator/concentrator CPU to be designed for processing the two effluent streams coming from a cesium ion-exchange (Cs-IX) CPU, which is currently in the design phase. Thus, this evaporator/concentrator CPU will be similar in mission to both EV-2 and EV-4 in the Case BETA flowsheet (Fig. 23). Preliminary design criteria were generated, outlining the mission

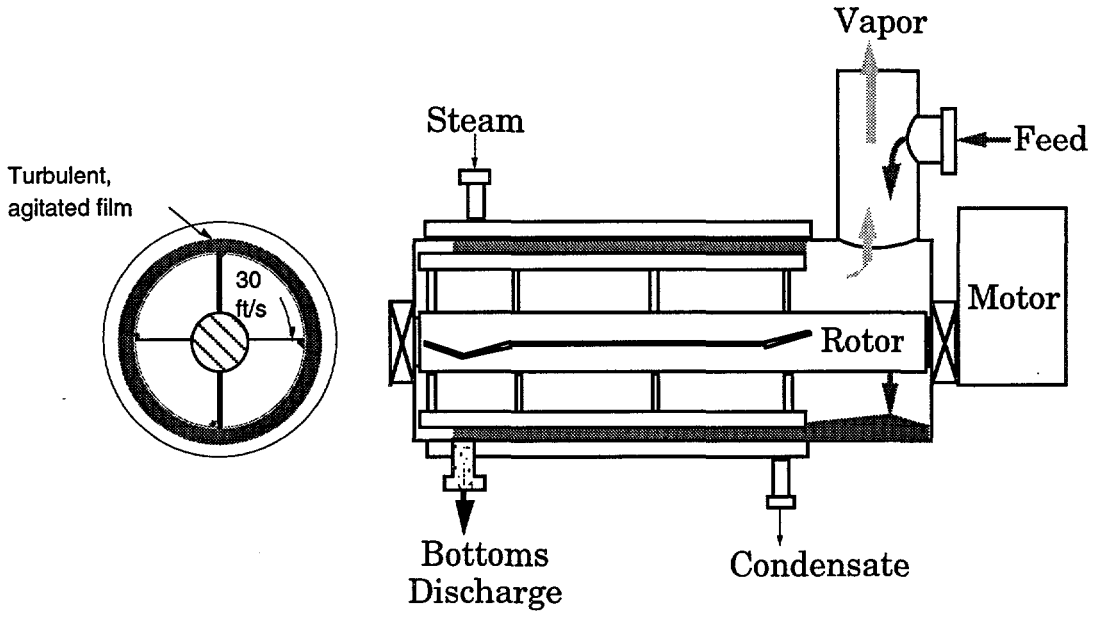

Fig. 28. Schematic of Artisan Rototherm

of the evaporator/concentrator CPU and the functional design requirements for such a unit. These preliminary design criteria were used to guide the drafting of a test plan, outlined under Sec. IV.F.2. A brief summary of the contents of the preliminary design criteria follows.

The CPU will be used in demonstrations for two years. During the first year, the CPU will be employed to concentrate the low-level waste (LLW) stream from which the cesium has been removed. The evaporator/concentrator system shall be designed such that maintenance-free operation is possible for this demonstration. After the LLW processing demonstration, the system will be returned to a state such that another year of maintenance-free operation is possible during demonstration of the high-level waste (HLW) processing. During the second year, the CPU will be used to process either a simulated or real acidic eluant from the Cs-IX CPU.

During the first year's demonstration, the evaporator/concentrator CPU will be used to process the raffinate from the Cs-IX CPU. The Cs-IX CPU and evaporator/concentrator CPU will operate in series, with the Cs-IX CPU removing the cesium from the contents of one Hanford tank and the evaporator/concentrator CPU concentrating the processed stream. Tank 241-AW-101, a 1,000,000 gal (4,000,000 L) double-shell tank, has been chosen for this demonstration. The chemical composition of the waste in Tank 241-AW-101 is given in Table 27; the radionuclide composition of the tank waste is listed in Table 28. The cesium-removal CPU is being designed to remove approximately 95% of the cesium. Other radionuclides will not be removed to a significant extent. The evaporator/ concentrator CPU will be designed to remove most of the free water from this stream, producing a thick but pumpable concentrate slurry.

The HLW processing demonstration for the evaporator/concentrator CPU is not fully specified at present. The purpose of the demonstration is to (1) prove the principle of nitric acid recovery from the Cs-IX CPU eluant, (2) design for operation in a radiation field similar to that encountered by EV-2 and EV-3 within Case BETA, and (3) concentrate the cesium-containing waste stream to a form suitable for neutralization and storage or direct feeding to the HLW vitrification facility.

Table 27. Chemical Composition of Tank 241-AW-101

Constituent	Average Concentration	Constituent	Average Concentration
Aluminum	1.0 E+00M	Sodium	1.0 E+01M
Arsenic	< 1.3 E-07M	Titanium	< 9.9 E-05M
Barium	< 6.8 E-05M	Uranium	9.4 E-04M
Bismuth	< 5.8 E-04M	Zinc	< 4.8 E-03M
Cadmium	< 1.1 E-05M	Zirconium	< 5.5 E-04M
Calcium	8.3 E-04M	Ammonia	1.5 E-02M
Chromium	3.1 E-03M	Carbonate	2.1 E-01M
Copper	< 3.8 E-04M	Chloride	1.5 E-01M
Iron	< 7.9 E-04M	Cyanide	1.0 E-03M
Lead	1.5 E-03M	Hydroxide	5.1 E+00M
Magnesium	2.2 E-03M	Fluoride	< 4.0 E-03M
Manganese	4.8 E-04M	Nitrite	2.2-E+00M
Mercury	7.8 E-07M	Nitrate	3.5 E+00M
Molybdenum	6.0 E-04M	Phosphate	2.2 E-02M
Potassium	1.1 E+00M	Sulfate	1.1 E-02M
Selenium	4.2 E-07M	TOC[a]	2.5 E+00 g/L
Silicon	< 4.4 E-03M	Water	4.4 E+01 wt%
Silver	< 3.1 E-04M	Density	1.6 E+00 g/mL

[a]TOC = total organic carbon.

Table 28. Radionuclide Composition of Tank 241-AW-101

Constituent	Average Concentration, Ci/L	Constituent	Average Concentration, Ci/L
^{3}H	7.07 E-06	^{129}I	3.03 E-07
^{14}C	3.70 E-07	^{134}Cs	1.53 E-03
^{60}Co	< 2.96 E-05	^{137}Cs	5.20 E-01
^{79}Se	4.80 E-07	^{137}Np	< 3.06 E-03
^{90}Sr	1.08 E-3	$^{239/240}Pu$	1.14 E-06
^{94}Nb	< 6.82 E-05	^{241}Am	1.20 E-06
^{99}Tc	1.52 E-04	$^{243/244}Cm$	5.33 E-08
^{106}Ru	< 3.70 E-03		

Because the system will be used to concentrate the basic tank waste and the acidic ion-exchange eluant, materials of construction must be carefully chosen to minimize corrosion. The processing capacity of the CPU will need to be 2.5 gal/min (9.5 L/min), with a peak capability of 5 gal/min (19 L/min). It is expected that decontamination factors (DFs) in the range of 10^6-10^7 will be required.

E. Evaporator Materials Evaluation

(A. E. V. Rozeveld)

Work was begun to determine the appropriate corrosion tests and candidate materials for the mobile evaporator. The fact that we are designing a unit to process both acidic and basic feeds

complicates matters somewhat, since alloying elements that provide corrosion resistance in one environment may not produce optimum resistance in the opposite environment. To date, discussions have been initiated with Allegheny Ludlum Corp. (Pittsburgh, PA), Haynes International Inc. (Kokomo, IN), and Inco Alloys International (Huntington, WV) to determine suitable alloys for testing. The ASTM specifications for corrosion testing tend to be guidelines rather than rigid specifications (except in some specific cases); the corrosion tests should reflect actual operating conditions as closely as possible. Some considerations are as follows:

- specimen shape and surface finish
- weld vs. general corrosion
- test solution temperature and velocity
- test duration

Test solution compositions will be modeled after the waste in Tank 241-AW-101 (Tables 27 and 28) and after the Cs-IX CPU eluant as estimated by the Aspen model for Case BETA (Sec. IV.B).

Plans are underway for completing corrosion tests of candidate materials. Planned tests include vapor, liquid junction, and liquid immersion testing. These tests will be completed by CC (Cortest Columbus) Technologies in Columbus, OH. Test materials currently under consideration include 304L and 316L stainless steel, AL-6XN, Incoloy 800, Inconel 625, Inconel 617, Incoloy 825, Inconel 690, Hastelloy G-30, and titanium. The corrosion rates in HNO_3, NaOH, and HNO_3-HF environments will be evaluated. The HNO_3-HF corrosion rates are of interest because CaF_2 may form some of the scale which will build up during evaporator operation; this scale is normally removed by flushing the unit with 1M HNO_3.

With regard to the laboratory-scale evaporator tests, there were some questions about the effect of HNO_3 on the evaporator's PVC components. We were informed by LICON that PVC and chlorinated PVC (CPVC) materials, of which the laboratory-scale evaporator is made, could possibly swell when exposed to nitric acid. A literature search was conducted, but nothing was found that addressed swelling. We thus set up our own immersion tests for PVC and CVPC in HNO_3; weight and dimensional changes were measured.

To obtain a preliminary assessment of the effect of HNO_3 exposure, samples were sawed from a piece of PVC pipe and a CPVC fitting. These samples were immersed in 2M and 16M HNO_3 at temperatures of 50, 60, and 70°C. Initially, four samples were immersed at 70°C (158°F) for 72 h. All the samples underwent a weight increase (see Table 29); the largest increase was 2.87%. Further samples were tested at 50°C and 60°C (122°F and 140°F), temperatures at which the evaporator will be run. These samples were immersed for 382 hours. All samples gained weight, as shown in Figs. 29 and 30.

Table 29. Weight Gain of Plastics Exposed to HNO_3 for 72 Hours

Sample No.	[HNO_3], M	Temp., °C	Wt. Gain, %
PVC-2	2	70	0.35
CPVC-2			0.46
PVC-4	16	70	1.75
CPVC-5			2.87

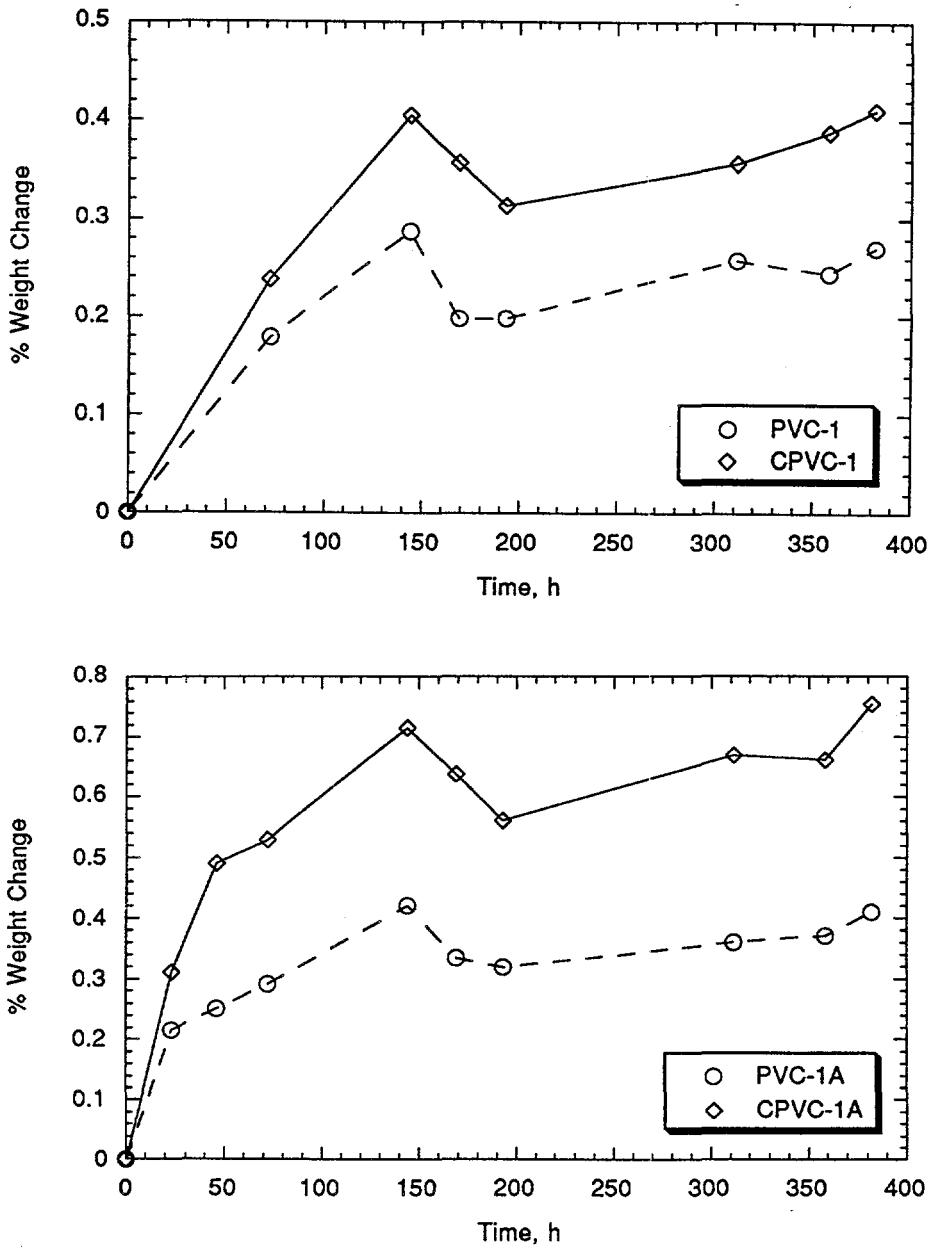

Fig. 29. Percent Weight Change of PVC and CPVC Samples in 2M HNO_3 at 50°C (top) and 60°C (bottom)

The American Society for Testing of Materials (ASTM 5260) lists three criteria for chemical resistance of PVC and CPVC: linear swelling, change in weight, and change in Shore hardness. These quantities are to be measured after exposure of standard specimens (ASTM 543) to the chemical for 30 days (720 h). Because of the irregular dimensions of our samples, change in weight was used to examine the resistance to HNO_3 in these tests. In ASTM 5260, a weight change of <1% is considered resistant, <10% marginally resistant, and >10% non-resistant. The largest weight changes for our samples at the most severe condition were 1.67% and 1.52% after 382 h. The estimated testing time with HNO_3 for the evaporator is 50-70 h. At 72 h, the largest weight increases were 0.81% and 0.84% in 16M HNO_3 at 60°C. These materials are not resistant to HNO_3 by ASTM standards, but we are not

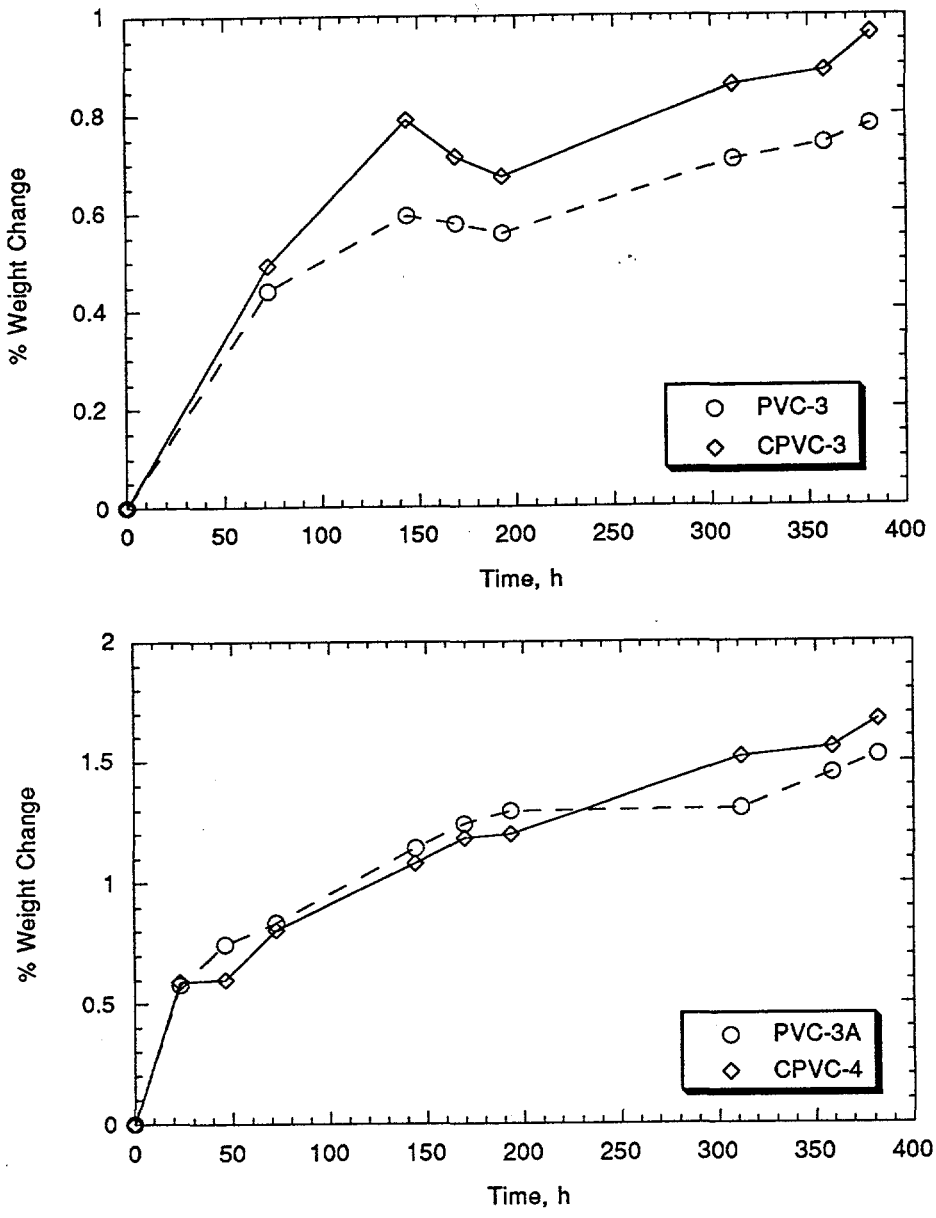

Fig. 30. Percent Weight Change in PVC and CPVC Samples in 16M HNO_3 at 50°C (top) and 60°C (bottom)

concerned with 720 h or more of exposure. Our test conditions (70 h or less) satisfy our requirements. Thus, in our case, the material can be considered resistant to HNO_3.

The PVC and CPVC samples tested for resistance to HNO_3 were weighed after 288 h out of solution to determine weight loss, if any. Weight loss did occur, and the data are tabulated in Table 30. Weight losses ranged from 0.25 to 0.63 wt%. The data from PVC and CPVC samples immersed in H_2O for 430 h under similar test conditions are reported in Table 31. These data confirm that some weight change occurs (0.28-0.41 wt%) in a mild environment such as deionized water. Again, data further support our conclusion that nitric acid can be processed in our laboratory-scale evaporator.

Table 30. Weight Loss after Exposure to Air for 288 h after Immersion Testing

Sample	Test Conditions (in HNO_3)	Weight after HNO_3 Exposure, g	Weight Loss, %
PVC-1	2M, 50°C	3.0349	0.25
CPVC-1		1.8583	0.33
PVC-1A	2M, 60°C	2.7944	0.34
CPVC-1A		1.2956	0.60
PVC-3	16M, 50°C	3.4745	0.26
CPVC-3		1.7396	0.34
PVC-3A	16M, 60°C	3.1358	0.63
CPVC-4		1.0831	0.45

Table 31. Weight Increase after Immersion Testing for 430 h in H_2O

Sample	Test Conditions	Initial Weight, g	Weight Increase, %
PVC-50	H_2O, 50°C	2.6084	0.28
CPVC-50		1.8270	0.29
PVC-60	H_2O, 60°C	2.9050	0.33
CPVC-60		1.8948	0.41

A literature search indicated that PVC and CPVC are resistant to swelling in 4-5M (~15%) NaOH at temperatures up to 60 and 80°C, respectively; the laboratory-scale evaporator will be operated at 50-60°C. We are interested in NaOH solutions because these are typically found in underground storage tanks at Hanford. Based upon this information, operation of our evaporator with NaOH solutions will not pose any materials-related problems.

The Signet flow sensors for the laboratory-scale evaporator have alumina bearings; a literature search and discussions with Technical Support at Signet verified that the bearings are resistant to HNO_3.

F. Laboratory-Scale Evaporator
(D. G. Wygmans)

A LICON model C-3 evaporator is being used for laboratory-scale evaporation studies. The unit is a typical LICON single-effect evaporator, with the major piping components made of plastic (PVC and CPVC). A computer-based data-acquisition system, along with appropriate sensors, is being added to the evaporator to monitor process and operational data. A test plan to guide the experimental work in support of the Tank Waste Remediation System (TWRS) was written, and the first test in the test plan was conducted. Studies were also undertaken to determine the long-term effects of acids on the plastic piping.

1. Data Acquisition System
(D. G. Wygmans)

The data-acquisition system is being designed to monitor the operation of the laboratory-scale evaporator. Our previous work had centered around choosing appropriate hardware and software for the system. This equipment was purchased during this report period. A Signet

magnetic-paddle-wheel-type flow meter, model number 8500, was selected for the concentrate loop. Paddle wheel sensors had previously been eliminated from consideration because of concerns over solids collection on the wheel. However, given the difficulty of finding a suitable sensor for this application and the ease with which this flow meter can be disassembled and cleaned, this concern has become less important.

As the software and hardware components arrived, the software design, hardware installation, wiring, and calibration procedures were undertaken. The design and installation were complete enough to use the data-acquisition system during the first of the laboratory-scale tests. Modifications to the data-acquisition system will be undertaken as necessary, including the addition of more sensors and the refinement of the software design.

2. Laboratory-Scale Test Plan
(D. G. Wygmans)

In support of the TWRS work, a battery of tests, using a number of waste-stream simulants, will be conducted with the LICON C-3 evaporator. A test plan was drafted to guide the experimental work. This plan is summarized below.

Initially, information regarding the following processing parameters will be sought:

- scaling tendencies and scale-removal techniques
- volume reduction and solids formation
- solids handling
- product quality
- decontamination factors (DFs)
- foaming tendencies and abatement
- boiling-point elevations
- distillate composition during acid evaporation

Much of the information gleaned from the tests will be qualitative in nature. The main indicators of DFs will be conductivity and pH measurements for the concentrate and distillate streams. Should further study of DFs be desirable, a samarium spike may be added to a feed so that samples can be sent to the University of Illinois for neutron activation analysis. Besides the information on the process parameters listed above, these tests will provide valuable operating experience, especially with the new data acquisition system.

Six simulated waste streams are foreseen as the feed solutions for Tests 1-6. Test 1 will use a feed stream simulating waste from Tank 241-AW-101 (Table 27). (According to current plans, Tank 241-AW-101 will be processed during the first year of the hot demonstration for the evaporator/concentrator CPU, currently scheduled for FY 1997.) The concentrations reported in Table 27 are of the raw waste as it exists in the tank; these concentrations could be diluted by as much as a factor of three during cesium removal. A major goal during Test 1 is to determine the concentration that can be achieved before solids formation becomes a problem.

Four of the remaining tests (Tests 2-5) will use feeds simulating four streams that may be generated during Case BETA-flowsheet (Fig. 23) processing of Hanford tank waste. The compositions of these four waste streams are highly variable and will likely change. Feeds to the

evaporator systems as specified in the Aspen model are given in Tables 32 through 35. The goals for each evaporator system, as specified in the Aspen model, are outlined below. This information will be used to guide the tests.

Table 32. Feed for Test 2 (EV-1 Feed Simulant)

Component[a]	Wt%	Concentration, M
H_2O	86.07	—
TDS	13.88	—
TSS	0.04	—
TOC	0.01	—
$Al(OH)_4^-$	2.98	4.08E-01
Cl^-	0.01	2.38E-03
$Cr(OH)_4^-$	0.11	1.17E-02
F^-	0.01	1.01E-02
Na^+	5.34	3.02E+00
OH^-	1.65	1.26E+00
Si	0.00	8.28E-05
CO_3^{2-}	0.03	7.39E-03
NO_2^-	0.14	3.99E-02
NO_3^-	1.45	3.05E-01
PO_4^{3-}	2.35	3.22E-01
SO_4^{2-}	0.03	3.61E-03

[a]TDS = total dissolved solids;
TSS = total suspended solids;
TOC = total organic carbon.

Table 33. Feed for Test 3 (EV-2 Feed Simulant)

Component	Wt%	Concentration, M
H_2O	98.07	—
TDS	1.93	—
TSS	—	—
TOC	—	—
$Al(OH)_4^-$	—	—
Cl^-	—	—
$Cr(OH)_4^-$	—	—
F^-	—	—
H^+	0.02	2.47E-01
Na^+	0.09	4.29E-02
Si	—	—
CO_3^{2-}	—	—
NO_2^-	—	—
NO_3^-	1.64	2.91E-01
PO_4^{3-}	—	—
SO_4^{2-}	—	—

Table 34. Feed for Test 4 (EV-3 Feed Simulant)

Component	Wt%	Concentration, M
H_2O	99.76	—
TDS	0.18	—
TSS	0.06	—
TOC	—	—
$Al(OH)_4^-$	0.01	1.68E-03
Cl^-	0.00	9.79E-06
$Cr(OH)_4^-$	0.00	4.82E-05
F^-	0.00	4.19E-05
Na^+	0.07	3.13E-02
OH^-	0.04	2.32E-02
Si	0.00	3.42E-07
CO_3^{2-}	0.00	3.05E-05
NO_2^-	0.00	1.04E-03
NO_3^-	0.01	1.26E-03
PO_4^{3-}	0.01	1.33E-03
SO_4^{2-}	0.00	1.49E-05

Table 35. Feed for Test 5 (EV-4 Feed Simulant)

Component	Wt%	Concentration, M
H_2O	82.01	—
TDS	17.99	—
TSS	0.00	—
TOC	0.06	—
$Al(OH)_4^-$	1.04	1.65E-01
Cl^-	0.03	1.47E-02
$Cr(OH)_4^-$	0.02	3.07E-03
F^-	0.08	6.30E-02
Na^+	5.65	3.68E+00
OH^-	1.05	9.26E-01
Si	0.00	5.15E-04
CO_3^{2-}	0.09	2.37E-02
NO_2^-	0.80	2.60E-01
NO_3^-	7.99	1.93E+00
PO_4^{3-}	0.63	9.89E-02
SO_4^{2-}	0.14	2.24E-02

Test 2 will simulate an LLW system for concentrating the alkaline supernatant liquid from sludge-washing operations. The Aspen model assumes that 67 wt% of the water in the feed will be recovered in the distillate, and that the concentrate will be a solution, with virtually no suspended

solids. Therefore, no concentrator is desired. Test 2 will use a simulant for EV-1 feed (Table 32) and will aim at attaining these water recovery and concentrate product goals.

Test 3 will simulate an LLW unit for recovering nitric acid from the Cs IX eluant while concentrating the cesium product. The recovered acid will be recycled back to the Cs IX system for reuse in regenerating the IX medium. The Aspen model assumes that 70 wt% of the acid and 99 wt% of the water in the feed will be recovered in the distillate. The concentrated, high-solids slurry will be neutralized and stored and eventually pumped to the HLW vitrification facility. Test 3 will use a simulant for EV-2 feed (Table 33).

Test 4 will simulate an HLW unit for concentrating the alkaline liquid centrifuged from the washed sludge. The Aspen model assumes that 99 wt% of the water in the feed will be recovered in the distillate. The concentrated, high-solids slurry will be returned to the centrifuge. Test 4 will use a simulant for EV-3 feed (Table 34).

Test 5 will simulate an LLW unit for concentrating the alkaline tank-waste supernatant liquid from which the cesium has been removed. The Aspen model assumes that 78 wt% of the water in the feed will be recovered in the distillate. The concentrated, high-solids slurry will be sent to the LLW vitrification facility. Test 5 will use a simulant for EV-4 feed (Table 35).

Since high-solids slurries are desired from EV-2, EV-3, and EV-4, concentrators will be needed as part of each of those systems. Tests 3-5 will determine how well the stated distillate recovery goals can be met in a LICON evaporator; it is understood that further concentration and distillate recovery in a concentrator will be needed. Results from the evaporator tests will be used in planning concentrator tests.

Test 6 will use a feed simulating a waste stream as retrieved from Hanford Tank 241-SY-101 (Table 36). The simulant accounts for a factor of 3.8 volume dilution during retrieval operations. This waste was chosen because it has been cited as a possible alternative for the feed stream to the evaporator/concentrator CPU during the hot demonstration. It is also important because

Table 36. Chemical Composition of Hanford Tank 241-SY-101 Simulant

Constituent	Concentration	Constituent	Concentration
Sodium	3.7E-00 M	Nitrate	7.9E-01 M
Aluminum	5.0E-01 M	Nitrite	9.6E-01 M
Chromium[a]	3.3E-02 M	Hydroxide	7.2E-01 M
Calcium	2.4E-03 M	Phosphate	2.8E-02 M
Iron	2.1E-03 M	Sulfate	1.7E-02 M
Potassium	3.5 E-02 M	TIC[b]	2.2E-01 wt%
Nickel	1.1E-03 M	TOC[c]	5.3E-01 wt%
Zinc	1.3E-04 M	Water	7.8E+01 wt%
Cesium	4.4E-05 M	Suspended Solids	none
Strontium	2.9E-06 M		
Fluoride	6.7E-03 M		
Chloride	9.3E-02 M	Density	1.2E+00 g/mL

[a]Cr(VI) is small compared to total Cr and is not added.
[b]TIC = total inorganic carbon, made up using carbonate.
[c]TOC = total organic carbon, made up using EDTA.

of its high concentration of organics, e.g., ethylenediamenetetraacetic acid, that are present in many Hanford tanks. Major concerns during this test include (1) when solids formation begins, (2) how far the waste can be concentrated effectively in a LICON evaporator, and (3) what problems are generated by the high concentration of organics.

The tests will not necessarily be run in numerical order. A safety review for evaporation of acidic solutions must be conducted before Test 2 can begin. In general, about 80 L of feed for each test will be used. (Arrangements are being made for acquisition of 200 L of the feed for Test 6.)

The first step in each test will be to attempt to evaporate the feed until about 8 L of concentrate remains in the concentrate tank, for a concentration factor (CF) of 10. At that time, the product distillate will be discharged from the system. This portion of the tests will take about a day (6-8 h) of evaporating near the system's capacity (15 L/h). At that point a decision will be made about whether further concentration is desired or feasible. If desired, evaporation of the concentrate can continue up to a CF of about 20; the laboratory-scale evaporator has a lower operating limit of about 5 L of concentrate. Furthermore, concentrated feed can be made and added to the concentrate tank should CFs beyond 20 appear desirable.

To determine scaling tendencies and solids-handling capabilities, extended operating times at high CFs will usually be desired. In such cases the distillate will be recycled to the concentrate tank once high CF's have been attained. Thus, the system can be made to cycle between two relatively high CFs (e.g., 10 and 20). One or two days of operation (8-16 h) in this recycle mode should be sufficient for predicting trends. Investigation into scale removal and flushing techniques will center around the use of acid solutions circulated through (although not necessarily evaporated in) the evaporator shell.

3. Test No. 1
(D. G. Wygmans)

Test 1 in the battery of tests planned for this project was begun. The laboratory-scale evaporator was used to process a feed simulating diluted waste from Hanford Tank 241-AW-101. The feed composition, given in Table 37, represents the tank waste diluted by a factor of three because this dilution will probably be necessary before the waste can be processed in the Cs-IX CPU.

Approximately 45 L of feed was evaporated down to 11 L of concentrate over about 8-1/2 hours of operation spanning three days. Thus, a feed CF of more than 4 was achieved. (The raw tank waste CF was about 1.4.) The boiling-point elevation (BPE) was about 14°C at this concentration factor. Figure 31 shows the CF and BPE over the length of the test. The data points for non-steady-state operation (startup) have been eliminated from the chart to make the temperature trends more continuous. The temperature fluctuations seen in the chart are largely due to the adjustment of operating parameters (e.g., cooling-water flow rate, heating water temperatures) during the run. As seen in Fig. 31, the BPE when a CF of 3 had been attained (original tank-waste concentration attained) was about 11°C.

No major operational difficulties were encountered during the testing. It appeared that any solids generated during the test settled in the tank as they were generated. The tank was stirred prior to processing each day, and for a short period the solids could be seen in the concentrate feed, making the solution opaque. However, within a few minutes the liquid was transparent again and remained that way throughout the day's processing. A foam could be seen in the evaporator-shell

Table 37. Chemical Composition of Feed Simulating Diluted Waste from Hanford Tank 241-AW-101

Compound	Mass,[a] g	Final Concentration,[b] M
Na_2CO_3	600	7.08×10^{-2}
Na_2SO_4	41.8	3.68×10^{-3}
NaCl	234	5.00×10^{-2}
$NaNO_2$[c]	5210	9.44×10^{-1}
$NaNO_3$	2050	3.01×10^{-1}
Na_2SiO_3	14.5	1.5×10^{-3}
NaOH	4920	1.54
$Al(NO_3)_3 \cdot 9\ H_2O$	9480	3.16×10^{-1}
$Mg(NO_3)_2 \cdot 6\ H_2O$	15.1	7.37×10^{-4}
$Na_3PO_4 \cdot 10\ H_2O$	222	7.30×10^{-3}
KOH	1630	3.63×10^{-1}
NH_4NO_3	32.0	5.00×10^{-3}

[a]Mass for 80 L of solution.

[b]Final composition of the 80 L of solution.

[c]Due to a calculation error too much sodium nitrite was added. The final nitrite concentration should have been 0.73M.

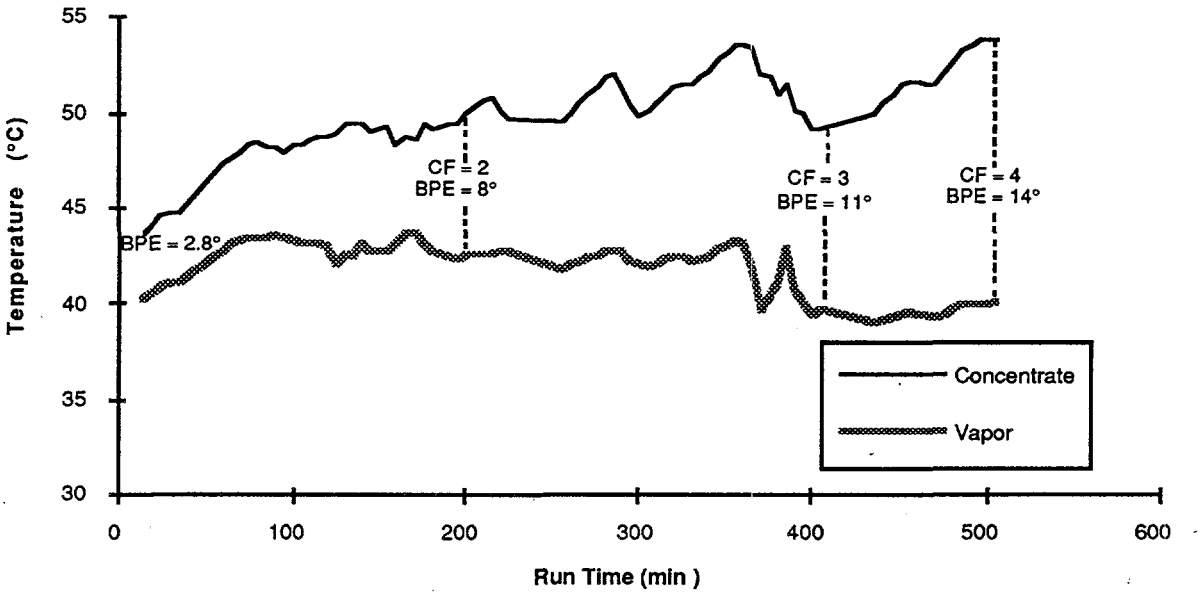

Fig. 31. Correspondence between Boiling-Point Elevation (BPE) and Concentration Factor (CF) during Test 1

sight glass window during the time when the solids were in suspension, but this foam went away as the liquid cleared up and did not return until the concentrate tank was stirred again. The evaporator-shell heat-exchanger tubes were pulled, dried, and weighed both before and after the 8-1/2 hours of testing. The tubes gained 1.2 g of mass over the course of the run, but this mass is most likely due not to scaling but to a film which seemed to coat all parts that were in contact with the concentrate. This film can be seen evenly distributed on the tube bundle and tube sheet, whereas scaling is expected to

be heaviest on the portions where boiling occurs on the tubes (i.e., on the top tube mostly and almost non-existent on the tube sheet).

The conductivity of the distillate rose rapidly at the beginning of the test and stabilized at about 70 μS/cm, where it remained throughout the remainder of the test. Measurements showed that the pH of the distillate was in the range of 9.5-11.0 throughout the test. It is suspected that the ammonia in the feed evaporated and then condensed in the distillate, raising the conductivity and pH of the distillate.

The testing so far indicates that the water of dilution can be evaporated from the tank waste without difficulty from solids generation, foaming, scaling, or boiling-point elevation. Because of undissolved solids in the feed, which were not expected in this simulant, the exact composition of the feed is in question. Further testing will be done on newly made simulant. Testing will attempt to determine any parameters that will limit the concentration factor that can be attained in a LICON evaporator for this feed.

V. TECHNICAL SUPPORT FOR ANL WASTE MANAGEMENT

(D. B. Chamberlain, C. Conner, K. Foltz, J. Sedlet, S. A. Slater, B. Srinivasan, and D. G. Wygmans)

The Separation Science and Technology Section is cooperating with ANL Waste Management to develop treatment processes for all liquid waste stored or being generated at ANL. Early work was directed toward the treatment of mixed waste slurries; a hydroxide/sulfide precipitation process followed by filtration was developed for this waste. Work was also completed in support of an evaporator/concentrator upgrade project. Technical support tasks in FY 1994 include (1) installation, testing, and startup of the new evaporators and concentrators, (2) testing of the mixed-waste treatment system, (3) development, installation, and testing of a TRU waste treatment system, and (4) development of a process to treat liquid scintillation cocktail waste.

A. Treatment of Mixed Waste

(D. B. Chamberlain)

The mixed-waste treatment system is designed to treat aqueous mixed wastes that contain hazardous metals (Pb, Cd, Cr, Ag, and Hg) and/or have a corrosive composition (pH >12.5 or <2). It consists of a chemical treatment which adjusts the pH and precipitates the metals by alkaline sulfide precipitation. The chemical treatment is followed by filtration, in which the solids are separated from the liquid by a variety of filters. A modular design allows the filtration scheme to be varied for research purposes and for treatment of different influents.

1. Chemical Treatment

a. Laboratory Tests of Chromium Solution Treatment

(B. Srinivasan and J. Sedlet)

Procedures for the treatment of Davies-Grey waste and Cr(VI)-containing waste in sulfuric acid were described in the previous semiannual report. During this reporting period, experimental work was performed to determine if the procedure devised for the latter waste [Cr(VI) in sulfuric acid] was applicable to Cr(VI) in nitric acid. This procedure consisted of the following steps:

- Determination of Cr(VI) concentration in the waste by titration of a small volume against a standard solution of ferrous sulfate.
- Reduction of Cr(VI) to Cr(III) in the bulk of the waste by the addition of the requisite amount of ferrous sulfate solution as determined in the titration.
- Precipitation of Cr(III) by the addition of base, which in this case was a calcium hydroxide slurry.

This procedure was found to be satisfactory for Cr(VI) in nitric acid solution, providing that the acid concentration was 5M or less.

b. Testing with Waste Simulant

(C. Conner)

The chemical treatment was tested using a waste simulant solution containing 2M HNO_3 and 25 g/L of copper nitrate. A lime slurry was prepared by mixing 800 g CaO in 10 L of

water. Hydrating the calcium oxide resulted in a 15°C temperature rise. The waste solution was then metered into the treatment vessel by means of a diaphragm pump and pH controller. When the controller stopped adding waste solution to the calcium hydroxide slurry at a pH of 10, the final temperature was 42°C. The pH controller was disabled and the sulfide controller activated. A 2M Na_2S solution was then metered into the treatment vessel. Sulfide addition was stopped by the controller when the meter indicated a voltage of -720 mV, at the final pH of 11.5*; this equates to total free sulfide concentration of ~1 ppm. The treated liquid was moved to a 50 L carboy for eventual filtration through the filter skid. The precipitate settled to the bottom of the carboy, leaving a clear supernatant. All of the equipment functioned exactly as planned, and this cold test successfully demonstrated the process, taking 2.5 h to complete. The system was then tested by using actual waste solutions.

c. Testing with Actual Waste
(C. Conner)

Several solutions of actual mixed waste were processed in the chemical treatment portion of the mixed-waste treatment system. Table 38 gives composition results from inductively coupled plasma-atomic emission spectroscopy (ICP-AES) analysis for the feed solutions. Table 39 shows the activity results from liquid scintillation counting of the samples reported in Table 38.

Table 38. Composition of Feed Solutions Used to Test the Mixed-Waste Treatment System

	Composition,[a] ppm									
No.	Se	As	Pb	Cd	Ag	Cr	Ba	U	Mo	Fe
RW 21120	<0.15	<0.15	66.3[b]	0.80	<0.02	1.11	0.14	N/A	N/A	N/A
RW 21336	<0.15	<0.15	34.1[c]	0.45	<0.02	0.60	0.20	N/A	N/A	N/A
RW 21358	<0.15	<0.15	6.0	1.36	<0.02	0.84	1.95	N/A	N/A	N/A
RW 21828	<0.15	<0.15	<100	<0.02	<0.02	<0.02	0.01	N/A	N/A	N/A
RW 22213[d]	N/A	N/A	<0.5	<0.5	N/A	24	<0.03	94	95	2200

[a]Analyzed by ICP-AES; N/A means not analyzed.
[b]Reanalyzed by ICP-AES; second analysis indicated 61.4 ppm lead.
[c]Reanalyzed by ICP-AES; second analysis indicated 31.9 ppm lead.
[d]This bottle contained Davies-Grey titration waste. Davies-Grey waste is well characterized and contains only chromium as a hazardous metal.

Processing these wastes, except for RW 21120, was accomplished by using our developed procedure. Unfortunately, the 30-min mixing step after addition of sulfide was inadvertently omitted. This mixing step ensures complete conversion of hydroxide precipitates to sulfide precipitates. A bottle of Davies-Grey titration waste, RW 22213, was also processed by the developed procedure and a modified version in which sodium hydroxide was used instead of calcium hydroxide. Sodium hydroxide was substituted to prevent the formation of calcium phosphate. Davies-Grey waste is rich in phosphoric acid (~3M), which forms a calcium phosphate sludge when neutralized with calcium hydroxide. This sludge makes subsequent filtration difficult. After

*Sulfide addition causes the pH of the solution to rise by conversion of the metal hydroxides to metal sulfides.

processing each of the wastes, a sample of the resultant slurry was taken. The solids were removed by filtration through a 0.2 μm filter, and the supernatant analyzed by ICP-AES. The results are shown in Table 40.

Table 39. Activity of Feed Samples from the Mixed-Waste Treatment System (determined by liquid scintillation counting)

	Activity, dpm/mL		
Feed Samples	Tritium	Beta	Alpha
RW 21120	216	<1	<1
RW 21136	53	28	27
RW 21358	430	238	<1
RW 21828	<1	<1	<1
RW 22213[a]	432[b]	88	209

[a]Results very unreliable for this sample. Precipitates in scintillation cocktail.
[b]Probably beta activity from higher energies.

Table 40. Composition of Supernatant Following Treatment

	Composition,[a] ppm									
No.	Se	As	Pb	Cd	Ag	Cr	Ba	U	Mo	Fe
RW 21120	<0.15	<0.15	13.4[b]	<0.02	<0.02	0.025	0.42	N/A	N/A	N/A
RW 21336	<0.15	<0.15	4.6	<0.02	<0.02	<0.02	0.17	N/A	N/A	N/A
RW 21358	<0.15	<0.15	6.0	<0.025	<0.02	<0.02	1.13	N/A	N/A	N/A
RW 21828	<0.15	<0.15	<100	<0.02	<0.02	<0.02	0.095	N/A	N/A	N/A
RW 22213[c]	N/A	N/A	<0.1	<0.05	N/A	1.1	<0.03	13	26	0.14
RW 22213[d]	N/A	N/A	<0.1	<0.05	N/A	<0.05	0.082	<1	0.15	<0.05

[a]Analyzed by ICP-AES.
[b]Reanalyzed by ICP-AES; second analysis indicated 12.0 ppm lead.
[c]Davies-Grey titration waste treated using NaOH.
[d]Davies-Grey titration waste treated using $Ca(OH)_2$.

In order to be classified as non-hazardous, the treated waste must meet the RCRA limits given in Table 41. As can be seen from the results in Table 40, all of the wastes treated were reduced to below RCRA concern, except for lead in RW 21120. In addition, Table 40 shows that treating Davies-Grey waste with $Ca(OH)_2$ is much more effective than NaOH at reducing the metal content of the supernatant. However, both reduced the chromium concentration to below RCRA concern.

The most likely cause for the failure to sufficiently precipitate lead from the waste in RW 21120 is the omission of the 30-min mixing step from the procedure. This omission did not allow for the complete conversion of $Pb(OH)_2$ to PbS. Lead hydroxide has a solubility ~10 ppm at pH=10. Thus, if insufficient sulfide was added to completely convert the lead hydroxide to sulfide, a concentration of ~10 ppm lead would be expected. To determine if the problem was indeed the slow conversion of $Pb(OH)_2$ to PbS, a sample of the mixture RW 21120 plus RW 21358 was taken and additional sulfide added. (Note: After the initial treatment of wastes RW 21120 and RW 21358, they were transferred to the same 50 L carboy.) Analysis results for this mixture are shown in Table 42, which shows all elements below RCRA limits.

Table 41. Resource Conservation and Recovery Act (RCRA) Limits for Toxic Metals

Metal	RCRA Limit, ppm
As	5.0
Ba	100.0
Cd	1.0
Cr	5.0
Pb	5.0
Hg	0.2
Se	1.0
Ag	5.0

Table 42. Analysis of Mixed Wastes RW 21120 and 21358 with and without Extra Sulfide

	Composition,[a] ppm						
	Pb	Cd	Cr	Ba	U	Mo	Fe
Normal Sulfide[b]	1.0	<0.05	<0.05	0.64	N/A	0.11	<0.05
Additional Sulfide	<0.1	<0.05	<0.05	0.71	N/A	0.14	<0.05

[a]Analyzed by ICP-AES.
[b]Sample is a mixture of these two treated effluents from the mixed-waste treatment system.

A 1-L sample of the RW 21120 and RW 21358 mixture was taken for testing. The sulfide concentration in this mixture was determined using a sulfide-specific electrode and meter. The sulfide concentration was below detection levels (~1 x 10^{-6}M). Since the treatment system stops sulfide addition at ~10 ppm (3 x 10^{-4}M), this indicates that additional conversion of hydroxide precipitate to sulfide precipitate occurred after the waste was removed from the treatment process, thus depleting the sulfide to below detection levels. To the mixture of RW 21120 and RW 21358, additional sulfide (10 ppm final concentration) was added over a 30-min period. The 10-ppm sulfide concentration stayed stable for several days, indicating no additional conversion of hydroxide precipitate to sulfide precipitate. This sample was then passed through a 0.2-μm filter and analyzed by ICP-AES (results in Table 42).

Adding additional sulfide to the RW 21120 and RW 21358 mixture reduced the lead from 1.0 ppm to <0.1 ppm; thus, adding more sulfide was effective. The 30-min mixing step to allow complete conversion of metal hydroxides to metal sulfides is very important to the success of the chemical treatment. A sample of the slurry generated after additional sulfide was added to the mixture of wastes RW 21120 and RW 21358 was submitted for analysis by the Toxicity Characteristic Leaching Procedure (TCLP). The solids were separated from the liquid portion and extracted according to the EPA's SW846 Method 1311. Digestion of the extracts used Method 3010A, which were then analyzed by ICP-AES Method 6010A. As can be seen in Table 43, the metal concentrations were below RCRA limits. Thus, the alkaline sulfide precipitation converted the mixed waste into two low level wastes (solid and liquid).

As an added benefit, the alpha and non-tritium beta activity in the supernatants was reduced following chemical treatment. Results from liquid scintillation analysis of

the samples are shown in Table 44 (compare with Table 39). Only those samples with sufficient liquid remaining after analysis by ICP-AES could be counted.

Table 43. Results from TCLP Analysis of Precipitate from Mixed-Waste Processing Equipment

Metal	Concentration, ppm	RCRA Limit, ppm
As	<0.5	5.0
Ba	1.06	100.0
Cd	0.02	1.0
Cr	0.04	5.0
Pb	<0.05	5.0
Se	<0.5	1.0
Ag	0.04	5.0
Hg[a]	0.012	0.2

[a]Mercury analyzed by cold vapor atomic absorption using EPA's SW846 Method 7470.

Table 44. Activity of Product Samples from the Mixed-Waste Treatment System

Product Samples	Activity, dpm/mL		
	Tritium	Beta	Alpha
RW 21120	38	<1	<1
RW 21358	268	129	<1
RW 22213[a]	<1	<1	<1
RW 21828	<1	<1	<1
RW 21136	27	<1	<1

[a]Davies-Grey waste treated using $Ca(OH)_2$.

2. Filtration
(D. G. Wygmans)

A versatile filtration system, incorporating a number of modules, has been designed as shown in Fig. 32. The modular design allows the filtration scheme to be varied for research purposes and for treatment of a variety of influents. As seen in Fig. 32, most modules can either be included in, or isolated from, the flow scheme, as desired.

The bag filter, with filter elements in the 20-40 μm range, traps the bulk of the solids. A bag filter combines the advantages of high solids loading capacity and low disposable-cartridge volume, making this a valuable front-end filter. Plumbing connections in parallel with the bag filter allow the later addition of a filter press or other pre-treatment options, if necessary.

Two prefilters in parallel are included to protect the hollow fiber filter (HFF) from solids loading. Back-flushable sintered-metal elements will normally be used as the prefilters. The metal elements are easily flushed with clean water by reversing the flow through them. If the nature

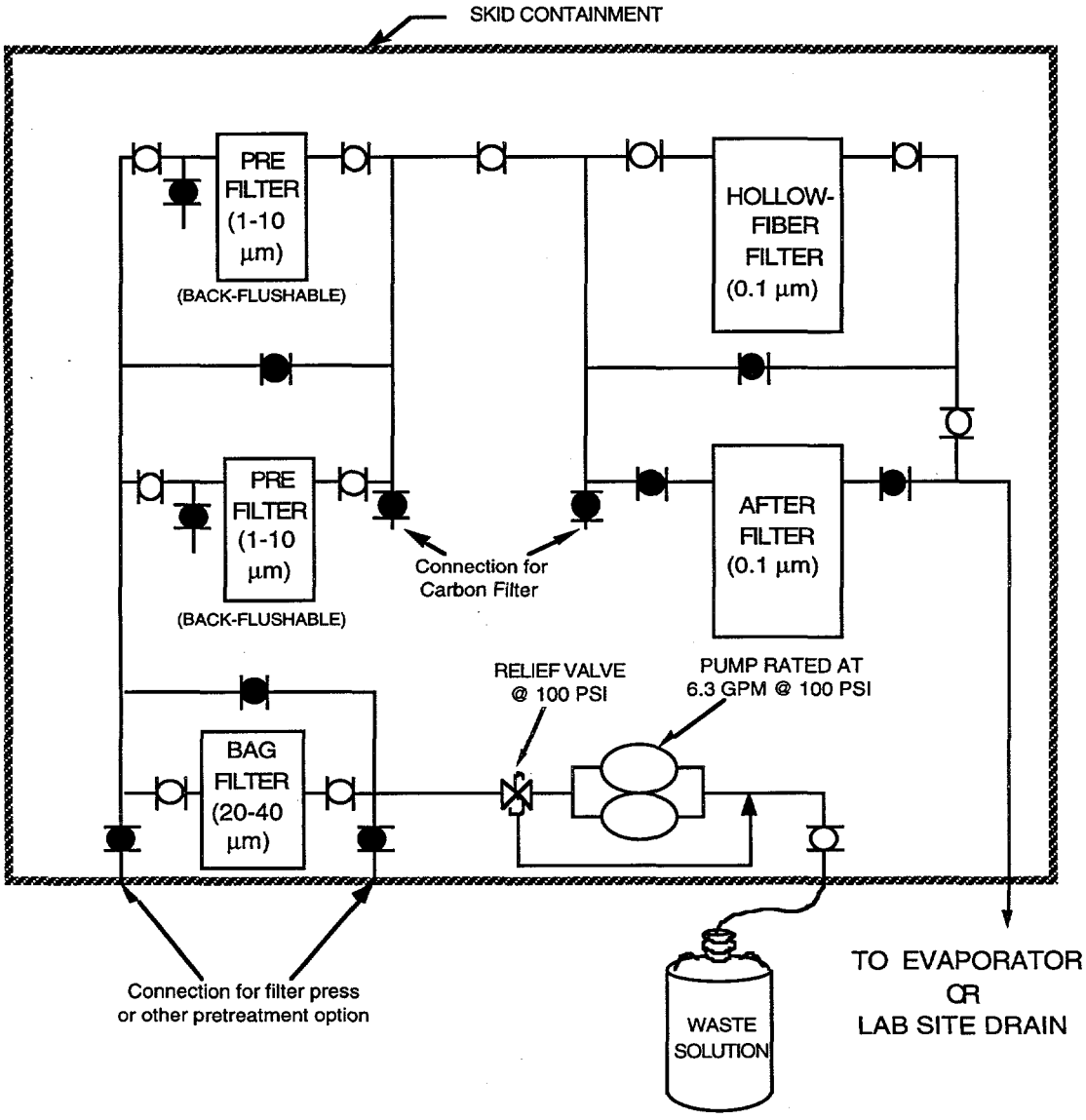

Fig. 32. Schematic for Filtration Skid

or size of the particles trapped by the filter makes flushing inefficient, the sintered-metal cartridge can be easily replaced by a disposable polypropylene cartridge. Pre-filter elements in the 1-10 μm pore size range will be used.

The open connection between the pre-filters and the HFF allows the addition of a carbon filter to adsorb dissolved organics from an aqueous stream. This addition may be necessary if streams containing dissolved organics are to be processed, since such organics would wet the pores of the HFF and plug it. A carbon filter has not been included in the present design for two reasons: (1) present plans do not include processing aqueous streams containing dissolved organics, and (2) incorporation of a suitably sized carbon filter would make the filter skid difficult to transport.

The after-filter, in parallel with the HFF, is included mainly as a backup for the HFF, for streams that cannot be run through the HFF (e.g., streams containing undissolved organics, which

cannot be absorbed by the carbon filter). Pore sizes for the after-filter cartridges will range from 0.1 to 1.0 μm.

The normal flow scheme, as shown in Fig. 32, will incorporate the bag filter, both prefilters, and the HFF. Filter housings accept industry-wide standard cartridges, allowing the use of cartridges in a wide variety of pore sizes available from many manufacturers. Polypropylene filter elements will receive the most use. Each filter housing has pressure gauges upstream and downstream and a sampling valve directly downstream to aid filtration studies.

The feed is pumped through the system by a variable-speed diaphragm pump. The diaphragm pump was chosen mainly because it is seal-less and self-priming, provides trouble free pumping of slurries, and is capable of running dry without damage. A pressure relief valve ensures that the design pressure is not exceeded. A pulsation dampener smooths out the flow pulses generated by the pump.

Operating procedures for the filtration system were written, and a manual is being compiled.

Startup testing on the system was completed. The purpose of this testing was to (1) gain experience in back flushing particulate from the pre-filter and the HFF, (2) test the written procedures for operating and back flushing the system, and (3) gather information regarding the performance of the filtration system during high solids loading of the filter elements. About 80 L of a copper sulfate mixture, generated during cold testing of the chemical treatment system, was processed in the filter skid. The bag filter, one pre-filter, and the HFF were put on-line for the processing.

The feed mixture was stirred during the test in an attempt to keep a high solids feed and quickly load up the filter elements with solids. Since normal processing will involve allowing the waste mixture to settle, then filtering the supernatant liquid only, the amount of solids run through the system in this test was extreme and may represent a full year's worth of solids during normal operation. Because of the rapid high solids loading of the bag filter during the test, a breach in the bag filter developed, so all the solids were loaded on the prefilter and the HFF. The filtrate was clear, indicating that all solids were trapped on the filters. Although the two filter elements underwent extreme solids loading, the back-flushing operations showed relative easy and efficient removal of the solids from these elements.

3. Permitting Requirements
(D. G. Wygmans)

Before processing could begin, documentation and permitting of the mixed-waste treatment system were required under the National Environmental Policy Act (NEPA) and the Resource Conservation and Recovery Act (RCRA). The former regulates work done by government agencies. The latter, which is mandated by the federal government but controlled at the state level, regulates the storage, handling, treatment, and shipment of hazardous wastes. Permit applications under NEPA and RCRA are processed through the ANL office for ESH/QA Oversight, which keeps programs informed of regulations, aids in filing applications, and coordinates treatability studies across the site.

The NEPA application was first submitted on July 23, 1993, requesting that the mixed-waste treatment system (chemical treatment, filtration, and concentration) be covered under

existing Categorical Exclusions (CXs). This request was rejected because of lack of clarity regarding whether the treatment system was to be used for long-term processing or for treatability studies. (If the system is to be used for long-term processing, an Environmental Assessment may be required; treatability studies, by definition, are limited in scope and duration and may be covered under a number of CXs already in place.) Re-submittal was made on September 13, 1993, requesting a CX for treatability studies. A CX was granted on October 27, 1993. After sufficient data have been gathered to prove the principle of the treatment system, another NEPA application will be filed to determine if an Environmental Assessment is needed.

Notification to the Illinois Environmental Protection Agency (IEPA), stating our intent to conduct mixed-waste treatability studies, was made on September 9, 1993. Under the RCRA, this notification is required a minimum of 45 days before the initiation of treatment. This notification, alongside compliance with the constraints defining a treatability study, constitutes compliance with the RCRA. The constraints for a treatability study include, among other things, the limit of 1000 kg on the amount of waste that can be treated in each study. Applications for a RCRA Part B permit, allowing the long-term processing of hazardous wastes, will be made soon so that the permit will be in place once the treatability studies are completed.

Two separate Safety Assessment Reviews (SAR) have been conducted: one for the chemical treatment and one for the filtration; SARs are filed and reviewed within the division in which the work is to occur. The purpose of the SAR is to identify and evaluate all safety-related issues associated with a project. The result of the SARs was to approve the system for processing mixed waste.

B. Transuranic Treatment of Waste
(S. A. Slater)

Aqueous waste solutions containing TRU elements are in temporary storage at the ANL Waste Management (WM) facilities. The TRU Waste Treatment Project involves the volume reduction of the aqueous TRU waste solution and the shipment of the waste to the Waste Isolation Pilot Plant (WIPP) in Carlsbad, New Mexico. The waste acceptance criteria for waste bound for WIPP, the carrier precipitation process to be studied for treating the TRU waste, and the initial results of laboratory-scale carrier precipitation tests are given.

1. Waste Acceptance Criteria
(S. A. Slater)

After processing, the TRU waste will be packaged so that it may be shipped and stored at the Waste Isolation Pilot Plant. The waste acceptance criteria are as follows:

(1) Wastes must be in solid form.

(2) If the waste is in the form of powder or ash or similar particulate material, which could become airborne easily, then the waste must be immobilized. If it can be shown that the waste form will not become easily airborne, then immobilization may not be necessary, and more economical means of fixing the waste can be adopted (see item 3 below).

(3) The ANL waste treatment methods are expected to yield sludge (combination of solids with appreciable amounts of liquid). Solid absorbents (e.g., bentonite, vermiculite) may be used to absorb the liquids.

(4) Residual liquid must not exceed more than 1% by volume in each drum.

(5) The immobilized wastes or absorbed wastes may be packaged in 55-gal drums. The absorbed waste must be packed in a secondary container (steel cans or plastic bags) to prevent the material from becoming airborne.

(6) The specific activity of the waste form shall be >100 nCi/g. The mass of the primary and secondary containers, liners, etc., is excluded from the specific activity calculations. However, the masses of immobilization agents or absorbent materials are included in the specific activity calculations. This could be a problem for some wastes if WIPP requires immobilization using grout or glass. Diluting a sludge whose activity is greater than 100 nCi/g could result in a waste form whose activity is less than 100 nCi/g. A waste package prepared in such a manner is not acceptable either to WIPP (because the specific activity is <100 nCi/g) or to Hanford (because it is in a grouted form).

(7) Explosives and compressed gases are not permitted in the waste containers.

(8) Transuranic-containing mixed wastes are permitted, but additional restrictions apply. They must meet the requirements in the WIPP RCRA Part A and Part B applications.

(9) The mass of a single TRU nuclide that can be placed in a drum is governed by the limits established by total activity and/or wattage considerations. The most restrictive of the two shall apply. Table 45 gives the most restrictive limit for each nuclide in both grams per drum and curies per drum. For all the nuclides, the most restrictive criterion is the wattage limitation, except for U-233, whose most restrictive criteron is the criticality limitation.

Table 45. Nuclide Limits per 55-gallon Drum in Units of Grams per Drum and Curies per Drum

Nuclide	Nuclide Limit in Grams per Drum	Nuclide Limit in Curies per Drum
U-233	2.00E+02	1.95E+00
Np-237	8.60E+03	6.13E+00
Pu-236	9.61E-03	5.16E+00
Pu-238	3.14E-01	5.43E+00
Pu-239	9.22E+01	5.80E+00
Pu-240	2.51E+01	5.77E+00
Pu-241	5.43E+01	5.65E+03
Pu-242	1.54E+03	6.10E+00
Am-241	1.55E+00	5.38E+00
Am-243	2.77E+01	5.59E+00
Cm-242	1.46E-03	4.89E+00
Cm-244	6.28E-02	5.14E+00
Cf-252	4.43E-03	2.41E+00

(10) Surface dose rate of the containers shall not be >200 mrem/h or 10 mrem/h at 2 m.

(11) Removable surface contamination shall not be >50 pCi/100 cm^2 alpha, and not >450 pCi/100 cm^2 beta/gamma.

(12) Packaging of the waste after processing will be done as follows[5] (however, further communications with WIPP are necessary to fill in the details, and no waste should be packaged without certification):

(a) The processed waste will be placed in 55-gal (280-L) drums with a 0.9-in. (2.3-cm) liner of high-density polyethylene. The drum lid will contain a carbon composite filter, and the rigid liner will be punctured.

(b) Vermiculite (#2 grade) will be used to immobilize the waste and twice as much absorbent as needed will be used. Reference 5 suggests using 43 gal (163 L) of vermiculite and 12 gal (45 L) of waste sludge per drum.

(13) Shipping of the waste drums to WIPP is governed by additional regulations mentioned in the WIPP waste acceptance criteria, but is not discussed in this document.

The next steps will be to obtain waste form requisitions from Waste Management to characterize the waste and then determine the steps required to process the waste. Currently, literature searches have been performed to locate relevant precipitation and ion-exchange techniques for the TRU elements: plutonium, neptunium, americium, curium, and uranium-233.*

2. Summary of Treatment Report
(S. A. Slater)

After a literature review of potential processes for treating TRU waste, carrier precipitation was chosen. Our recommendation for carrier precipitation is based on its potential for success and ease and cost of implementation and operation. Carrier precipitation is considered the simplest, most robust, and least costly chemical procedure. The technology is relatively simple; the TRU elements are recovered in a solid phase and a single solution remains to be treated by evaporation/concentration. Evaporation/distillation is a close second. While it is a simple procedure, environmental, safety, and health concerns would make its implementation difficult.

Among the potential carrier precipitation methods, ferric hydroxide has the greatest prospect of early success and will be studied first. In addition, magnetite ($FeO \cdot Fe_2O_3$ or Fe_3O_4) will be evaluated. Boyd and Klochen[6,7] were able to obtain high decontamination factors (approximately 10,000) with magnetite in one precipitation step.

The reverse-strike precipitation can be used if the first (direct strike) precipitation is not sufficient in removing the TRU elements. This second precipitation will be more effective if the solution is acidified first or if a homogeneous precipitation is used. Diphonix and TRU•SPEC columns will also be evaluated for polishing. A homogeneous precipitation will usually produce a more compact and more easily filterable precipitate.

A treatment flow diagram is given in Fig. 33. This figure is intended to show the path of waste through the TRU treatment process and the fate of the various process streams. This diagram

*U-233 exhibits TRU characteristics at concentrations greater than 100 nCi/g.

assumes that carrier precipitation is the waste treatment method and the wastes are classified as being TRU waste and not just waste containing low levels of TRU components. It is also assumed that the TRU concentrations in the waste are high enough that the solid precipitate would be TRU (i.e., >100 nCi/g). A discussion of this treatment tree follows. After the first precipitation step, the resulting slurry is filtered to separate the solids from the liquid. The total solids content and the total alpha activity of the filtrate are then measured. If the filtrate is greater than 100 nCi/g (decision junction A in Fig. 33), then the filtrate must be sent to a second precipitation step. (A column polishing step could also be used at this point.) If the filtrate contains less than 100 nCi/g, then a calculation is needed to determine whether the solids, if processed in the evaporator/concentrator system, will be TRU or nonTRU waste (decision junction B). This decision depends upon the TRU concentration remaining in solution and the amount of dissolved solids present. If TRU waste will be produced, then the filtrate must be sent to the second precipitation step and not processed in the evaporator/ concentrator system.

If TRU waste will not be generated during waste concentration, a decision needs to be made on whether to process the filtrate in the evaporator or concentrator (decision junction C). This decision depends upon the solids content. For high solids, the waste should be concentrated in the concentrator. For low solids, the waste can first be processed in the evaporator. The limit of <0.07 (alpha) dpm/mL for the evaporator distillate is derived from DOE Order 5400.5 and determines whether this solution can be discharged to Sawmill Creek at ANL (decision point D).

If the filtrate from the first precipitation step is greater than 100 nCi/g (decision junction A), a second precipitation is needed. After the second filtration of TRU waste, the total solids and alpha content of the filtrate are determined. Decision junction A is then used again to determine what to do with this waste. The filtrate at this point in the process should be less than 100 nCi/g. On the basis of the feed and filtrate analysis or a separate solids sample analysis, the solids from the second precipitation step will either be TRU or nonTRU. If the precipitate is TRU, the solids will be sent to the WIPP; if nonTRU, the waste will be sent to Hanford as LLW (decision junction D).

A plan was prepared describing the laboratory studies needed to develop a process for treating TRU waste at ANL. This plan is being released as an ANL topical report.[8]

3. Initial Laboratory Tests
(S. A. Slater and J. Sedlet)

Experimental work was begun on carrier precipitation methods for removing TRU elements from waste solutions. Laboratory-scale (5-10 mL) tests were performed using ferric hydroxide precipitation to remove ^{241}Am and ^{239}Pu from acid solution. The following generic procedure was used for the precipitations:

(a) A known amount of 1M ferric nitrate [$Fe(NO_3)_3$] solution was pipetted into a centrifuge tube.

(b) A known amount of 1M acid was pipetted into the same centrifuge tube.

(c) The solution was spiked with a known amount of ^{241}Am or ^{239}Pu.

(d) After mixing the solution for a few seconds, a known amount of 1M or 6M sodium hydroxide (NaOH) was added to the solution to precipitate ferric hydroxide [$Fe(OH)_3$].

(e) The final suspension was mixed for a few seconds, then centrifuged for 5 min.

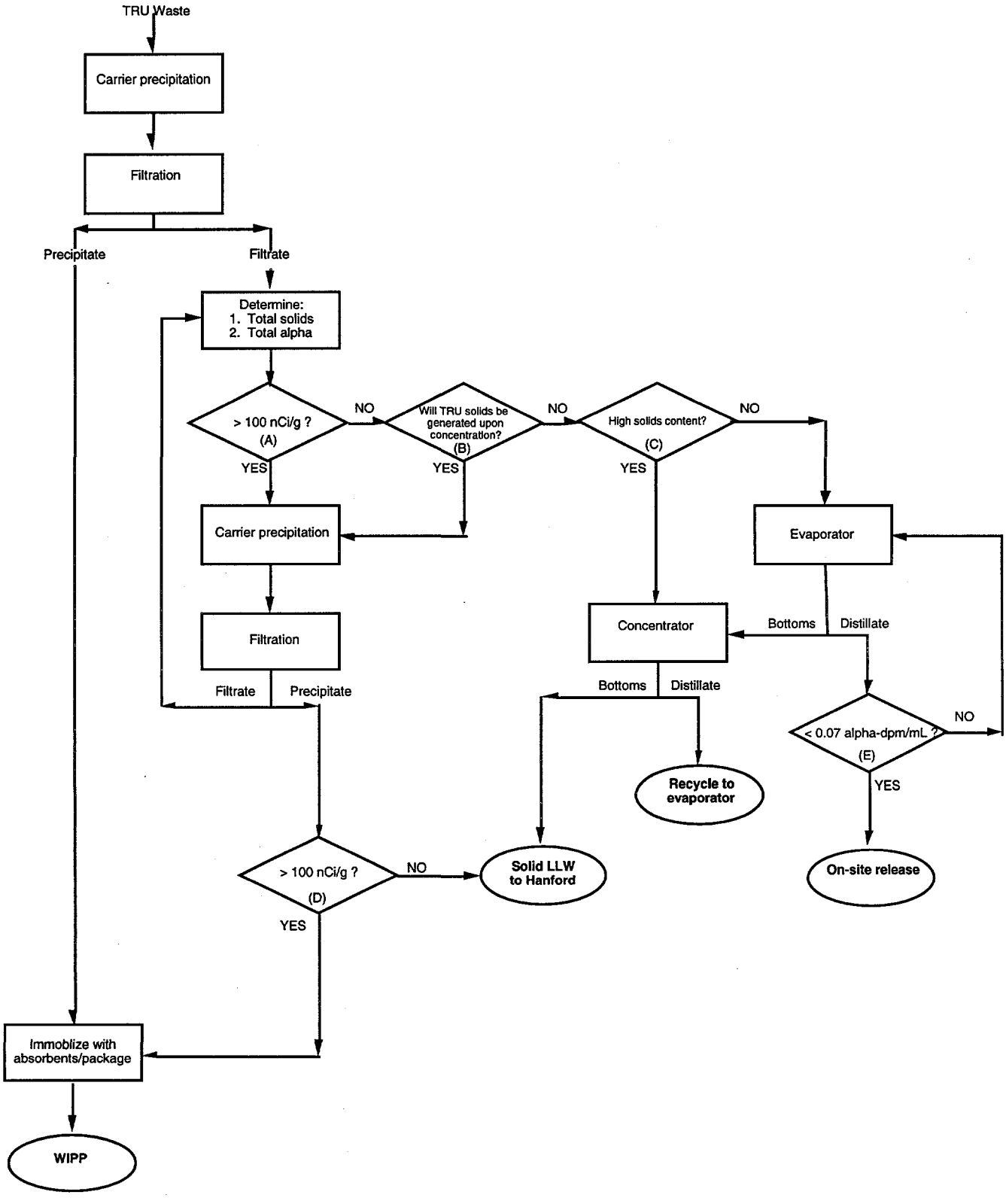

Fig. 33. Flow Diagram for TRU Waste Treatment

(f) The supernatant was pipetted off, and duplicate aliquots were taken for counting.

(g) The precipitate was dissolved in concentrated nitric acid by heating in a water bath.

(h) A volume of 2-4 mL of deionized water and 200 μL of concentrated phosphoric acid (H_3PO_4) was added to the solution of the precipitate to make it colorless for efficient counting (phosphates form a colorless complex with ferric ions).

(i) Duplicate aliquots of the precipitate solution were taken for counting.

(j) A known amount of ferric nitrate solution (second strike) was added to the supernatant from the first precipitation (direct strike), and steps e-i were repeated.

(k) The alpha activity in the aliquots was measured by liquid scintillation counting.

Table 46 gives the results of the precipitations that have been run. Run A is the first precipitation or direct strike, and Run B is the second strike; both are described in the generic precipitation procedure. In Table 46, the initial conditions of the precipitation are given: the amount of Fe(III) per milliliter of solution, the activity of the radioactive spike, acidic conditions of the solution before precipitation, any reducing agents that were used, and the final volume in which the precipitation took place. The final volume is the volume after the addition of sodium hydroxide.

The results that are given in Table 46 include the material balance and the distribution of the actinides between the precipitate and the supernatant. In determining how efficient the carrier precipitations were, the nCi/mL of activity of the supernatant and the nCi/g of activity of the precipitate were calculated. The weight of the precipitate was calculated from the amount of iron added, with the assumption that the precipitate corresponded to the formula $Fe(OH)_3$. The decontamination factor (DF), which is defined as the total activity of the feed (initial nCi/mL) divided by the total activity of the supernatant, was calculated for both the direct-strike and the second-strike precipitation steps. Finally, the overall DF was calculated for each test.

The poor material balances obtained in some of the tests are attributed to problems in counting the solutions of the ferric hydroxide precipitate. For the second strike, counting the supernatant resulted in large statistical errors. The problems encountered in counting the precipitate solution are believed to be due to poor emulsification of the sample in the scintillation cocktail and incomplete decolorization of the iron. These problems are being studied.

The Am-241 test 1 was successful, with an overall DF of 5.07×10^4, and the supernatant activity was reduced from 335 to 0.01 nCi/mL. The Pu-239 precipitations were also successful. However, the precipitates were gelatinous and, as expected for ferric hydroxide, will be difficult to filter. When the plutonium was reduced with sodium bisulfite, the precipitate had finer particles, which were black. The Pu-239 tests showed trends in the data based on the amount of Fe^{3+} used in the precipitations and use of sodium bisulfite ($NaHSO_3$) to reduce the plutonium to the III valence state. As a trend, the higher the Fe^{3+} concentration, the higher the decontamination factor. In tests 3 and 4, sodium bisulfite was used, and this solution appears to increase the efficiency of the precipitations (higher decontamination factors) at Fe^{3+} concentrations of 0.8 mg/L.

In tests 3 and 4, sodium bisulfite was added in an attempt to reduce Pu(IV), the starting oxidation state, to Pu(III). The bisulfite ion will reduce Fe(III) to Fe(II), and magnetite may have precipitated. Without the reducing agent (tests 5 and 6), ^{239}Pu decontamination factors were small (10-50). Magnetite precipitations will be studied hereafter.

Table 46. Results of Precipitations[a]

Test No.	Isotope	Conditions	mg Fe/mL	Initial Spike nCi	Initial Spike nCi/mL[b]	Final Vol., mL	SN, nCi/mL	PPT, nCi/g	DF	Overall DF	% SN	% PPT	Mat. Bal., %
1A	Am-241	1M HNO_3	0.79	2548	335	7.60	1.48	1.70E+05	2.27E+02		0.44	76	77
1B	Am-241				1.48		0.01	9.79E+02	2.23E+02	5.07E+04	0.45	100	100
1A	Pu-239	1M HNO_3	4.10	922	111	8.31	0.10	1.33E+04	1.07E+03		0.09	93	93
1B	Pu-239				0.10		< 0.01	8.96E+00	7.21E+01	7.74E+04	1.39	79	80
2A	Pu-239	1M HNO_3	0.72	922	111	8.31	4.28	6.89E+04	2.59E+01		3.86	85	89
2B	Pu-239				4.28		0.01	1.53E+03	4.19E+02	1.09E+04	0.24	49	49
3A	Pu-239	1M HNO_3	0.77	922	118	7.81	0.64	7.95E+04	1.87E+02		0.54	99	99
3B	Pu-239	1M $NaHSO_3$			0.64		< 0.01	6.44E+02	1.42E+02	2.65E+04	0.70	149	150
4A	Pu-239	1M HNO_3	4.40	922	118	7.81	0.01	1.32E+04	1.51E+04		0.01	93	93
4B	Pu-239	1M $NaHSO_3$			0.01		ND	4.59E-01		1.51E+04	ND	49	49
5A	Pu-239	1M HNO_3	3.60	1845	399	4.62	8.31	4.26E+04	4.82E+01		2.08	83	85
5B	Pu-239				8.31		0.17	1.01E+03	4.80E+01	2.31E+03	2.08	73	75
6A	Pu-239	1M HNO_3	1.80	1845	399	4.62	7.63	1.08E+05	5.25E+01		1.91	93	95
6B	Pu-239				7.63		0.79	1.61E+03	9.60E+00	5.04E+02	10.42	72	83

[a] A = first precipitation, B = second strike, ND = not distinguishable from background activity level, SN = supernatant, PPT = precipitate, DF = decontamination factor, Mat. Bal. = material balance.

[b] All concentrations calculated after the addition of NaOH.

C. Treatment of Scintillation Cocktail Waste
(B. Srinivasan and K. Foltz*)

The overall goal of this research project is to develop methods that will efficiently extract TRU elements from liquid scintillation cocktail waste by using liquid-liquid extraction and demulsification techniques yet will minimize volume changes in the resulting aqueous and organic phases.

In this report period, preliminary experiments were completed to determine the amount of irradiated neodymium spectroscopic solution required to achieve acceptable counting statistics for future experiments with simulated liquid scintillation cocktail wastes. We chose Nd-147 for use as an analog to Am-241. The neodymium solution used for experiments was the Standard Reference Material 3185 (Neodymium Spectroscopic Solution containing 9.98 ± 0.02 mg/mL Nd in 10% HNO_3). The solution was irradiated to produce Nd-147 by using the facility at the University of Illinois TRIGA Reactor for 2 hours at 1.5 MW. The specific activity of the Nd-147 after irradiation was approximately 10^6 dps/mL. Counts accumulated under the Nd-147 photopeak at 91.1 keV were used for determining neodymium concentrations. Further experiments are needed to evaluate other test conditions (different complexants, organic/aqueous ratios, and temperatures).

D. Evaporator/Concentrator Upgrade
(D. B. Chamberlain)

Waste Management's (WM) existing evaporator/concentrator system (located in ANL's Building 306) for low-level waste is approximately 30 years old and cannot achieve the decontamination factors that are required for on-site disposal of the distillate stream. Therefore, WM decided in FY 1992 that two new evaporators should be purchased to replace the existing two units. In addition, two new concentrators were purchased to replace the existing concentrator. We have helped in the design, selection, and placement of this equipment.

Both new evaporators and one of the concentrators will be used to process low-level radioactive waste. The concentrate from the evaporators would then be pumped into the concentrator, where the remaining water would be evaporated. The product from the concentrator, a thick solids slurry, is discharged directly into a 55-gal drum. The piping diagram (Fig. 34) shows the connections between these three units.

The second concentrator is being purchased to process mixed waste, that is, waste containing radioactive and hazardous components. To simplify training and maintenance requirements, this unit will be identical to the low-level waste concentrator. Because of RCRA requirements, this unit will be operated independently of the other concentrator and the evaporators.

Following a competitive bid process, the evaporator contract was awarded to LICON, Inc. (Pensacola, FL), and the concentrator contract was awarded to Artisan Industries (Waltham, MA).

1. Design of LICON Evaporator
(D. Chamberlain and D. Wygmans)

Design of the LICON evaporators for Waste Management continued through this period. LICON's evaporators are Model C-90 and rated at 1.5 gal/min (5.7 L/min) distillate-production capacity. The electrical ladder, general arrangement, and piping and instrumentation

*Graduate student at University of Illinois, Champaign-Urbana.

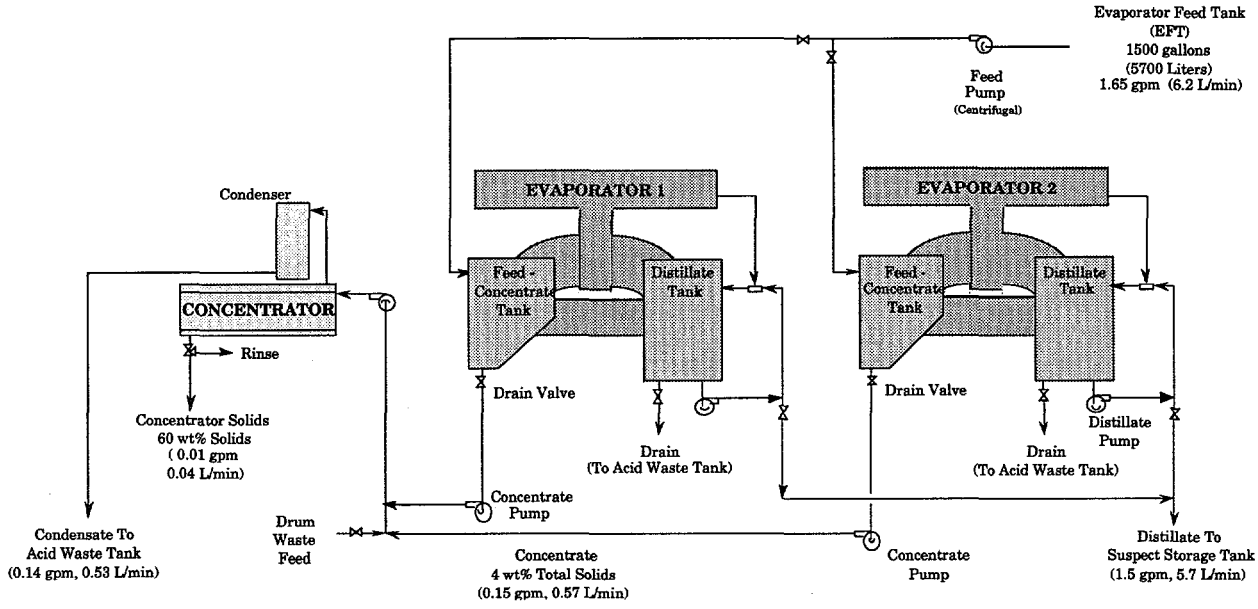

Fig. 34. Piping Schematic for Low-Level Waste Evaporators and Concentrator

drawings were approved for construction. Testing of the two evaporators at LICON's facilities is scheduled for the summer of 1994, with installation of the units expected to be completed at ANL by December 1994.

2. Procurement and Testing of Artisan Rototherms
(D. Chamberlain and D. Wygmans)

Artisan Industries, Inc. (Waltham, MA), was awarded the contract for fabrication of two concentrators with capacities of 0.15 gal/min (0.57 L/min). Artisan's unit, called a Rototherm, is a horizontal, agitated film unit capable of producing high-solids-content waste slurries. This unit is transportable and capable of remote operation and control.

In an Artisan Rototherm, the agitator rotates at approximately 30 ft/s (9 m/s), which generates a thin film on the hot walls of the vessel. In this thin film, the remaining water is evaporated, and then passes up through the vapor duct. The concentrated slurry/solids move down the unit, where they fall from the unit through the bottoms discharge (into a 55-gal drum). In an Artisan unit, the blades do not touch the vessel walls.

Fabrication of the two concentrators was completed in mid-December 1993, and performance tests at Artisan were completed on December 20-23, 1993. To test these units, a simulant of a concentrated ANL waste solution was prepared and shipped to Artisan. These chemicals were shipped dry--Artisan added water and then adjusted the pH. Enough chemicals were shipped to Artisan to prepare 110 gal (416 L) of feed solution. The composition of this solution is given in Tables 47 and 48.

Both units were tested at Artisan on December 20 and 21, 1993; testing of the second unit went much more smoothly than the first unit because of lessons learned on the first unit. The first unit was tested with heat tape and temporary insulation in place, while the second was tested without either. This was done so that the tests could be completed in one day. Since heat losses were

Table 47. Chemicals Required to Prepare 208 L (55 gal) of Feed for Artisan Performance Tests

Chemical Compound	Chemical Name	Mass, g
$NaHCO_3$	Sodium bicarbonate	3914
Na_2SO_4	Sodium sulfate	2225
NaCl	Sodium chloride	1398
$NaNO_2$	Sodium nitrite	812
$Mg(NO_3)_2 \cdot 6H_2O$	Magnesium nitrate	702
$NaH_2PO_4 \cdot H_2O$	Sodium phosphate monobasic	456
$Ca(NO_3)_2 \cdot 4H_2O$	Calcium nitrate	188
NaF	Sodium fluoride	156
$LiNO_3$	Lithium nitrate	72.8
$Na_2SiO_3 \cdot 9H_2O$	Sodium metasilicate	177
$NaNO_3$	Sodium nitrate	38.3
$Na_2B_4O_7 \cdot 10H_2O$	Sodium borate	25.5
$Ni(NO_3)_2 \cdot 6H_2O$	Nickel nitrate	11.8
$CuSO_4 \cdot 5H_2O$	Copper sulfate	4.41
$MnSO_4 \cdot H_2O$	Manganese sulfate	0.26

Table 48. Composition of Simulated Feed for Artisan Performance Tests

Species	Concentration, mg/L
B	13.9
Ca	153
Cu	5.4
Mg	320
Na	13300
Ni	11.4
Si	84
F	340
Cl	4070
SO_4	7240
NO_3	2580
NO_2	2110
HPO_4	1540
HCO_3	13700

not that much greater for the second unit than the first, having the insulation in place really did not change the test procedure for the second unit. A schematic of an Artisan pilot-plant Rototherm unit is shown in Fig. 35. The test setup for Waste Management's units was very similar.

The units were not completely ready for these tests. Additional instrument calibrations (steam flow, temperatures, conductivity) were required because it appeared that most readings were in error or could not be substantiated. Valve labeling was incomplete; instrument and alarm labeling on the instrument panel was nonexistent. The operations manual was also incomplete--there was also some confusion on materials supplied in the pinch valve and on the number of tubes in the preheater.

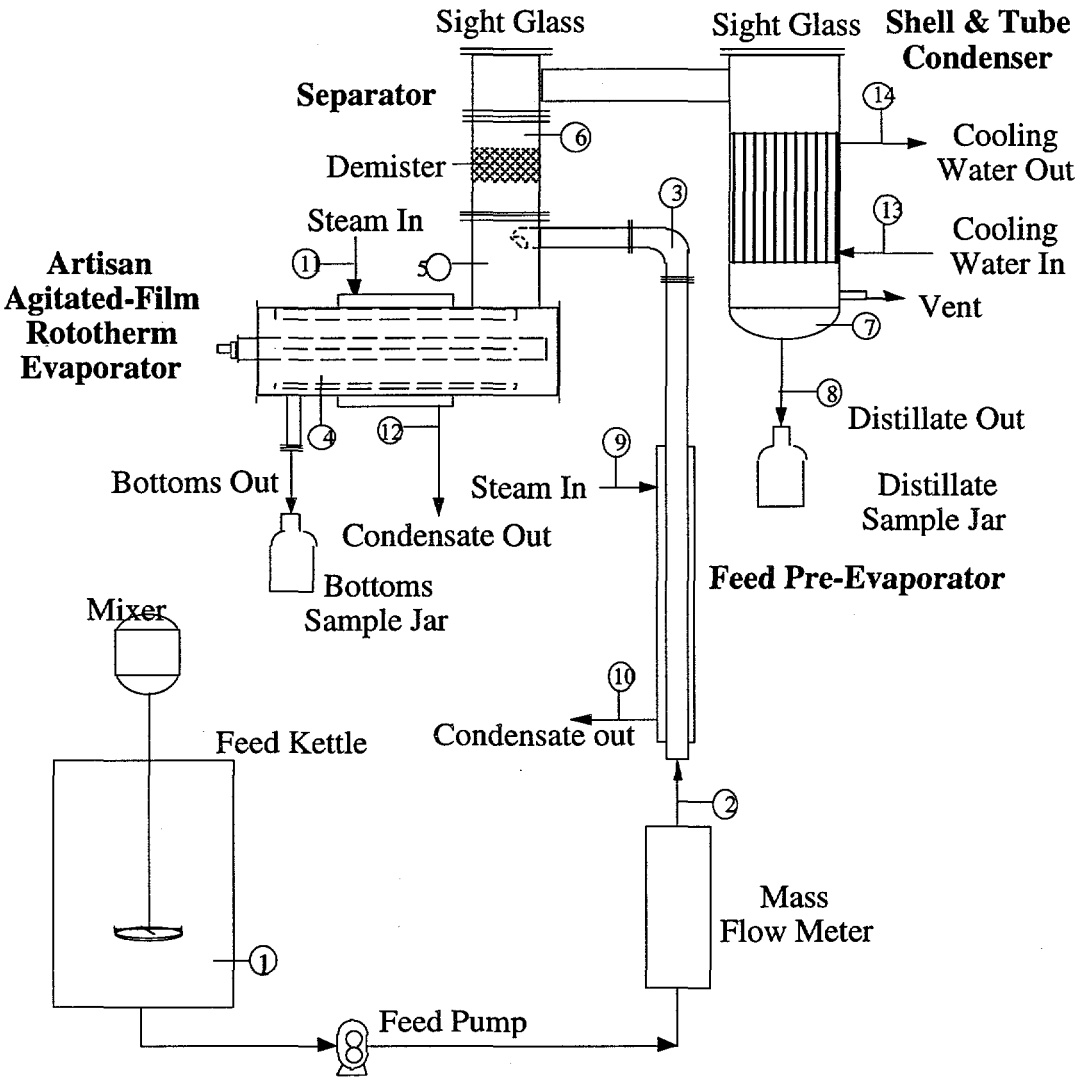

Fig. 35. Schematic of Artisan Pilot-Plant Rototherm

The documents provided in the manual did not give any such information. In spite of these problems, the units appeared to work well and should be more than adequate for Waste Management's use.

Test duration was only about half the 6 h given in our initial specifications. Once various tests at different operating conditions were completed and steady-state operation achieved, it seemed unnecessary to continue the tests for another 3-4 h, and we terminated the tests early.

Without boiling in the preheater, the capacity required in our specifications (distillate flow rate of 0.15 gal/min or 0.57 L/min) could not be achieved. In these tests, only 70% of the required capacity was achieved. However, by allowing phase change in the preheater, the Rototherm exceeded our design goals. Artisan had designed the system assuming boiling in the preheater, and they believe that scaling will not be a problem. With preheater steam pressure at 20 psi (140 kPa) and the Rototherm at 80 psi (550 kPa), satisfactory operation and product quality were achieved at about the design flow rate.

After successfully completing the performance tests, both concentrators were delivered to ANL. Installation will proceed once the evaporators are delivered from LICON (summer of 1994).

3. Limits on Alpha Activity in the Evaporator/Concentrator System
(C. Conner)

As part of technical support to Waste Management, we developed criteria that set a limit on the quantity of TRU material that can be fed to the evaporator. To set this limit, the following four criteria could not be exceeded:

- maximum derived air concentration (DAC) for the high bay in Building 306.
- generation of TRU waste in the concentrator bottoms (>100 nCi/g).
- alpha in the distillate >0.07 dpm/mL.
- quantities of material that could cause criticality.

a. Maximum Derived Air Concentration

The first step was to perform a DAC calculation to determine the maximum amount of alpha activity allowable in Bldg. 306 high bay. The following formula takes a number of factors into account such as the various levels of containment and dispensability of the material:

$$q = \frac{0.02 \cdot C_{DAC} \cdot 2000 \cdot V \cdot lv}{f_a \cdot f_r} \qquad (5)$$

where

q = total activity of dispersible material (μCi) allowed (0.02 = 2% of C_{DAC} is the policy value for dispersible radioactive material)

C_{DAC} = the DAC value for the specified nuclide (μCi/m^3)

2000 = number of hours in a work year

V = room volume (m^3; Bldg. 306 high bay, 4400 m^3)

lv = effective air changes per hour (h^{-1}; Bldg. 306 high bay, 0.6 h^{-1})

f_a = maximum fraction of airborne material (hooded enclosure, 10^{-2}-10^{-3}; glovebox, 10^{-6}-10^{-8})

f_r = fraction of material that could become airborne inside containment over 2000 h (liquids, 10^{-2}-10^{-3}; powders, 10^{-1}-10^{-2})

For the following values, conservative estimates were used. A value of 10^{-2} was assumed for f_a. The concentrator bottoms dump into a vented drum; this configuration is similar to a fume hood (f_a = 10^{-2}-10^{-3}). A 10^{-2} value was also assumed for f_r. The concentrator bottoms have a toothpaste-like consistency and are, therefore, somewhere between a solid and liquid (f_r equals 10^{-2}-10^{-3} for liquids; 10^{-1}-10^{-2} for solids). The high bay has a room volume of 4400 m^3 with an air flow rate of 440 m^3/min; thus the theoretical air changes in the high bay is 6 h^{-1}. However, applying a 0.1 mixing factor (mixing factor suggested by ANL Environmental Safety & Health Manual), the

effective number of air changes is 0.6 h^{-1}. Using all these values, we calculated the maximum allowable amount of activity (q) for four isotopes (Table 49).

Table 49. Maximum Amount of Alpha Activity in Concentrator Bottoms Collection Drum (existing system)

Isotope	C_{DAC},[a] µCi/m³	Maximum Activity, µCi	
		Current System	New System
Pu-239	2.5E-6	2620	2.6 E+7
Am-241	2.5E-6	2620	2.6 E+7
U-235	1.7E-5	17,800	1.8 E+8
U-238	1.7E-5	17,800	1.8 E+8

[a]From ANL Environmental Safety & Health Manual.

Assuming a worst case (that all of the alpha activity in the concentrator bottoms is due to Pu-239 or Am-241), the activity limit for the current system is 2620 µCi. For a safety margin, we suggest a limit of 1300 µCi.

Once the new drum discharge system, with a sealed drum cover is installed, these limits will increase. The f_a for this new system will be 10^{-6}, because it has a configuration similar to a glovebox ($f_a = 10^{-6}$-10^{-8}). The f_r remains at 10^{-2}. Using these values to compute the maximum allowable activity for the new system gives the quantities shown in Table 49. Because of these high maximums, TRU waste would be generated long before these values are exceeded.

The evaporator feed tanks (EFTs) are all sealed systems. Therefore, they have an $f_a > 10^{-6}$. Because of the type of confinement for these tanks, the DAC limit for this room would be large, and handling the slightly elevated levels of alpha activity in the EFTs will not be a problem.

b. Determination of the Potential for TRU Waste Generation

The limit for TRU waste is 100 nCi/g; for a margin of safety we suggest a limit of 50 nCi/g. To determine if TRU waste will be generated requires that total alpha and the total solids in a sample be measured. Once the total alpha and total solids are measured, divide the alpha activity by the total solids to determine if TRU waste could be generated. For example, a sample from a 1500 gal (5700 L) EFT containing 100 nCi/L of alpha activity was found to have 10 g/L total solids. The total alpha present in the 5700 L is

$$\text{Total alpha (µCi)} = \frac{100\ \text{nCi/L} \cdot 5700\ \text{L}}{1000\ \text{nCi/µCi}} = 570\ \text{µCi} \qquad (6)$$

Since 570 µCi is less than the 1300 µCi processing limit given above, this waste could be processed.

If the waste was evaporated to dryness, the total solids generated would be

$$10\ \text{g/L} \cdot 5700\ \text{L} = 57{,}000\ \text{g solids} \qquad (7)$$

Since these solids contain 570 µCi of alpha activity, the TRU content would be

$$\frac{570\ \mu Ci}{57000\ g} \cdot 1000\ nCi/\mu Ci = 10\ nCi/g \quad (8)$$

Since this waste is below the 50 nCi/g limit specified above, the resulting concentrated waste will not be TRU. The result calculated in Eq. 8 can alternatively be calculated from the concentration of alpha activity and the concentration of solids:

$$\frac{100\ nCi/L}{10\ g/L} = 10\ nCi/g \quad (9)$$

c. Alpha Discharge Limits for the Distillate

To meet the sewer discharge limits, the evaporator/concentrator distillate must contain less than 0.07 dpm alpha/mL (3.2×10^{-5} nCi/mL). Estimates of the DF (concentration in the feed/concentration in distillate) for the current evaporator system are not available. However, the system currently processes waste containing 0.005-0.02 nCi/mL of alpha activity, and the distillate meets the 0.07 dpm alpha/mL discharge limit. Since estimates for the DFs in the system are not available, we suggest that an initial upper limit of 0.1 nCi/mL of alpha activity in the feed be set to meet the alpha discharge limits for the distillate. It may be necessary to decrease this level if the distillate fails to meet the discharge limits. Since the distillate is collected in a suspect waste tank (SWT), distillate failing to meet the alpha discharge limit may be evaporated to reduce the activity levels to below discharge limits.

The new evaporator system has an estimated DF of 100,000. (A DF of 100,000 is conservative for the LICON units being installed; DFs > 1,000,000 have been observed in similar units.) Using this value and the alpha discharge limit of 0.07 dpm/mL, we calculated that the evaporator bottoms can contain up to 3.2 nCi/mL. Assuming that a concentration factor of 7.5 is obtained in the evaporator [e.g., 1500 gal (5680 L) of feed is evaporated to 200 gal (760 L) before going to the concentrator], the feed can contain 0.43 nCi/mL and still meet the alpha discharge limits for the distillate.

d. Criticality

Due to the small quantities of fissile material involved (<500 mg Pu-239), criticality is not an issue. In addition, there are administrative controls in place that do not allow critical quantities of transuranic isotopes in the building.

4. Wastes to Be Processed Directly in the Concentrator

Once the new concentrator system is installed, wastes can be fed directly to the concentrator. Wastes containing solids or large quantities of dissolved solids would be good candidates for direct concentrator processing. However, the same limits still can not be exceeded: generation of TRU waste in the concentrator bottoms (>100 nCi/g), maximum DAC for the 306 high bay, and quantities of material that could cause criticality. The above analysis showed that the maximum allowable alpha activity in the high bay to be 1300 μCi (includes safety factor of two). Gross alpha analysis of a sample of the waste will indicate whether or not it exceeds this limit.

To determine if TRU waste will be generated requires the total solids in a sample to be determined by evaporation, followed by weighing the residue. Once the total solids are determined,

divide the alpha activity by the total solids number to determine if TRU waste could be generated. For example, a sample from a 20 L carboy containing 10 μCi/L alpha activity was found to contain 500 g/L total solids.

To determine if TRU waste would be generated, divide the concentration of alpha activity by the concentration of solids:

$$\frac{10\ \mu Ci / L \bullet 1000\ nCi/\mu Ci}{500\ g/L} = 20\ nCi/g \qquad (10)$$

Since 20 nCi/g is less than the suggested limit of 50 nCi/g, TRU waste will not be generated if this waste is processed.

5. Guidelines for Adding Alpha-Containing Waste

The following are some step-by-step guidelines for adding alpha-contaminated waste to the evaporator system:

a. Sample an EFT that is almost full and determine gross alpha (nCi/mL) and total solids (g/mL). Alpha activity levels in the EFT typically range from 0.005-0.02 nCi/mL.

b. Determine the maximum amount of alpha activity allowed in EFT so that TRU waste is not generated in the concentrator bottoms. Use

$$MA = 50\ nCi/g \bullet TS \qquad (11)$$

where MA = maximum alpha in the EFT (nCi/mL) and TS = total solids determined in step a.

c. Mix several likely candidate wastes together and obtain the gross alpha (nCi/mL). Wastes greater than 100 nCi/g cannot be added.

d. Determine if this activity level exceeds the guideline for generating distillate, that is, >0.07 dpm/mL alpha. The maximum EFT concentration for the current system is 0.1 nCi/mL alpha (may need to be decreased if distillate fails to meet the alpha discharge limits). The maximum EFT concentration for the new system is 0.43 nCi/mL alpha.

e. If the activity calculated in step b is less than the limit set in step d, go to step g.

f. If the activity calculated in step b is greater than the limit set in step d, set the maximum amount of alpha activity allowed in the EFT to 0.43 nCi/mL.

g. Determine if the amount of alpha activity calculated in step b or step f exceeds the DAC limit (1300 μCi for existing system; 1.3 $x10^7$ μCi for new system). Do not forget to reduce the DAC limit by the amount of activity already contained in a partially full drum. For example, if the concentrator bottoms are to be discharged

into a drum already containing 300 μCi of activity, the EFT could only contain 1000 μCi of activity instead of 1300 μCi.

h. Multiply the MA calculated in step b or step f by the volume of the EFT:

$$TA = \frac{AC \bullet V}{1000\ nCi/\mu Ci} \tag{12}$$

where TA = total alpha in EFT (μCi)

AC = Alpha concentration in the EFT from step a (nCi/mL)

V = Volume of EFT (mL)

If the total alpha in the EFT is less than the DAC limit, then alpha-contaminated waste can be added to the EFT. To calculate the volume of the alpha-containing waste to add, use

$$WV = \frac{V \bullet (MA - AC)}{(WA - MA)} \tag{13}$$

where WV = Volume of alpha-contaminated waste to add to the EFT (mL)

V = Volume of the EFT (mL)

MA = The alpha concentration calculated in step b or step f (nCi/mL)

AC = Alpha concentration in the EFT from step a (nCi/mL)

WA = Concentration of alpha in the waste to be added from step c (nCi/mL)

i. If the total alpha calculated in step d exceeds the DAC, then determine the quantity of waste to add, use

$$WV = \frac{DAC - AC \bullet V}{WA} \tag{14}$$

where WV = Volume of alpha-contaminated waste to add to the EFT (mL)

DAC = The DAC limit calculated in step g (nCi)

AC = Alpha concentration in the EFT from step a (nCi/mL)

V = Volume of the EFT (mL)

WA = Concentration of alpha in the waste to be added from step c (nCi/mL)

j. Add the volume of waste calculated from Eq. 13 or 14 to the EFT.

VI. MAGNETICALLY ASSISTED CHEMICAL SEPARATION

The activities of the magnetically assisted chemical separation (MACS) program include: (1) developing a design unit for testing our method for TRU simulant waste treatment, and (2) testing particles for gamma radiation damage.

A. Unit Design

(L. Nuñez, B. A. Buchholz, and S. B. Aase)

A fluidized-bed application for laboratory-scale testing of the MACS process has been designed (Fig. 36). The fluidized bed will contain paramagnetic charcoal/magnetite particles coated by CMPO and transuranic radioisotopes in solution. The fluidized bed is designed for a 10 L capacity operated in a batch countercurrent fashion. The process will operate like a conventional multistage pulsed column used in solvent extraction, except that (1) one phase is a solid, (2) the solid-to-liquid phase ratio is typically 0.5-5 kg/100 L (versus a 30-300 L/100 L liquid-to-liquid phase ratio for a solvent extraction column), and (3) pulsing is done magnetically rather than mechanically. The magnetically stabilized fluidized bed allows for a compact design and limited mechanical parts compared to solvent extraction and ion-exchange separation systems. The TRU elements are extracted by the CMPO, and once loaded, the charcoal/magnetite particles will be separated easily by the application of an external magnetic field. Liquid TRU waste will be pumped into the bottom of the column to disperse and fluidize the MACS particles throughout the waste. As the waste fluid flow increases, the upward forces of buoyancy and drag on the particles will balance the downward force of gravity. To pulse the particles in the column, magnetic coils are placed around the outside of the column on a slant so that the particles will move along the magnetic lines of force. The coils can be alternately activated and deactivated to provide vertical motion of the particles in the column.

B. Gamma Radiolysis

(B. A. Buchholz)

The MACS particles were irradiated with a high-intensity ^{60}Co gamma-ray source. All particle samples were mixed with one of five solutions [deionized water; 0.1, 2, and 5M HNO_3; and simulant for Plutonium Finishing Plant (PFP) waste] and vacuum sealed in quartz tubes. The sealed tubes were rotated end-over-end during irradiation and acquired the ambient air temperature of the ^{60}Co cell, approximately 30°C. The expected doses to the particles were estimated to determine the exposure time of the particles to the ^{60}Co source. Dose rates were determined by measuring the change in optical density of blue cobalt glass. The water equivalent dose rate was multiplied by the ratio of the electron density of the particles to the electron density of water to obtain a dose rate to the particles. Upon completion of the irradiations, the quartz vials were opened, and the particles were separated from the contact solutions. The quartz vials containing particles in 5M HNO_3 were coated with deposits of a sticky yellow organic material. The partition coefficients of the irradiated particles were measured by using 2M HNO_3 spiked with ^{241}Am.

The ability of the MACS particles to extract americium from 2M HNO_3 solutions was found to depend on the radiation dose, strength of acid in contact with the particles, and contact time of the acid with the particles. Figure 37 depicts the variation in K_d value for absorbed doses of 1, 2.6×10^4, 2.6×10^5, and 5.9×10^6 rad, respectively equivalent to 0, 10, 100, and 2000 cycles of use processing PFP acid waste. The decline in extraction capacity with increase in dose is most prevalent with the 5M acid. The K_d values quoted at 1 rad dose are for particles exposed to the stated acid for five hours but not placed in the ^{60}Co cell. Based on the slight decrease in extraction capacity of the 0.1M HNO_3 for no dose and 10 cycles, it appears as though the acid in the contact solutions is responsible for most of

the decline in K_d values. Figure 38 shows the change in K_d value with contact time in 0.1, 2, and 5M HNO_3 with no irradiation. The sharp drop in extraction capability for particles in contact with 5M HNO_3 suggests that the acid may be dissolving the coating or dissolving the iron in the magnetite.

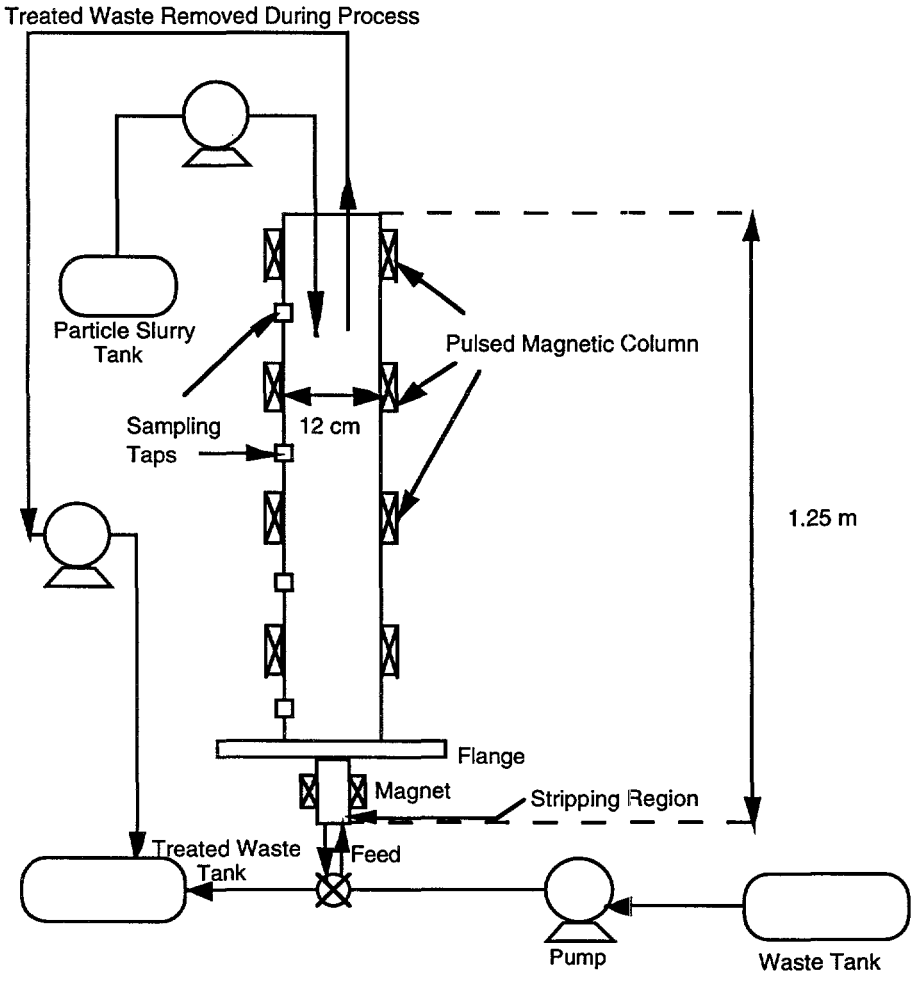

Fig. 36. Process Diagram for MACS Fluidized Bed

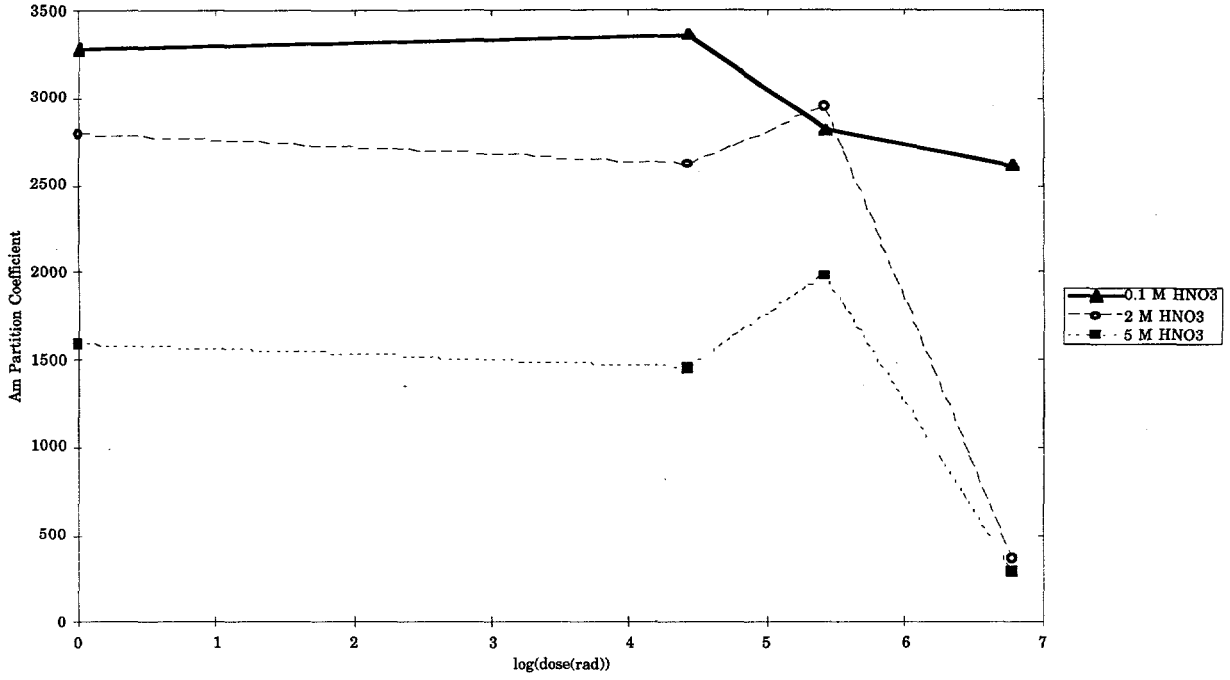

Fig. 37. Change in Americium Partition Coefficients from 2M HNO_3 as a Function of Absorbed Dose for Three Different Contact Solutions. Particles coated with 1.36M CMPO in TBP, and all partition coefficients measured with ^{241}Am in 2M HNO_3.

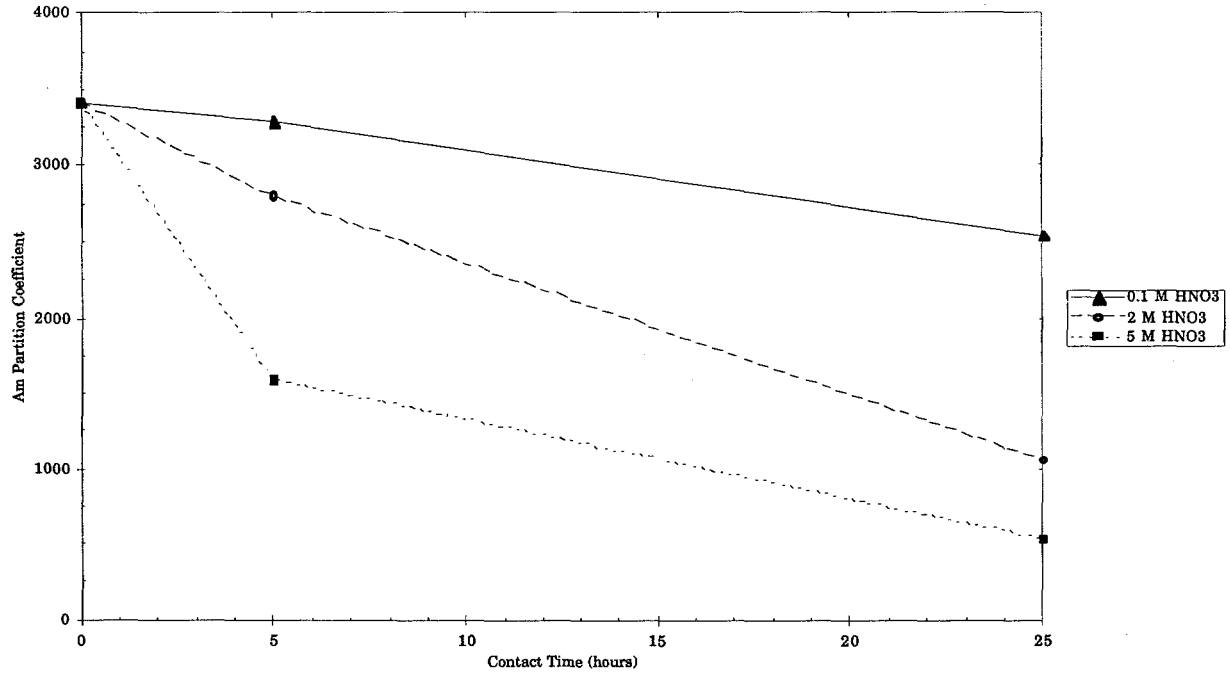

Fig. 38. Change in Americium Partition Coefficients from 2M HNO_3 as a Function of Contact Time in Three Nitric Acid Solutions with No Irradiation. Particles coated with 1.36M CMPO in TBP, and all partition coefficients measured with ^{241}Am in 2M HNO_3.

VII. PROCESSING OF ^{99}Mo TARGET

(J. C. Hutter, B. Srinivasan, and G. F. Vandegrift)

Molybdenum-99 is a precursor of Tc-99m, which is used in several medical applications. It must be produced by one of two methods of controlled nuclear reactions: neutron bombardment of Mo-98 and fission of U-235. In neutron bombardment of Mo-98, the Mo-99 is generated by the nuclear reaction Mo-98 (n,γ) Mo-99. This method is not amenable to full-scale production because its product has a low specific activity.[9] Mo-99 is currently being produced by the fission of U-235, i.e., U-235 (n,f) Mo-99. The Mo-99 is recovered by dissolving the irradiated target and purifying the Mo-99 recovered from the dissolver solution. This process has many variations, but its common feature is that high-enriched uranium (HEU) targets are used for its production.

Recent legislation in the United States requires that the export of HEU be curtailed to prevent nuclear weapons proliferation. To meet these new requirements, Mo-99 must be produced with low-enriched uranium (LEU). As a part of the Reduced Enrichment Test Reactor (RERTR) Program, we are working on processes to produce Mo-99 from LEU targets instead of HEU targets. Two promising LEU targets, under development at Argonne, contain either uranium metal or uranium silicide. These targets can be substituted for the HEU-UO_2 or various HEU-UAl_x alloys now in use.

A. Uranium Silicide Targets

(J. C. Hutter and B. Srinivasan)

For the last several years, uranium silicide fuels have been under development as LEU targets for Mo-99. The use of silicide is aimed at replacing the HEU-UAl_x alloy in the basic dissolution process practiced by both the Institute National Des Radioelements (IRE), Fluerus, Belgium, and Comision Nacional de Energia Atomica, Buenos Aires, Argentina. The targets do not readily dissolve in base. In acid, silica is precipitated in the dissolution process, and the Mo-99 cannot be recovered from the solution.[10] In 1987, Kwok was able to dissolve the uranium silicide in alkaline hydrogen peroxide at 70°C. Kwok's dissolution apparatus is shown in Fig. 39. This vessel was used to dissolve quantities of up to 0.3 g U_3Si_2 in 100 mL of liquid. According to Kwok's original description, initially, the target was placed in 3.0M NaOH to remove the cladding. Once the cladding was dissolved, the cladding solution was removed, and a 1:1 ratio of 3M NaOH and 30 wt% hydrogen peroxide was used to dissolve the remaining uranium silicide.[11] In 1989, the following optimized procedure was proposed to dissolve uranium silicide targets.[12] A dissolver is loaded with irradiated targets. Initially, the cladding and the aluminum in the fuel matrix are dissolved in 3M NaOH. (The addition of $NaNO_3$ was suggested to keep hydrogen production to a minimum.) A gas sparge, during the dissolution, is proposed to remove the gaseous fission products and mix the dissolver contents. Once the cladding is dissolved, the flocculent in the solution is removed from the dissolver, leaving the dense uranium silicide behind. This solution is filtered, then returned to the dissolver. Next, a 30 wt% solution of hydrogen peroxide is added dropwise until the uranium silicide is completely dissolved. After this time, the dissolver solution is heated to destroy the hydrogen peroxide complex and allow the dissolved uranium to precipitate. This solution is filtered to recover the uranium, and then it is acidified for subsequent recovery of Mo-99 in the same way as currently done for uranium aluminide targets.

Recently, we initiated experiments to optimize the silicide dissolution process. During the dissolution process, two chemical reactions occur, the autodestruction of hydrogen peroxide and the dissolution of uranium silicide. A literature search revealed very little data about the autodestruction of hydrogen peroxide in sodium hydroxide solutions. One source[13] simply mentioned that the autodestruction reaction is catalyzed in base, but no quantitative data were given. Experiments were

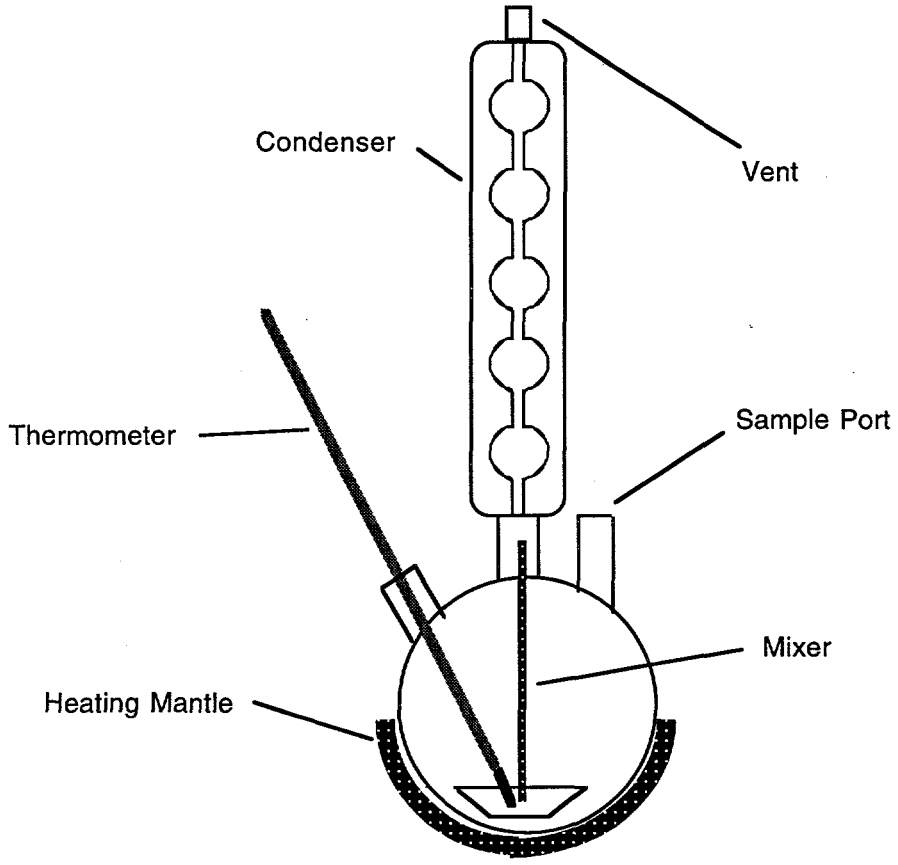

Fig. 39. Dissolution Apparatus Used to Collect Rate Data

completed to quantify the autodestruction rate in various NaOH solutions over the temperature range 70-100°C. The autodestruction reaction is exothermic, and its kinetics must be understood to design a dissolver with the proper heat transfer characteristics so that the dissolution process can be safely controlled.

The autodestruction of hydrogen peroxide

$$2H_2O_2 \rightarrow 2H_2O + O_2 \qquad (15)$$

has a first-order dependence on the concentration of hydrogen peroxide. The rate expression is

$$\frac{dC}{dt} = -kC \qquad (16)$$

where C = concentration of hydrogen peroxide, mol/L

t = time, min

k = first-order rate constant, min^{-1}

Equation 16 can be rearranged and can be integrated with the initial condition $C = C_0$ at $t = t_0$, to yield Eq. 17:

$$\ln \frac{C}{C_0} = -k (t - t_0) \tag{17}$$

To determine k, the isothermal destruction of a completely mixed batch of hydrogen peroxide in a sodium hydroxide solution was measured over time. From a plot of ln C/C_0 vs. time the slope equal to -k is determined. Since this equation has the form y = mx+b, a least squares fit of the data was used to statistically minimize the errors in the measurements of C.

Kwok's dissolver (Fig. 39) was used to collect the rate data for the hydrogen peroxide autodestruction reaction. A 1000 mL glass round bottom flask was used as the reaction vessel. Attached to the flask was a 40 cm Allihn condenser (Fisher Scientific), which ensured that vaporized water and hydrogen peroxide were returned to the flask. A thermometer was inserted into the liquid to monitor the temperature. A 380 W heating mantle was used to manually control the temperature at various set points. Temperature control within 1°C was possible during the course of the experiments. A glass shaft and Teflon impeller (Fisher Scientific) were used to mix the reactor contents after addition of reagents. During the experiments, the generation of oxygen gas bubbles, caused by the decomposition of hydrogen peroxide, was adequate to mix the flask contents.

The destruction of hydrogen peroxide is exothermic, and it is a function of the composition of the peroxide solution (from data in Ref. 13). The heat of mixing is not included since it is negligibly small compared to the heat of reaction (0.4-1.2 kJ/mol). Initially, the reactor was filled with 30 mL of a sodium hydroxide solution and heated to 10°C less than the target temperature. The experiment was started by adding 40 mL of 30 wt% hydrogen peroxide to the flask. Since the peroxide was stored at 0°C, initially the flask contents cooled slightly, then as the reaction began the reactor contents heated up to temperatures as high as 95°C. Within a few minutes, the reactor contents cooled to one of the target temperatures of 70, 80, or 90°C, and the temperature could be maintained at this target temperature by using the heating mantle. Once the set point temperature was reached, the clock was started, and 0.1-0.2 mL grab samples were removed at set time intervals up to 120 min. The grab samples were quickly cooled to 0°C in an ice water bath to slow the reaction down before they were introduced into 52 mL of 1M H_2SO_4 and 0.15M KI for titration with 0.1M sodium thiosulfate to determine the hydrogen peroxide concentration.[14] Once the concentration-vs.-time data were obtained, the rate constant was determined from Eq. 17.

Typical experimental data plot as straight lines on a logarithmic scale (Fig. 40). The straight lines in Fig. 40 indicate that the data fit a first-order dependence well. The curve for 2.57M NaOH at 70°C reflects the lowest destruction rate observed, while the curve for 0.128M NaOH at 90°C reflects the highest measured rate.

The rate constants for the three NaOH concentrations tested were calculated and are displayed in an Arrhenius plot in Fig. 41. The activation energies and collision frequencies were determined from a least squares fit of the data in Fig. 41 (see Table 50). Data for glass and stainless steel* were taken from the literature.[15] In water, a 30 wt% solution of hydrogen peroxide is slightly acidic and

*The autodestruction of H_2O_2 is catalyzed by stainless steel; therefore, its rate of destruction is proportional to the surface area of stainless steel per volume of solution. The curve shown is for one condition given in Lin et al.[15]

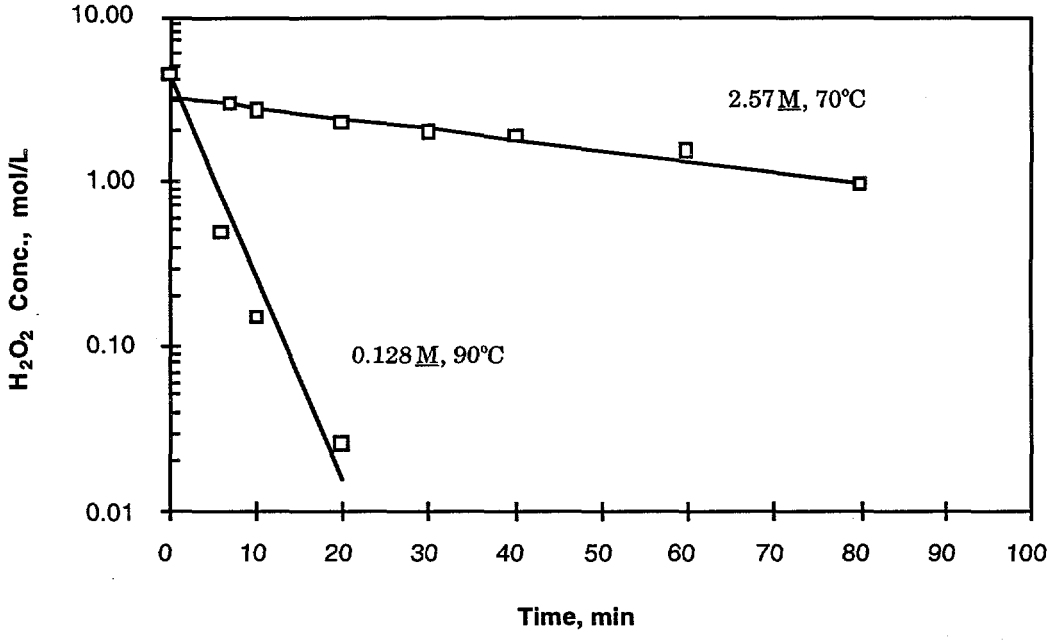

Fig. 40. Typical Concentration vs. Time Results for the Peroxide Reaction (Eq. 15)

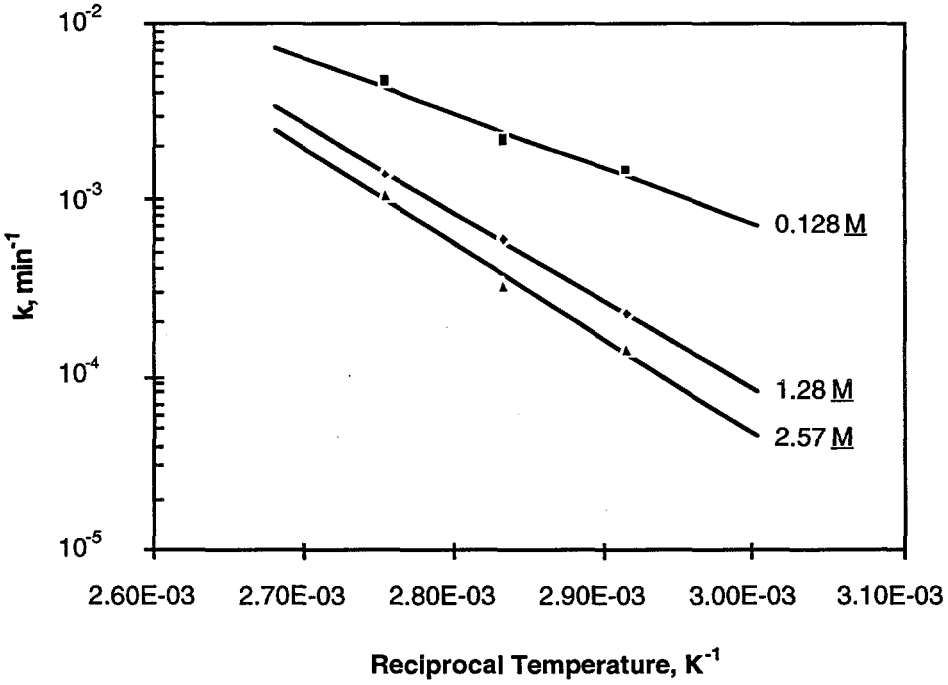

Fig. 41. First-Order Rate Constants for Destruction of Hydrogen Peroxide in Alkaline Media in Glass

Table 50. Activation Energies (E_a) and Collision Frequencies (A) for Hydrogen Peroxide Destruction

Condition	E_a, kJ/mol	A, min^{-1}
Water on glass[a]	66.9	2.40E+05
Water on stainless steel[a]	61.9	1.50E+07
0.128M NaOH	60.5	1.32E+08
1.28M NaOH	96.0	5.57E+12
2.57M NaOH	104.1	5.82E+13

[a]From Lin et al.[15]

has a pH of about 4. Our experimental data were collected for sodium hydroxide (basic) solutions at concentrations of 0.128-2.57M.

As shown in Table 50, the activation energy for hydrogen peroxide destruction in aqueous solutions is 61-67 kJ/mol, which is substantially less than the energy of the O-O bond, 200 kJ/mol.[14] Due to the low activation energy, it is likely that the rate-controlling step in the reaction does not involve the breakage of the O-O bond.[15] The activation energy in 0.128M NaOH was similar to the result in water; however, the activation energy in high NaOH concentrations was substantially larger, which contributes to greater stability of hydrogen peroxide in more concentrated NaOH solutions. Thus, to minimize destruction of hydrogen peroxide in the dissolution procedure, low temperatures and high base concentrations should be used. Also, if the dissolution is done in water alone, the destruction rate of hydrogen peroxide is lower still. The highest destruction rate was found in 0.128M NaOH at 90°C.

Experiments are planned to study the kinetics of the silicide dissolution. Once the rate data are collected, the optimum dissolution conditions will be identified. Under these conditions, a 5-g irradiated miniplate will be dissolved to demonstrate the effectiveness of the dissolution procedure.

B. Uranium Metal Foil Target
(B. Srinivasan)

The LEU-metal foil target is expected to replace the HEU-UO_2 target that was used to produce ^{99}Mo using the Union Carbide Reactor facilities in Tuxedo, New York. The reactor facilities were shut down in February 1990. Since that time, Nordion of Canada has been the supplier of ^{99}Mo to the U.S. market. The future production of ^{99}Mo in the U.S. is likely to use the metal foil target in some other reactor facility operated by the Department of Energy. In that case, the post-irradiation processing of the LEU-metal foil target will be done using the Cintichem process, a process that was developed to recover molybdenum from the HEU target. The first step in the Cintichem process was the dissolution of the HEU-UO_2 target that was electroplated on the inside surface of a stainless steel cylinder. It appears that a mixture of 0.8M nitric acid and 2M sulfuric acid was used for the dissolution.[16] The exact composition of the dissolver solution and the chemistry behind the dissolution reaction can only be guessed from a process flowsheet prepared by Merrick for use by the Los Alamos National Laboratory (LANL). The flowsheet is of limited use not only because some of the details are lacking, but also because of errors. It is necessary to obtain a copy of the original document to verify the details of the Cintichem process.

The first step in the recovery of ^{99}Mo from irradiated LEU-metal foil targets is to develop a satisfactory scheme for the dissolution of uranium metal in a mixture of nitric and sulfuric acids. The

main goal of this work is to obtain a solution at the end of dissolution that is similar to the Cintichem process solution. In this manner, further processing of this solution to recover the molybdenum can proceed along the same lines as the Cintichem process with minimum modifications.

The R&D work on the dissolution method began in January 1994, using depleted uranium metal foil samples (^{235}U content is about 0.3% in contrast to 19.7% in LEU), with the same thickness as in the proposed LEU target (125 μm). These dissolutions were carried out in pure nitric acid and in various nitric and sulfuric acid mixtures. The dissolution temperature was also varied. The rate of dissolution under different conditions is given in Table 51.

Table 51. Dissolution Rates of Uranium Metal Foil in Nitric Acid and in Mixtures of Nitric and Sulfuric Acids

Conc., mol/L		Rate,[a] mg/(min•cm^2)			
Nitric	Sulfuric	25°C	40°C	59°C	84°C
4	–	Very slow[b]	–	–	0.76[c]
4	0.54	≥0.03[d]	–	–	3.1
8	–	0.09	0.15	≥0.42	1.5
8	0.54	0.29	0.70	1.7	4.0
8	1.1	0.52	1.5	4.7	
12	–	≥0.2	0.73	1.6	4.0
12	0.54	1.81	5.64	9.3	21
12	1.1	5.9	12.6	35	
16	–	≥0.2	–	–	6.0
16	0.54	–	–	–	102

[a]The rates of dissolution represent an average value. The initial rates for dissolution, where determined, were higher than the average values shown in this table. The samples were not stirred during dissolution.

[b]The dissolution rate is very slow. There is no appreciable change in the mass of the foil even after 164 h.

[c]This rate was obtained at 95°C, not 84°C.

[d]The ≥ sign means that the exact time for complete dissolution was not known. Several of these experiments were done overnight or over the weekend and complete dissolution had occurred during this period.

The rates of dissolution for the uranium metal foil given in Table 51 are semi-quantitative measurements, for two reasons: First, the foil is not pure uranium metal; the surface of the foil appears to be oxidized. Therefore, the rates correspond to the dissolution of the mixture of metal and its oxide, and not pure metal. The actual target after irradiation is expected to have an oxide covering; therefore, the above rate experiments are relevant. Second, the time required for dissolution was determined by visual inspection of the total disappearance of the foil, which invariably coincided with the cessation of gas evolution. Such visual observations yield only approximate values.

Despite the semi-quantitative data, some general conclusions are possible. For a given nitric acid concentration, the rate of dissolution is higher in nitric-sulfuric acid mixtures than in pure nitric acid alone; also, the rate is higher when the mixture contains a higher concentration of sulfuric acid. The rate of dissolution increases with increased temperature. A desirable rate for dissolution for the

actual target is about 3 mg/(min•cm^2). At this rate, a typical LEU-target foil will require about 30 min for complete dissolution (see Table 52).

Table 52. Time Required for Complete Dissolution of Typical Uranium Metal Target Foil[a]

Dissolution Rate, mg/(min•cm^2)	Dissolution Time, min
1	101
3	34
10	10

[a]Mass of foil = 15.7 g
Dimensions = 10 cm x 8 cm x 0.013 cm (thick)
Surface Area = 12 in.^{2} or 77.4 cm^2
Surface Area for Dissolution = 2 x 77.4 cm^2

The above data show that several combinations of nitric and sulfuric acid mixtures and temperatures will yield the desirable dissolution rate of 3 mg(min•cm^2). The important point is that the solution at the end of dissolution has to resemble the Cintichem solution. That composition, as best as we can estimate from the Cintichem flowsheet, is as follows: uranium concentration of 1M, sulfuric acid concentration of about 2M, and little or no nitric acid. We plan additional experiments to ensure that the foil is dissolved within about 1 or 2 h and the solution approximates the Cintichem solution in composition. In addition, we need to design a dissolver apparatus that can withstand the heat evolved and pressure increase accompanying the dissolution reaction. To minimize waste generation, the dissolver apparatus has to be used for several dissolutions before it is discarded. For designing the apparatus, we need experimental data on the heat of reaction and on the composition and amount of gases released.

REFERENCES

1. M. J. Steindler et al., *Chemical Technology Division Annual Technical Report, 1991*, Argonne National Laboratory Report ANL-92/15, p. 95 (1992).

2. R. A. Leonard, "Solvent Characterization Using the Dispersion Number," Sep. Sci. Technol. 30 (7-9), 1103-1122 (1995).

3. W. Richmond, *Conceptual Design Report: Cesium Demonstration Unit/BNFL*, E/B-SD-W236B-RPT-008-Rev. 03 (1994).

4. S. A. Barker, E. B. Schwenk, and J. R. Devine, "Materials Evaluation for a Transuranic Processing Facility," Westinghouse Hanford Company Report WHC-SA-0963-FP (1990).

5. U.S. Department of Energy, *TRUPACT-II Content Codes (TRUCON)*, Department of Energy Report DOE/WIPP 89-004, Revision 3 (July 1989).

6. T. E. Boyd and R. L. Klochen, *Ferrite Treatment of Actinide Waste Solutions: Continuous Processing of Rocky Flats Process Waste*, U.S. Atomic Energy Commission Report RFP-3476 (1983).

7. R. L. Klochen, *Actinide Removal from Aqueous Solution with Activated Magnetite*, U.S. Atomic Energy Commission Report RFP-4100 (1987).

8. S. A. Slater, D. B. Chamberlain, C. Conner, J. Sedlet, B. Srinivasan, and G. F. Vandegrift, *Methods for Removing Transuranic Elements from Waste Solutions*, Argonne National Laboratory Report ANL-94/43 (November 1994).

9. A. A. Sameh and H. J. Ache, "Production Techniques of Fission Mo-99," *Fission Molybdenum for Medical Use, Proceedings of the Technical Committee*, International Atomic Energy Agency, Karlsruhe, IAEA-TECDOC-515, pp. 47-64 (1987).

10. K. A. Burrill and R. J. Harrison, "Development of the Mo-99 Process at CRNL," *Fission Molybdenum for Medical Use, Proceedings of the Technical Committee,* International Atomic Energy Agency, Karlsruhe, IAEA-TECDOC-515, pp. 35-46 (1987).

11. G. F. Vandegrift, J. D. Kwok, S. L. Marshall, D. R. Vissers, and J. E. Matos, "Continuing Investigations for Technology Assessment of Mo-99 Production from LEU Targets," *Fission Molybdenum for Medical Use, Proceedings of the Technical Committee*, International Atomic Energy Agency, Karlsruhe, IAEA-TECDOC-515, pp. 115-128 (1987).

12. G. F. Vandegrift, J. D. Kwok, D. B. Chamberlain, J. C. Hoh, W. E. Streets, S. Vogler, H. R. Tresh, R. F. Domagala, T. C. Wiecek, and J. E. Matos, "Development of LEU Targets for Mo-99 Production and Their Chemical Processing Status 1989," 12th Int. Meeting, Reduced Enrichment for Research and Test Reactors, Proceedings, Berlin, September 10-14, 1989, pp. 421-433 (1989).

13. W. C. Schumb, C. N. Satterfield, and R. L. Wentworth, *Hydrogen Peroxide*, Reinhold Publishing Corp., New York (1955).

14. A. I. Vogel, *A Textbook of Quantitative Inorganic Analysis*, Lowe & Brydone, Ltd., London (1960).

15. C. C. Lin et al., "Decomposition of Hydrogen Peroxide in Aqueous Solutions at Elevated Temperatures," *Int. J. Chem. Kin.* 23, 971-987 (1991).

16. H. Arino, H. H. Kramer, J. J. McGovern, and A. K. Thornton, "Production of High Purity Fission Product Molybdenum-99," U.S. Patent 3,799,833 (1974).

Distribution for ANL-97/21

Internal:

D. B. Chamberlain
C. Conner
D. W. Green
J. E. Harmon
J. E. Helt
E. P. Horwitz
J. J. Laidler
R. A. Leonard
C. J. Mertz
L. Nuñez
J. Sedlet
S. A. Slater
M. J. Steindler
D. M. Strachan
G. F. Vandegrift (5)
R. D. Wolson
TIS Files

External:

DOE-OSTI (2)
ANL-E Library
ANL-W Library
Manager, Chicago Operations Office, DOE
J. C. Haugen, DOE-CH
A. L. Taboas, DOE-CH
Chemical Technology Division Review Committee Members:
- H. U. Anderson, University of Missouri-Rolla, Rolla, MO
- E. R. Beaver, Monsanto Company, St. Louis, MO
- D. L. Douglas, Consultant, Bloomington, MN
- R. K. Genung, Oak Ridge National Laboratory, Oak Ridge, TN
- J. G. Kay, Drexel University, Philadelphia, PA
- R. A. Osteryoung, North Carolina State University, Raleigh, NC
- G. R. St. Pierre, The Ohio State University, Columbus, OH

B. A. Buchholz, Lawrence Livermore National Laboratory, Livermore, CA
L. Chen, Naperville, IL
M. K. Clemens, Lisle, IL
M. Dinehart, Los Alamos National Laboratory, Los Alamos, NM
D. Dong, Owens-Corning Science and Technology Center, Grandville, OH
L. Holton, Pacific Northwest National Laboratory, Richland, WA
J. C. Hutter, Marmora, NJ
S. C. T. Lien, USDOE, Office of Technology Development, Germantown, MD
G. J. Lumetta, Pacific Northwest National Laboratory, Richland, WA
C. P. McGinnis, Oak Ridge National Laboratory, Oak Ridge, TN
A. C. Muscatello, Rocky Flats Plant, Golden, CO
A. L. Olson, Lockheed Idaho Technology Company, Idaho Falls, ID
M. Palmer, Los Alamos National Laboratory, Los Alamos, NM
G. Pfennigworth, Martin Marietta Energy Systems, Oak Ridge, TN
M. C. Regalbuto, Amoco Oil Company, Naperville, IL
A. Rozeveld, Eaton Rapids, MI
B. Srinivasan, Woodridge, IL
J. L. Swanson, Pacific Northwest National Laboratory, Richland, WA

I. R. Tasker, Waste Policy Institute, Gaithersburg, MD
D. W. Tedder, Georgia Institute of Technology, Atlanta, GA
M. Thompson, Westinghouse Savannah River Company, Aiken, SC
T. A. Todd, Lockheed Idaho Technology Company, Idaho Falls, ID
S. Yarbro, Los Alamos National Laboratory, Los Alamos, NM